ELECTRICAL PROPERTIES OF IONIC CRYSTALS

A thesis submitted for the degree of

Doctor of Philosophy in the

University of London

by

JOHN HARRISON BEAUMONT, B.Sc., A.R.C.S.

Department of Chemistry,
Imperial College,
London, S.W.7.

October, 1965.

ABSTRACT

A review has been made of the recent literature pertinent to the electrical conductivity and polarisation of uni-univalent ionic salts. Special attention has been given to the results obtained for potassium chloride.

Pure and strontium-doped hydroxyl-free KCl crystals have been prepared by pre-treating the melt with Cl_2. The crystals were grown by the Stockbarger technique with the KCl in a graphite crucible, sealed under vacuum in a spectrosil vessel.

The temperature dependence of the A.C. electrical conductivity of these crystals has been studied. To interpret the data, a program has been developed for the Atlas computer which, given the conductivity parameters, generates the ionic conductivity as a function of temperature. This has been used in conjunction with a minimisation routine to determine values of all the parameters for KCl. Using the Stasiw and Teltow association theory, the value of the association energy for strontium-cation vacancy complexes in KCl was found to be 0.42 eV. The following enthalpy values were also found: for cation vacancy migration, 0.709 eV; for anion vacancy migration, 1.04 eV; for the formation of a pair of Schottky vacancies,

2.26 eV. The corresponding entropies were: for cation vacancy migration, (0.155 - 0.193) x 10^{-3} eV/deg.; for anion vacancy migration (0.54 - 0.58) x 10^{-3} eV/deg.; for the formation of a pair of Schottky vacancies, 0.463 x 10^{-3} eV/deg.

A dramatic reduction in the extrinsic conductivity of the nominally pure crystals, has been observed subsequent to heating them in an atmosphere of oxygen and water vapour.

Simple expressions have been derived for the space charge capacitance and conductance of doped KCl. These contain a blocking parameter which allows for the possibility of partial discharge of ions at the electrodes. Extensive measurements have been made on the strontium-doped crystals, to determine whether the predictions of this expression are correct. These have shown that the inclusion of the condition for partial blocking does not provide any substantial improvement in the agreement between the theory and the experimental data.

ACKNOWLEDGMENTS

I wish to express my gratitude to my supervisor, Dr. P.W.M. Jacobs, D.Sc., for his continual interest, guidance and advice throughout this work. I also wish to thank Professor R. M. Barrer, F.R.S., for the provision of research facilities in this College.

Thanks are due to Dr. C. C. Klick who made arrangements with the U.S. Naval Research Laboratory, for analyses and for the provision of a piece of zone refined crystal.

I would like to thank the University of London Institute of Computer Science, for the provision of computing facilities.

Finally, I must thank the Science Research Council, for the award of a Studentship from 1962 to 1965.

CONTENTS

1. INTRODUCTION

1.01 General introduction

All the charge transport properties of potassium chloride which have been studied in this work are assumed to result from two mechanisms: A polarisability of the crystal as a whole and motion of the individual ions through the lattice. The first mechanism gives rise to a displacement current when an electric field is applied to the crystal. The current results from an elastic displacement of the ion nuclei and a displacement of the electrons relative to the nuclei. This contributes to the admittance of the crystal as the dielectric constant in a high frequency A.C. field.

The second mechanism is the one which is largely used to interpret the experimental results and requires some justification. The best evidence comes from auto-diffusion of tracer ions and from transference number determinations.

The crystal structure is maintained throughout these experiments showing that the overall result is the movement of ions within their own sublattice. The diffusion experiments (Aschner, 1954; Laurent and Bernard, 1957) clearly demonstrate this property under the influence of

a concentration gradient.

The transference number measurements need more careful examination. By putting three or more slices of crystal between metallic electrodes and passing a known charge through the system, it has been shown (Tubandt et al., 1931; Kerkhoff, 1951) that the mass of the central slice remains unchanged and the changes in mass of the end cylinders and electrodes satisfy Faraday's law. These results yield the transport number for each ion and show the conduction to be entirely ionic within the accuracy of the experiment. Thus the central slice must have allowed a net flow of ions of each sign in a direction appropriate to the field, by a mechanism involving ions moving within their own sublattice.

There are three processes which could lead to ionic mobility. One is the direct exchange of adjacent ions on the same sublattice, energetically, however, this would be very unfavourable. Another mechanism which has been proposed requires several ions to change place simultaneously in a closed ring. This would be more favourable in terms of energy requirements, than the direct exchange process. The third and most likely possibility involves the formation of lattice imperfections, enabling the ions to move with a lower activation energy. Such an imperfection may be created by an ion moving into an interlattice position

(interstitial site) leaving a vacant lattice site. The formation of such defect pairs was first proposed by Joffé (1923) although they are generally referred to as Frenkel (1926) defects. With these defects, the mobility may result from movement of an interlattice ion from one interstitial site to the next, ultimately to return to a lattice site created by another interstitial ion. Alternatively an interlattice ion could displace a lattice ion of the same sign, to form another interstitial ion. A repetition of this process, called the interstitialcy mechanism, would enable ions to move through the lattice. Mobility may also occur via the vacancy mechanism by which neighbouring lattice ions jump into the vacancy created by the interstitial ion. Another possible imperfection comprising a pair of vacancies may occur by the overall result of moving a pair of lattice ions from the bulk to a surface, e.g. a grain boundary or a free surface of the crystal. Mobility could follow by the vacancy mechanism described above. Creation of the vacancies in this case can be regarded as starting by a surface ion jumping up to form an element of a new or partially created surface. The surface vacancy then diffuses into the bulk by a series of subsequent ion jumps. If there are equal numbers of lattice sites for both cations and anions, as in KCl,

this mechanism alone produces equal numbers of cation and anion vacancies. Vacancy pairs created in this way will be referred to as Schottky defects (Schottky, 1935).

All of these processes could contribute to diffusion but energy considerations suggest motion aided by imperfections to be the most likely. Only the latter processes could contribute to conductivity for it is only in these that there can be a net flow of ions under the influence of an electric field.

1.02 Equilibrium numbers of defects.

Statistical mechanics enables a theoretical determination of the numbers of defects in an otherwise perfect lattice. (The following derivation is based upon that given by Fowler and Guggenheim, 1952.) Consider a crystal A^+B^- with N ion pairs in it, N_A positive ions and N_B negative ions. Let the total number of lattice sites be N^l, comprising $\frac{1}{2} N^l$ A lattice sites and $\frac{1}{2} N^l$ B lattice sites. Let the numbers of A and B vacancies be respectively N_A^V and N_B^V and the numbers of A and B interstitials be N_A^i and N_B^i. Then we have

$$1.02.1 \qquad \tfrac{1}{2} N^l = N_A + N_A^V - N_A^i$$

$$1.02.2 \qquad \tfrac{1}{2} N^l = N_B + N_B^V - N_B^i$$

$$1.02.3 \qquad N_A = N_B = N$$

whence

$$1.02.4 \qquad N_A^V - N_A^i = N_B^V - N_B^i$$

Let h_A^V be the energy (excluding lattice frequency changes) required to remove an ion A from an internal lattice point to a new surface lattice point leaving a vacancy. Considering the ions as independent oscillators, as in an Einstein model, and assuming only nearest neighbour frequencies are affected by the presence of a vacancy, let the increase in energy arising from modification of one degree of freedom of the frequencies of the z nearest neighbours to a vacancy be $z(v + \frac{1}{2})h(\nu_A^V - \nu)$. Where v is an integer, the vibrational quantum number and ν is the undisturbed frequency. Let h_B^V and $z(v + \frac{1}{2})h(\nu_B^V - \nu)$ be the corresponding quantities for an ion B. Similarly, let h_A^i, $z_i(v + \frac{1}{2})h(\nu_A^i - \nu)$ and h_B^i, $z_i(v + \frac{1}{2})h(\nu_B^i - \nu)$ be the energies required to take an A and B ion respectively from a surface lattice point to an interstitial position. Where ν_A^V etc. are the frequencies of the nearest neighbours to the defects along a line joining the defect to the nearest neighbour.

Assuming the defects do not interact, the excess energy of this imperfect configuration over that of the perfect crystal is

1.02.5

$$\Delta E = N_A^V h_A^V + \sum_j [(v_j+\tfrac{1}{2})h\nu_A^V - (v_j+\tfrac{1}{2})h\nu]$$

$$+ N_A^i h_A^i + \sum_k [(v_k+\tfrac{1}{2})h\nu_A^i - (v_k+\tfrac{1}{2})h\nu]$$

$$+ N_B^V h_B^V + \sum_n [(v_n+\tfrac{1}{2})h\nu_B^V - (v_n+\tfrac{1}{2})h\nu]$$

$$+ N_B^i h_B^i + \sum_m [(v_m+\tfrac{1}{2})h\nu_B^i - (v_m+\tfrac{1}{2})h\nu]$$

Where each vibrational state being considered is characterised by the vibrational quantum numbers v_j, v_k, v_n, v_m, integers which may be arbitrarily assigned. There will be N_A^V z terms in the first pair of summations, N_A^i z_i in the second, N_B^V z in the third and N_B^i z_i in the last pair.

The total number of energetically equivalent configurations in a KCl lattice type, which has N^l interstitial sites, is given by

1.02.6

$$\Pi = \frac{\frac{1}{2}N^l!}{N_A^V!(\frac{1}{2}N^l - N_A^V)!} \cdot \frac{\frac{1}{2}N^l!}{N_B^V!(\frac{1}{2}N^l - N_B^V)!} \cdot \frac{N^l!}{N_A^i! N_B^i! (N^l - N_A^i - N_B^i)!}$$

From 5 and 6 the complete partition function for the crystal is K(T) Γ(T) where K(T) is that for the perfect crystal and

1.02.7

$$\Gamma(T) = \sum_{N_A^V, N_A^i, N_B^V, N_B^i} \sum_{o}^{p-1} {}_{v_j, v_k, v_n, v_m} \prod e^{-\Delta E/kT}$$

Subject to restrictions 1 and 2

The summations over the vibrational quantum numbers may be carried out first. Each may be done independently; a typical one is

$$I = \sum_{v_j=o}^{p-1} \exp - \frac{1}{kT}\left[\sum_j (v_j+\tfrac{1}{2})h\nu_A^V - \sum_j (v_j+\tfrac{1}{2})h\nu \right]$$

$$I = \left[\sum_{v_j=o}^{p-1} \exp \frac{-1}{kT}\left[(v_j+\tfrac{1}{2})h\nu_A^V - (v_j+\tfrac{1}{2})h\nu \right] \right]^{N_A^V z}$$

$$I = \exp\left[-N_A^V z h(\nu_A^V - \nu)/2kT\right] \left[\frac{1-\exp(-ph\nu_A^V/kT)}{1-\exp(-h\nu_A^V/kT)}\right]^{N_A^V z} \left[\frac{1-\exp -h\nu/kT}{1-\exp -ph\nu/kT}\right]^{N_A^V z}$$

If the highest quantum number, p-1, is chosen sufficiently large such that $\exp(-ph\nu/kT) \ll 1$ for all T encountered, then the expression reduces to

$$I = \exp\left[-N_A^V z h(\nu_A^V - \nu)/2kT\right] \left[\frac{1-\exp(-h\nu/kT)}{1-\exp(-h\nu_A^V/kT)}\right]^{N_A^V z}$$

Above 230°K, the Debye temperature for KCl, where the Einstein approximation is valid, $kT > h\nu$ and

$$I = \exp[-N_A^V z h(\nu_A^V - \nu)/2kT]\ (\nu/\nu_A^V)^{N_A^V z}$$

$$I = \exp - \frac{N_A^V z}{kT}[\tfrac{1}{2}h(\nu_A^V - \nu) + kT \log(\nu_A^V/\nu)]$$

Carrying out all the summations over the v quantum numbers 1.02.8

$$\Gamma(T) = \sum_{N_A^V, N_A^i, N_B^V, N_B^i} \prod \exp - \frac{1}{kT}\Big[N_A^V[h_A^V + \tfrac{1}{2}zh(\nu_A^V - \nu) + kTz \log(\nu_A^V/\nu) + N_A^i[h_A^i + \tfrac{1}{2}z_i h(\nu_A^i - \nu) + kTz_i \log(\nu_A^i/\nu) + N_B^V[h_B^V + \tfrac{1}{2}zh(\nu_B^V - \nu) + kTz \log(\nu_A^V/\nu)] + N_B^i[h_B^i + \tfrac{1}{2}z_i h(\nu_B^i - \nu) + kTz_i \log(\nu_B^i/\nu)]\Big]$$

Expressions similar to $\log \Gamma(T)$ can be shown rigorously, by the method of steepest descents, to have a very sharp, unique maximum. The total contribution to $\log \Gamma(T)$ comes from terms in the immediate neighbourhood of the maximum. At the maximum N_A^V, N_B^i, etc., take on their equilibrium values; since the insertion of an extra slowly varying term, e.g. N_A^V or N_B^i in the summation does not alter the maximum. Thus if $\Gamma(T)$ be abbreviated to $\sum H$ and at the maximum $N_A^V = N_A^{V*}$, the equilibrium value of N_A^V is given by

$$\overline{N}_A^V = \frac{\sum N_A^V H}{\sum H} = N_A^{V*} \frac{H_{MAX}}{H_{MAX}} = N_A^{V*} \cdot \text{Log } \Gamma(T)$$

may thus be equated to the log (max.term) and the condition for this maximum will yield the equilibrium numbers of defects.

Using Stirling's formula for large factorials Log N! = N LogN -N and Lagrange's method to determine the maximum of a function of several dependent variables

$$\left[-\frac{1}{kT}\left\{h_A^V+\tfrac{1}{2}zh(\nu_A^V-\nu)+kTz\log\left(\frac{\nu_A^V}{\nu}\right)\right\}+\log\left(\frac{\frac{1}{2}N^1-N_A^V}{N_A^V}\right)\right]dN_A^V$$

$$+\left[-\frac{1}{kT}\left\{h_B^V+\tfrac{1}{2}zh(\nu_B^V-\nu)+kTz\log\left(\frac{\nu_B^V}{\nu}\right)\right\}+\log\left(\frac{\frac{1}{2}N^1-N_B^V}{N_B^V}\right)\right]dN_B^V$$

$$+\left[-\frac{1}{kT}\left\{h_A^i+\tfrac{1}{2}z_ih(\nu_A^i-\nu)+kTz_i\log\left(\frac{\nu_A^i}{\nu}\right)\right\}+\log\left(\frac{N^1-N_A^i-N_B^i}{N_A^i}\right)\right]dN_A^i$$

$$+\left[-\frac{1}{kT}\left\{h_B^i+\tfrac{1}{2}z_ih(\nu_B^i-\nu)+kTz_i\log\left(\frac{\nu_B^i}{\nu}\right)\right\}+\log\left(\frac{N^1-N_A^i-N_B^i}{N_B^i}\right)\right]dN_B^i$$

$$+\left[\tfrac{1}{2}\log\left(\frac{\frac{1}{2}N^1}{\frac{1}{2}N^1-N_A^V}\right)+\tfrac{1}{2}\log\left(\frac{\frac{1}{2}N^1}{\frac{1}{2}N^1-N_B^V}\right)+\log\left(\frac{N^1}{N^1-N_A^i-N_B^i}\right)\right]dN^1=0$$

subject to the restrictions

$$\tfrac{1}{2}dN^1=dN_A^V-dN_A^i=dN_B^V-dN_B^i$$

Assuming N_A^V, N_A^i, N_B^V, $N_B^i \ll \frac{1}{2}N^1$ at the maximum, then $\frac{1}{2}N^1 \sim N$ and the conditions simplify to

$$\left[-\frac{1}{kT}\left\{h_A^V+\tfrac{1}{2}zh(\nu_A^V-\nu)+kTz\log\left(\frac{\nu_A^V}{\nu}\right)\right\}+\log\frac{N}{N_A^V}\right]dN_A^V$$

$$+\left[-\frac{1}{kT}\left\{h_B^V+\tfrac{1}{2}zh(\nu_B^V-\nu)+kTz\log\left(\frac{\nu_B^V}{\nu}\right)\right\}+\log\frac{N}{N_B^V}\right]dN_B^V$$

$$+ \left[- \frac{1}{kT} \left\{ h_A^i + \tfrac{1}{2} z_i h(\nu_A^i - \nu) + kTz_i \log\left(\frac{\nu_A^i}{\nu}\right) \right\} + \log \frac{2N}{N_A^i} \right] dN_A^i$$

$$+ \left[- \frac{1}{kT} \left\{ h_B^i + \tfrac{1}{2} z_i h(\nu_B^i - \nu) + kTz_i \log\left(\frac{\nu_B^i}{\nu}\right) \right\} + \log \frac{2N}{N_B^i} \right] dN_B^i = 0$$

subject to the restriction

$$dN_A^V - dN_A^i = dN_B^V - dN_B^i$$

One equilibrium value will be given by:

$$- \frac{1}{kT} \left[h_A^V + \tfrac{1}{2} zh(\nu_A^V - \nu) + kTz \log(\nu_A^V/\nu) \right] + \log(N/N_A^V) - \log \lambda = 0$$

Therefore

$$N_A^V/N = \frac{1}{\lambda} \exp - \frac{1}{kT} \left[h_A^V + \tfrac{1}{2} zh(\nu_A^V - \nu) + kTz \log(\nu_A^V/\nu) \right]$$

similarly

$$N_B^V/N = \lambda \exp - \frac{1}{kT} \left[h_B^V + \tfrac{1}{2} zh(\nu_B^V - \nu) + kTz \log(\nu_B^V/\nu) \right]$$

$$N_A^i/2N = \lambda \exp - \frac{1}{kT} \left[h_A^i + \tfrac{1}{2} z_i h(\nu_A^i - \nu) + kTz_i \log(\nu_A^i/\nu) \right]$$

$$N_B^i/2N = \frac{1}{\lambda} \exp - \frac{1}{kT} \left[h_B^i + \tfrac{1}{2} z_i h(\nu_B^i - \nu) + kTz_i \log(\nu_B^i/\nu) \right]$$

These expressions may be abbreviated to the following

1.02.9 $\quad N_A^V/N = \frac{1}{\lambda} \exp(-g_A^V/kT) \qquad N_B^V/N = \lambda \exp(-g_B^V/kT)$

$$N_A^i/2N = \lambda \exp(-g_A^i/kT) \qquad N_B^i/2N = \frac{1}{\lambda} \exp(-g_B^i/kT)$$

λ may be found by substituting 9 in 4 giving

1.02.10

$$\lambda^2 = \exp - \frac{1}{kT}(g_A^V - g_B^V) \left[\frac{1 + 2 \exp - \frac{1}{kT}(g_B^i - g_A^V)}{1 + 2 \exp - \frac{1}{kT}(g_A^i - g_B^V)}\right]$$

It is now convenient to express these results in terms of quasi chemical equilibrium constants, if we let

1.02.11

$$K_1 = \exp - \frac{1}{kT}(g_A^V + g_B^V), \qquad K_A = 2 \exp - \frac{1}{kT}(g_A^i - g_B^V),$$

$$K_B = 2 \exp - \frac{1}{kT}(g_B^i - g_A^V)$$

In terms of these 9 and 10 become

1.02.12

$$N_A^V/N = K_1^{\frac{1}{2}}\left(\frac{1 + K_A}{1 + K_B}\right)^{\frac{1}{2}}, \qquad N_B^V/N = K_1^{\frac{1}{2}}\left(\frac{1 + K_B}{1 + K_A}\right)^{\frac{1}{2}}$$

$$N_A^i/N = K_A K_1^{\frac{1}{2}}\left(\frac{1 + K_B}{1 + K_A}\right)^{\frac{1}{2}}, \qquad N_B^i/N = K_B K_1^{\frac{1}{2}}\left(\frac{1 + K_A}{1 + K_B}\right)^{\frac{1}{2}}$$

Three limiting cases of the expressions 12 are of interest.

1. If $K_A \ll 1$, $K_B \ll 1$ all the imperfections are A and B vacancies present in equal numbers - Schottky defects.

1.02.13

$$N_A^V/N = N_B^V/N = \exp - \frac{1}{2kT}(g_A^V + g_B^V)$$

or as a quasi chemical equilibrium

$$N_A^V . N_B^V / N^2 = \exp - \frac{1}{kT}(g_A^V + g_B^V)$$

2. If $K_A >> 1$, $K_B << 1$ all the imperfections are A vacancies and A interstitials in equal numbers - Cationic Frenkel defects.

1.02.14

$$N_A^V / N = N_A^i / N = \sqrt{2} \exp - \frac{1}{2kT}(g_A^V + g_A^i)$$

or as a quasi chemical equilibrium

$$N_A^V . N_A^i / N^2 = 2 \exp - \frac{1}{kT}(g_A^V + g_A^i)$$

3. If $K_A << 1$, $K_B >> 1$ Anionic Frenkel defects will predominate.

1.02.15

$$N_B^V / N = N_B^i / N = \sqrt{2} \exp - \frac{1}{2kT}(g_B^V + g_B^i).$$

Using lattice theory the following energies may be calculated:

E_A^V The energy required to take a positive ion from a lattice site to a position at rest at infinity.

E_B^V The energy required to take a negative ion from a lattice site to a position at rest at infinity.

E_A^i The energy required to take a positive ion from infinity to an interstitial position.

E_B^i The energy required to take a negative ion from infinity to an interstitial position.

E_c The lattice energy per ion pair.

If volume changes associated with defect creation are neglected the following relations hold

$$h_A^V + h_B^V = E_A^V + E_B^V - E_c$$

$$h_A^V + h_A^i = E_A^V + E_A^i , \qquad h_B^V + h_B^i = E_B^V + E_B^i$$

$$h_A^i - h_B^V = E_A^i - E_B^V + E_c , \qquad h_B^i - h_A^V = E_B^i - E_A^V + E_c$$

Table 1 summarises the results of lattice calculations for some alkali halides. If the dominant terms in the exponents of equations 11 are the h values (they will be more dominant at low temperatures) KBr, KCl and NaCl satisfy the limiting case 1 and should only exhibit Schottky defects. In AgBr $K_A >> 1$ and $K_B << 1$ experiment confirms in this case that cationic Frenkel defects predominate. There is no substantial experimental evidence to confirm the presence of Schottky defects in KCl but it is generally assumed the results of the lattice calculations are correct. For KCl at 1000°K neglecting vibrational terms $K_A = e^{-11.6 \times 1.14}$, $K_B = e^{-11.6 \times 3.01}$.

The energy $(g_A^V + g_B^V)$ in 13 is generally referred to as the Gibbs free energy of formation of a Schottky defect, however, it is clearly apparent that it does

TABLE 1

Results of theoretical calculations for the alkali halides

Material	(Ref.)	E_A^V	E_B^V	$E_A^V+E_B^V-E_c$	Δh_1	Δh_2
KCl	(1)	4.655	4.900	2.393		
KCl	(3)	4.54	4.63	2.01	1.13	1.18
NaCl	(3)	4.89	4.76	1.77	0.87	1.11

Material	(Ref.)	E_A^i	E_B^i	$E_A^V+E_A^i$	$E_B^V+E_B^i$	Interstitial (Δh_1)	(Δh_2)
KCl	(2)	-1.12	0.50	3.53	5.40	1.31	1.89
						0.87	0.44
NaCl	(2)	-2.26	1.62	2.63	6.38	1.26	2.16
						0.74	0.04
KBr	(2)	-0.97	1.51			1.30	2.21
						0.87	0.19

All values in the table are in eV. Where the Born Mayer Verwey and Born Mayer repulsive potentials were both used, the results for the former are put in the table. E_c for KCl was taken as 7.162 eV and for NaCl 7.88 eV. (Δh_1) and (Δh_2) are activation energies for the movement of cation and anion interstitials respectively. Two values are quoted for each, the upper for motion in the (100) direction, the lower for motion in the (111) direction (interstitialcy mechanism).

REFERENCES:

(1) Boswarva, 1965.

(2) Tharmalingam, 1964.

Tharmalingam, 1963.

(3) Guccione et al, 1959.

not include the configurational free energy arising from π in equation 7. The free energy may be split into enthalpy and entropy terms

1.02.16

$$g_A^V + g_B^V = h - T\,s$$

where

$$h = H_A^V + H_B^V , \qquad s = S_A^V + S_B^V$$

From equation 9

1.02.17

$$S_A^V = -kz \log\left(\frac{\nu_A^V}{\nu}\right) \qquad S_B^V = -kz \log\left(\frac{\nu_B^V}{\nu}\right)$$

1.02.18

$$H_A^V = h_A^V + \tfrac{1}{2}zh(\nu_A^V - \nu) \qquad H_B^V = h_B^V + \tfrac{1}{2}zh(\nu_B^V - \nu) .$$

Finally, for KCl

1.02.19

$$N_A^V . N_B^V = K_1 = e^{-(h-T\,s)/kT}$$

1.03 Doping of KCl with divalent impurities.

If it were possible to incorporate divalent cation impurities into an alkali halide lattice this would necessarily introduce defects. Consider a strontium chloride ion triplet being substitutionally inserted in a KCl lattice. One Cl^- ion and the Sr^{2+} ion could occupy an anion and cation site respectively. Two possibilities

remain for the extra Cl^- ion. It can enter an interstitial position, possibly adjacent to the Sr^{2+} ion to compensate its extra charge: or it can occupy an anion site, in this case it would necessarily be accompanied by a cation vacancy to retain the lattice structure of equal numbers of anion and cation sites. If the host lattice shows predominant Schottky disorder as in KCl the latter possibility is more likely.

If the defects in the two possible cases are ionised from their position next to the Sr^{2+} ion, the energies required to create them on the basis of the lattice calculations for KCl (Table 1) are

interstitial formation $E_B^i = 0.5$ eV

cation vacancy formation $(E_A^V+E_B^V-E_c)-E_B^V = -2.51$ eV.

Hence cation vacancies will be predominantly introduced since this requires much less energy. It is generally true that the imperfections introduced by impurities are of the same type as those predominantly present in the pure imperfect host crystal. Thus one of the conditions for Schottky defect formation, namely $K_B << 1$ is equivalent to the condition for the introduction of cation vacancies by impurities, i.e. $E_B^i > E_A^V - E_c$.

No lattice calculations have been made to determine the relative stability of an impurity with a cation

vacancy adjacent to it as compared to an interstitial anion.

Conductivity measurements indicate very strongly that impurities do introduce imperfections in the manner described. At sufficiently high temperatures these defects ionise and contribute to the mobility of the lattice ions.

1.04 Numbers of defects in KCl containing divalent impurities.

Let the number of divalent impurities be N_d and assume the defects introduced by these, namely cation vacancies, are readily ionised from the divalent impurities. Then using the same notation as in 1.02 and considering Schottky disorder only, the number of ion pairs AB is:-

1.04.1 $$N = N_A = N_B - 2N_d$$

and as before

1.04.2 $$\tfrac{1}{2}N^1 = N_a + N_A^V + N_d$$

1.04.3 $$\tfrac{1}{2}N^1 = N_B + N_B^V$$

Combining these equations

1.04.4 $$N_B^V = N_A^V - N_d$$

Let the partition function be $K(T)\Lambda(T)$ where $K(T)$ is the partition function for a crystal containing N_d ionised impurities but otherwise perfect. Then assuming no defect interactions, and leaving out the steps discussed in 1.02:

1.04.5

$$\Lambda(T) = \sum_{\substack{N_A^V, N_B^V \\ \text{subject to} \\ \text{restrictions} \\ 3 \text{ and } 2}} \frac{\frac{1}{2}N^1!}{N_A^V!(\frac{1}{2}N^1 - N_A^V)!} \cdot \frac{\frac{1}{2}N^1!}{N_B^V!(\frac{1}{2}N^1 - N_B^V)!} \exp - \frac{1}{kT}\left[(N_A^V - N_d)g_A^V + N_B^V g_B^V\right]$$

Then, as before, differentiating to find a maximum and using the condition for the dependent variables

1.04.6 $$dN_B^V = dN_A^V$$

1.04.7 $$N_A^V/N = \frac{1}{Q}\exp(-g_A^V/kT), \quad N_B^V/N = Q \exp(-g_B^V/kT)$$

Substituting in 4 to find Q

1.04.8 $$\frac{1}{Q} = \frac{N_d/N \pm \left[(N_d/N)^2 + 4 \exp(-1/kT)(g_A^V + g_B^V)\right]^{\frac{1}{2}}}{2 \exp(-g_A^V/kT)}$$

Taking the positive sign to avoid a negative result

1.04.9 $$N_A^V/N = \left[1 + (1 + 4K_1N^2/N_d^2)^{\frac{1}{2}}\right]N_d/2N$$

This result and the similar one for N_B^V/N could be more readily obtained using a quasi chemical equilibrium approach and the condition for equal numbers of lattice sites, e.g.

1.04.10 $$N_A^V . N_B^V/N^2 = K_1$$

1.04.4 $$N_B^V = N_A^V - N_D$$

Eliminating N_B^V between 4 and 10 yields 9 immediately, then N_B^V may be found immediately from 10.

1.04.11 $$N_B^V/N = K_1 N/N_A^V$$

1.05 Defect interactions.

The two treatments given in 1.04 and 1.03 ignore interactions among the defects. It is clearly possible in the case of doped crystals that there might be strong interaction between the doubly charged impurity ion and its accompanying vacancy. For large separations the defects can be regarded as point charges, cation and anion vacancies being virtual negative and positive charges respectively. In this case the interaction energy relative to infinite separation can be expressed as

$$\pm \frac{e^2}{\epsilon r}$$

where ϵ is the static dielectric constant of the crystal and r the separation.

When determining the interaction energy for small separations, lattice theory must be used to take into account the polarisation of individual ions. Bassani and Fumi (1954), using Born-Mayer lattice theory, have calculated the decrease in energy relative to infinite separation of a cation vacancy on the next nearest

neighbour position to a divalent cation, E_1. Similar calculations have been made by Tosi and Airoldi (1958) for the binding energy of a cation vacancy on the fourth nearest neighbour position from a divalent cation, E_2. The results of these calculations together with the binding energy of a cation and anion vacancy on nearest neighbour sites, E_3 (Tosi and Fumi, 1958) and on third nearest neighbour sites, E_4 (Tosi and Airoldi, 1958); are summarised in Table 2.

TABLE 2

Theoretical association energies for complexes

Lattice	E_3(eV)	E_4(eV)	Impurity	E_1(eV)	E_2(eV)
NaCl	0.6	0.28	$CdCl_2$	0.38	
			$CaCl_2$	0.38	
			$SrCl_2$	0.45	0.41
KCl	0.72	0.38	$CdCl_2$	0.32	
			$CaCl_2$	0.32	
			$SrCl_2$	0.39	0.49

The surprising fact that $E_2 > E_1$ for $KCl/SrCl_2$ arises from the strong polarisation of the Cl^- ion lying between

the Sr^{2+} ion and its cation vacancy. This particular result is confirmed qualitatively by e.p.r. measurements on Mn^{2+} in NaCl and KCl (Watkins, 1959; Watkins and Walker, 1956). These experiments show a similar inversion of E_1 and E_2 in going from NaCl to KCl.

1.06 Calculation of defect concentrations in an impure crystal with association.

Considering only divalent cation doping of a crystal showing predominantly Schottky defects. Let the mole fractions of cation and anion vacancies be x_1 and x_2 respectively. Let the mole fraction of impurities and complexes be c and x_k respectively. The complex is to be regarded as a tightly bound impurity vacancy pair. On the basis of 1.05 the ground state of the complex can be taken as having an association energy E_1 and the first excited state, an energy E_2. Applying the mass action law to the quasi chemical equilibrium,

unassociated impurity ion	+	unassociated vacancy	$\rightleftharpoons$	vacancy complex
$c-x_k$		x_1		x_k

1.06.1 $$K_2 = \frac{x_k}{x_1(c-x_k)}$$

In addition the condition derived in 1.04 will hold

1.06.2 $$K_1 = x_1 x_2$$

Since the lattice configuration must be maintained there will be equal numbers of cation and anion sites, hence

1.06.3 $$x_1 - x_2 = c - x_k$$

The number of cation-anion vacancy pairs may be treated on the same basis as the impurity complexes. If their concentration at equilibrium is x_p then

1.06.4 $$K_3 = \frac{x_p}{x_1 x_2}$$

The presence of vacancy pairs does not affect the condition 3; hence they will not affect the concentrations of unassociated vacancies at equilibrium. Vacancy pairs will not contribute to conductivity since they are a neutral species. From equation 1

$$x_k = \frac{x_1 K_2 c}{1+x_1 K_2}$$

Combining this with 2,

1.06.5 $$x_k = \frac{K_1 K_2 c}{x_2+K_1 K_2}$$

Eliminating x_1 using 5 and 2 in equation 3

$$\frac{K_1}{x_2} - x_2 = c - \frac{K_1 K_2 c}{x_2 + K_1 K_2}$$

$$\frac{K_1}{x_2} - x_2 = \frac{x_2 c}{x_2 + K_1 K_2}$$

1.06.6 $$(K_1 - x_2^2)(x_2 + K_1 K_2) = x_2^2 c$$

1.06.7 $$x_2^3 + x_2^2 (c + K_1 K_2) - x_2 K_1 - K_2 K_1^2 = 0$$

This cubic may be solved for x_2 in terms of K_1 and K_2. The corresponding value of x_1 is obtained by substituting x_2 in equation 2.

The equilibrium constants K_2 and K_3 could be interpreted on the basis of statistical thermodynamics but with present knowledge could not be evaluated. K_2 will be of the general form (Lidiard, 1957)

1.06.8 $$K_2 = \sum_s z_s e^{-\zeta_s / kT}$$

where z_s and $-\zeta_s$ are the number of orientations and the Gibbs free energy of association (although $+\zeta_s$ is referred to in most of the literature as the association energy) respectively for a complex in its s^{th} state. In a KCl lattice $z_o = 12$, $z_1 = 6$. The entropy of association is usually assumed to be zero since it cannot be determined accurately and is probably small.

If the vacancy is to be regarded as associated only when it is in the second nearest neighbour position to the Sr^{2+} then

1.06.9 $$K_2 = 12e^{\xi/kT}$$

This is the expression for $K_2(T)$ first given by Stasiw and Teltow (1947). On the basis of the values of E_1 and E_2 this assumption is not valid; according to the calculations the first two terms would be

1.06.10 $$K_2 = 12e^{0.39/kT} + 6e^{0.49/kT}$$

Deviations from ideality of the mixtures of component defects may be taken into account by introducing activity coefficients. In equations 1 and 2, x_1, x_2 and c are replaced by x_1f_1, x_2f_2, and cf_i. The activity coefficients may be derived using the Debye-Hückel theory developed for dilute solutions (Lidiard, 1954,a). The results are

1.06.11 $$\text{Log } f_1 = \log f_2 = \log f_i = -\frac{q^2}{2\epsilon kT}\frac{\chi}{1+\chi R}$$

where χ the Debye-Hückel screening constant is given by

1.06.12 $$\chi^2 = \frac{8\pi q^2 x_1}{V\epsilon kT}$$

R is the separation below which a vacancy impurity pair are to be regarded as complexed, q the charge on the ion, V the volume per molecule of the pure salt and ϵ the dielectric constant of the crystal.

Lidiard has examined the solution of equations 1, 2, 3, 11 and 12 for a model containing a high impurity concentration such that $x_2 << x_1$. In addition he assumed coulombic interaction at all separations and only ground state complexes, hence

1.06.13 $$\zeta = \frac{e^2}{\sqrt{2}\epsilon a} \equiv kT_o$$

where a is the undisturbed anion-cation separation. The solution obtained in terms of the degree of association $p = x_k/c$ is

1.06.14 $$\frac{p}{(1-p)^2} = 12c \exp\left[\frac{T_o}{T} - \frac{2(2\pi\sqrt{2})^{\frac{1}{2}}(T_o/T)^{3/2}[(1-p)c]^{\frac{1}{2}}}{1+4(\pi\sqrt{2})^{\frac{1}{2}}[(1-p)cT_o/T]^{\frac{1}{2}}}\right]$$

For a given reduced temperature T/T_o, the expression gives a slower rise of p with concentration and a well reduced limiting value at high concentrations. It also indicates a more rapid decay of p with increasing temperature.

Allnatt and Cohen (1964) have attempted to take into account the long range coulombic interactions in a more sophisticated way, by means of cluster expansions of the partition function. The technique is similar to that first used by Mayer to obtain virial coefficients for a non-ideal gas. For coulombic interactions, however, the convergence of terms in the virial expansion is very slow.

Allnatt and Cohen conclude that application of the Debye-Hückel theory at temperatures below 500°C and concentrations greater than 10^{-4} mole fraction should be viewed with caution. They cannot, however, estimate the accuracy of the simple theory in these regions. This limitation excludes application of their theory to most conductivity work.

1.07 Statistical theory of conductivity in a KCl lattice.

For a crystal in which Schottky defects predominate the ionic mobility arises from ions jumping into adjacent vacancies on their own sublattice. Regarding the vacancy as the mobile unit, the probability per unit time w that it jumps in the (100) direction may be obtained from statistical mechanics (Wert, 1950).

1.07.1 $$w = 4 \nu \exp(-\Delta g/kT)$$

Where ν is the frequency with which the next nearest neighbour ions to the vacancy vibrate against it and Δg is the free energy required to raise one of these ions from its equilibrium position to the energy col in the direction of the vacancy. The factor 4 arises from there being 4 ions which can jump into the vacancy enabling it to move a distance a (the anion-cation separation) in the (100) direction.

For a negative ion vacancy in an electric field E along the (100) direction, the height of the col will be reduced by an amount $\frac{1}{2}eaE$. The col will be increased by the same amount in the opposite direction. Thus the probability per unit time that the anion vacancy jumps in the direction of the field will be increased to

1.07.2 $$w' = 4\nu \exp - \frac{1}{kT}(\Delta g - \tfrac{1}{2}eaE)$$

The probability with which the vacancy jumps against the field will be reduced to

1.07.3 $$w'' = 4\nu \exp - \frac{1}{kT}(\Delta g + \tfrac{1}{2}eaE)$$

Thus the net probability with which such vacancies jump in the direction of the field will be

1.07.4

$$\Delta w = w' - w'' = 4\nu \exp(-\Delta g/kT)[\exp(eaE/2kT) - \exp(-eaE/2kT)]$$

1.07.5 $$\Delta w = 2w \sinh(eaE/2kT)$$

The mobility μ or the velocity per unit field with which the vacancy moves in the direction of the field will be

1.07.6 $$\mu = \Delta w\, a/E$$

For the fields used in practice $Eae \ll kT$ thus

1.07.7 $$\Delta w \sim 2w \cdot \tfrac{1}{2}\left[1 + \frac{eaE}{2kT} - 1 + \frac{eaE}{2kT}\right]$$

1.07.8 $\Delta w = weaE/kT$

Therefore

1.07.9 $\mu = wea^2/kT$

The same result would be obtained for fields applied along different axes of the crystal, due to the cubic symmetry of the KCl lattice.

The electrical conductivity arising from the motion of the anion vacancies will be

1.07.10 $\sigma_2 = Nx_2e\mu = \frac{4Nx_2e^2a^2}{kT} \nu \exp(-\Delta g/kT)$

Where N is the number of K^+ ions per unit volume and x_2 is the mole fraction of anion vacancies. Using the subscript 1 to denote cation vacancy properties and 2 to denote the anion vacancy parameters, the total conductivity for both carriers will be

$$\sigma = \sigma_1 + \sigma_2$$

whence

1.07.11 $\sigma = N(x_1e\mu_1 + x_2e\mu_2)$

1.07.12 $\sigma = \frac{4Na^2e^2}{kT}[x_1\nu_1\exp(-\Delta g_1/kT) + x_2\nu_2\exp(-\Delta g_2/kT)]$

This result may be combined with the expressions for x_1 and x_2 found in 1.04 (neglecting association). Two limiting cases of 1.04.9 and 1.04.11 are of special interest.

1) $x_1 \sim x_2 \gg c$, i.e. when the impurity mole fraction is much less than that of the thermally produced defects. This will be true in pure crystals at high temperatures. In this case 1.04.9 and 1.04.11 reduce to 1.02.13. Using the notation of 1.02.19

1.07.13

$$\sigma = \frac{4Na^2e^2}{kT}\left[\nu_1 \exp - \frac{1}{kT}(\tfrac{1}{2}h - \tfrac{1}{2}Ts + \Delta g_1) + \nu_2 \exp - \frac{1}{kT}(\tfrac{1}{2}h - \tfrac{1}{2}Ts + \Delta g_2)\right]$$

Writing Δg_1 and Δg_2 in terms of entropies and enthalpies

$$\Delta g_1 = \Delta h_1 - T\,\Delta s_1$$

$$\Delta g_2 = \Delta h_2 - T\,\Delta s_2 ,$$

1.07.14

$$\sigma = \frac{4Na^2e^2}{kT} \exp(s/2k)\left[\nu_1 \exp - \frac{1}{kT}(\tfrac{1}{2}h + \Delta h_1 - T\,\Delta s_1) + \nu_2 \exp - \frac{1}{kT}(\tfrac{1}{2}h + \Delta h_2 - T\,\Delta s_2)\right]$$

Now if $\nu_2 \sim \nu_1 = \nu$, $\Delta s_1 \sim \Delta s_2 = \Delta s$ and $\Delta h_2 \sim \Delta h_1 = \Delta h$

1.07.15

$$\sigma = \frac{8\nu a^2e^2N}{kT} \exp \frac{1}{2k}(s + 2\Delta s) \exp - \frac{1}{kT}(\tfrac{1}{2}h + \Delta h)$$

and a graph of log σT against $1/T$ will be a straight line of slope $-(\frac{1}{2}h + \Delta h)/k$.

2) $x_1 \sim c \gg x_2$. In general this will be satisfied at low temperatures, when the impurity content is much

higher than the thermal defect concentration and

1.07.16

$$\sigma = \frac{4Na^2e^2}{kT} [\nu_1 c \exp(-\Delta g_1/kT)]$$

1.07.17

$$\sigma = \frac{4Na^2e^2 \nu_1 c}{kT} \exp(\Delta s_1/k)\exp(-\Delta h_1/kT)$$

A plot of log σT against $1/T$ will be a straight line of slope $-\Delta h_1/k$.

On the basis of these two results a log σT versus $1/T$ plot will comprise two straight lines linked by a region, "the knee", where neither approximation holds. This is roughly true for the experimental data. The slope of the high temperature line $-\frac{1}{k}(\Delta h + \frac{1}{2}h)$ is the greater. The conductivity is said to be "intrinsic" in this region, since the position and slope of the line will be independent of impurity content. The conductivity in the low temperature region is referred to as "extrinsic", because the position of the straight line plot will be a function of impurity content.

The full expression for conductivity using the simple Stasiw and Teltow association theory may be obtained by substituting x_1 and x_2 from 1.06 into 12. Clearly impurity

vacancy association will only affect the extrinsic conductivity. To estimate the effect an expression will be derived for the conductivity concentration isotherm when $x_1 >> x_2$ is satisfied. Using the simple association theory

1.07.18 $$x_1 \sim c - x_k$$

1.07.19 $$\frac{x_k}{x_1(c-x_k)} = K_2$$

eliminating x_k between 18 and 19

$$c = K_2 x_1^2 + x_1$$

A short cut to the isotherm can then be taken in the following way:

1.07.20
$$c = K_2 x_1^2 \left(\frac{N^2e^2\mu_1^2}{N^2e^2\mu_1^2}\right) + x_1\left(\frac{Ne\mu_1}{Ne\mu_1}\right)$$

But from 17 and 11 $\sigma = Ne\mu_1 x_1$

1.07.21 $$c = \frac{K_2\sigma^2}{N^2e^2\mu_1^2} + \frac{\sigma}{Ne\mu_1}$$

Equation 21 shows that the isotherms are parabolic. The effect of association on the log σT versus $1/T$ plot will be to make the extrinsic region slightly concave towards the $1/T$ axis.

It is convenient to express the simple association theory of conductance, without approximations, in terms of more readily available experimental parameters. These are the mobility ratio $\phi = \mu_2/\mu_1$, $y = x_1/x_o$ and the intrinsic conductivity $\sigma_o = Nex_o(\mu_1 + \mu_2)$. Then for Schottky disorder, as before

1.07.22 $$K_1 = x_1 x_2 = x_o^2$$

1.07.23 $$x_1 - x_2 = c - x_k$$

1.07.24 $$K_2 = \frac{x_k}{x_1(c-x_k)}$$

In general

$$\sigma = Ne(x_1\mu_1 + x_2\mu_2)$$

$$(\mu_1 + \mu_2)\frac{\sigma}{\sigma_o} = \mu_1(x_1/x_o) + \mu_2(x_2/x_o)$$

1.07.25 $$\frac{\sigma}{\sigma_o} = \frac{y + \phi/y}{1 + \phi}$$

solving for y

1.07.26 $$y = \tfrac{1}{2}\frac{\sigma}{\sigma_o}(1 + \phi) + \left[\left[\tfrac{1}{2}\frac{\sigma}{\sigma_o}(1 + \phi)\right]^2 - \phi\right]^{\frac{1}{2}}$$

Using the relation 1.06.6 obtained by combining 2, 3 and 1

$$x_2^2 c = (K_1 - x_2^2)(x_2 + K_1 K_2)$$

and expressing it in terms of the parameters defined above

$$c = (y^2 - 1)(x_2 + K_1 K_2)$$

$$c = (y - \tfrac{1}{y})(x_o + yK_2 K_1^{\frac{1}{2}} x_o)$$

1.07.27

$$\frac{c}{x_o} = (y - \tfrac{1}{y})(1 + yK_2 K_1^{\frac{1}{2}})$$

When interpreting experiments ϕ is obtained first in the best possible way, this generally involves approximations. Then y is derived from 26 using direct measurements of σ and σ_o. By plotting $\phi/(y - \frac{1}{y})$ in equation 27 against y, where c is the analytical concentration of impurities, a straight line should result with intercept x_o. The slope of this line yields K_2. From equation 25

$$\sigma = Ne\mu_1 x_o (y + \phi/y)$$

Using the x_o and y values, estimates of μ_1 as a function of temperature may be made. All the conductance parameters are obtainable from these results. This treatment was first given by Stasiw and Teltow (1947) and later reviewed by Lidiard (1957).

Lidiard (1957) has included the effect of long range coulombic interactions upon mobility. He considered a model which satisfies the condition $x_1 >> x_2$ and derived $\dot{p}$ using the Debye-Hückel association theory mentioned in 1.06. The mobility was then modified according to Onsager's theory developed for ions of a finite size. The final expression is

1.07.22

$$\sigma = \left(\frac{\mu_1 e}{2a^3}\right) c(1-p)\left[1 - \frac{2(2\pi\sqrt{2})^{\frac{1}{2}}}{3(\sqrt{2}+1)} \cdot \frac{c^{\frac{1}{2}}(1-p)^{\frac{1}{2}}(T_0/T)^{3/2}}{(1+2\chi a)(\sqrt{2}+2\chi a)}\right]$$

where $2\chi a = 4(\pi\sqrt{2})^{\frac{1}{2}} c^{\frac{1}{2}}(1-p)^{\frac{1}{2}}(T_0/T)^{\frac{1}{2}}$

It must be emphasised that this expression is derived assuming coulombic interactions at all ranges down to nearest neighbour separation. Diagrammatic plots of $(c/\alpha\sigma)$ versus $\alpha\sigma$, where $\alpha = 2a^3/\mu_1 e = 1/\mu_1 Ne$ (a is the anion-cation separation), are shown in Fig.1. The horizontal line (1) $c/\alpha\sigma = 1$ will be obtained if there is no association (equation 17). A straight line (2) of intercept 1 and gradient K_2 represents the result expected on the basis of the Stasiw and Teltow association theory (equation 21). The curve (3) represents equation 22.

The mobility μ_s of a species s is related to its self diffusion coefficient D_s by the Nernst-Einstein

FIG 1

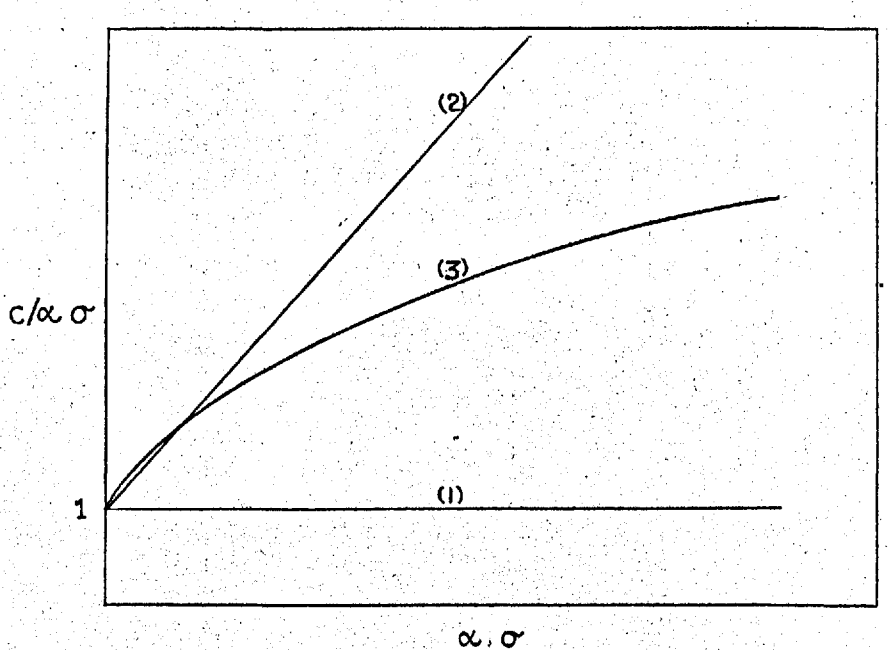

relationship

1.07.23 $$\mu_s/D_s = q_s/kT$$

where q_s is the charge on s. In terms of the conductance σ_s and the concentration N_s this relation may be rewritten

1.07.24 $$\sigma_s/D_s = N_s q_s^2/kT$$

D_s is related to the tracer diffusion coefficient D_{Ts} by

$$D_{Ts} = f_s D_s$$

Where f_s is the correlation factor arising from the distinguishability of tracer ions; its value depends upon the jump mechanism and the nature of the lattice. For tracer diffusion via vacancies in a KCl lattice $f_s = 0.7815$ (Compaan and Haven, 1956). The above relation does not hold in the presence of vacancy pairs which contribute to diffusion but not to electrical conductivity.

From studies of the temperature and concentration dependence of the diffusion coefficient for divalent impurities substitutionally incorporated in an alkali halide lattice; it is possible to obtain association energies for impurity vacancy complexes. This approach is reviewed by Lidiard (1957).

1.08 Previous experimental work.

A comprehensive summary of early experimental results may be found in the theses of Allnatt (1959) and Maycock (1962). An excellent review at the time is that given by Lidiard (1957) who reexamined almost all the previous results in the field of ionic conductivity. Table 3 summarises activation energies from KCl conductivity plots. Most of these were obtained by merely drawing tangents to a plot of log σT or log σ against $1/T$. The parameters found in the only comprehensive analyses of the conductivity of alkali halide single crystals are given in Table 4.

Etzel and Patterson (1958) identified absorption bands at 185 mμ in NaCl and 204 mμ in KCl as arising from OH^- ions. They further showed that when $CaCl_2$ was added to NaCl or $SrCl_2$ to KCl the absorption band was absent. The presence of the OH stretching frequency in the infra red of the doped crystals indicated that hydroxyl groups were still in the crystal despite the absence of the U.V. absorption. Doping of NaCl with $CdCl_2$ did not affect the 185 mμ band. These results were interpreted as a destruction of the OH^- band in the U.V. by the divalent cations Sr^{2+} and Ca^{2+} with the possible formation of $CaOH^+$ or $Ca(OH)_2$. If this is so the presence of OH^- should affect the conductivity of crystals doped with

TABLE 3

Activation energies for conductance and diffusion in KCl

	Activation Energy (eV)	
(1) Conductance	Extrinsic	Intrinsic
Phipps and Partridge (1929)	0.99	2.02
Lehfeldt (1933)	0.89	2.06
Brennecke (1940)		1.99
Kelting and Witt (1949) ($+CaCl_2$)	0.79	
" " " ($+SrCl_2$)	0.86	
" " " ($+BaCl_2$)	0.94	
Wagner and Hantelmann (1950) (pellets + $SrCl_2$)	0.78	1.82
Aschner (1954) (and diffusion)	0.68	
Kobayashi and Tomiki (1960)	0.75	
Gründig (1960) ($+CaCl_2$)	0.77	
Biermann (1960)	0.79	
Pierce (1961) ($+SrCl_2$)	0.76	
Kanzaki et al. (1962)	0.83	
Gründig (1965)		2.01-1.79
Dreyfus and Nowick (1962) (average of literature values)	0.84	1.95
(2) Anion Diffusion		
Laurent and Bernard (1957)		2.0
Ewles and Jain (1957)	1.86	
Barr et al. (1960)		1.9 - 2.6
(3) Cation Diffusion		
Armilear and Chemla (1956)		1.74
Laurent and Bernard (1957)		1.5

Sr^{2+} or Ca^{2+}. Later work (Patterson, 1962) showed a sharp increase of the 204 mμ band in KCl crystals drawn in the presence of an $O_2 + H_2O$ atmosphere. The intensity of the band increased in proportion to the time the melt was exposed to this atmosphere. This increase was ascribed to a hydroxyl-rich layer on the melt created by continuous reaction between the salt and the moist oxygen.

A series of qualitative observations have been made by Lüty (1963) relating to simultaneous measurements of conductivity and optical absorption. He found that KCl crystals grown from melts with the composition 2×10^{-3} mole fraction KOH and 1×10^{-3} $CaCl_2$ had a lower extrinsic conductivity than those grown without the addition of KOH. After treating the doubly doped conductivity specimens with chlorine at 700°C and just under an atmosphere pressure, the conductivity rose by a factor of about 10. This corresponded to a value similar to that for the crystals singly doped with 1×10^{-3} $CaCl_2$ and grown in air. The chlorination also diminished the OH stretch absorption in the infra red. From analytical and optical measurements Lüty deduced that Ca^{2+} and OH^- combined in the ratio 1:2 probably forming $Ca(OH)_2$. If this species occupies two lattice sites, as suggested by Lüty on the basis of its size, the Ca^{2+} would no longer contribute to

the extrinsic conductivity. His argument that the reaction in the solid would release a vacancy pair which could contribute to diffusion is incorrect. Any excess vacancy pairs released by such a reaction would merely be destroyed by diffusion to a surface. Their concentration is only governed by the relation 1.06.4. Lüty concludes that all crystals grown in air show a lower extrinsic conductivity than corresponds to their true cation impurity content. In his air-grown crystals, using analytically pure material, later chlorination showed that only between 3 and 30% of the impurities contributed to the conductivity. Redfern and Pratt (1964) have attempted to dope NaCl with anions using Na_2SO_4 and Na_2O_2. The only effect, a depression of the extrinsic conductivity, suggests that the result of doping has been to introduce OH^- or O^{2-} and reduce the effective cation content.

Although no significance is generally attached to it, Etzel and Patterson (1958) found that $CaCl_2$ additions to NaCl destroyed a fluorescent centre present in crystals grown in oxygen. The fluorescence was later attributed to an O_2^- molecule ion located on an anion site (Känzig and Cohen, 1959; Rolfe et al., 1961). The O_2^- fluorescence is also present in KBr and KCl crystals grown in oxygen. Additions of $CdCl_2$ to NaCl did not affect the

O_2^- fluorescence.

In view of the above findings, conductance data aimed at determining association energies for impurity vacancy complexes should be viewed with caution. The presence of OH^- could have two obvious effects. It might reduce the active concentration of doping agents, e.g. Sr^{2+} and Ca^{2+} below the analytical concentration. In addition spurious temperature dependence of conductivity could arise from dissociation of impurity - OH^- complexes.

Gründig (1963) obtained extremely pure hydroxide free crystals by the zone refining of KCl and KBr in graphite crucibles. Both the crucible and starting material were chlorinated at high temperatures to destroy OH^- and remove impurities as volatile chlorides. Gründig (1960) has estimated values for the association energies of calcium-vacancy complexes. In KCl the association energy was 0.52 ± 0.04 eV (cf. Table 2) and in KBr 0.56 ± 0.04 eV. These values are obtained as twice the difference of the high and low temperature slopes of a plot of log σ versus $1/T$ in the extrinsic region. Gründig justifies this procedure for association energies of ~ 0.5 eV, his doping levels of $3 - 50 \times 10^{-5}$ mole fraction and when the low-temperature tangent is taken below about $100^{\circ}C$. However, considerable precipitation is probably occurring at this

temperature and the method is likely to overestimate association energies. In addition plots of log σT versus $1/T$ should have been used to conform with the conductivity theory in 1.07. A rough estimate of the correction is given below.

$$\frac{d(\log \sigma T)}{d(1/T)} = \frac{d(\log \sigma)}{d(1/T)} + \frac{d(\log T)}{d(1/T)}$$

By plotting log T against $1/T$ the correction term is $\sim -0.04 \times 2$ which would further reduce the association energies, and not inconsiderably.

In a more recent paper Gründig (1965) has demonstrated the necessity of considering both anion and cation contributions to conductance in the intrinsic regions of KCl and KBr. For a very pure crystal of KCl the tangent to a plot of log σ versus $1/T$ at the highest temperature in the intrinsic region has a slope 2.01 ± 0.03 eV whereas just above the knee the slope is 1.79 ± 0.03 eV. For KBr the high temperature slope is 2.06 ± 0.03 eV, the low temperature gradient is 1.67 ± 0.03 eV. Clearly the intrinsic region must be represented as a sum of two exponentials, using the full expression 1.07.13. Gründig assumes that one slope represents a temperature region where anions dominate, the other a region where cations dominate. Then from 1.07.14 the difference in the slopes for KCl,

0.22 eV = $|\Delta h_1 - \Delta h_2|$, similarly for KBr $|\Delta h_1 - \Delta h_2|$ = 0.39 eV. In this case Gründig points out that plotting log σ rather than log σT does not greatly influence the result. This is due to the smaller temperature difference between the points at which the slopes are taken. The curvature in the intrinsic region and its interpretation have been noted before (Allnatt and Jacobs, 1962).

Relative contributions of anion conductance σ_2 and cation conductance σ_1 are usually expressed in terms of transference numbers. The cation transference number t_1 and that of the anions t_2 being defined as

1.08.1

$$t_1 = \frac{\sigma_1}{\sigma_1+\sigma_2} = 1 - t_2 ,$$

the total conductance being $\sigma = \sigma_1 + \sigma_2$.

Several direct measurements of t_1 in KCl have been made by electrolysing crystals and pellets. A summary of previous results as a function of temperature is given by Allnatt and Jacobs (1962), they include transference numbers obtained by a more complete analysis of the curvature in the intrinsic region. The most unambiguous results are those of Kerkhoff (1951), carried out on single crystals. He accompanied the transference number determinations with conductivity measurements before and after

electrolysis. Only in this way can it be shown with certainty that values are significant in that they are determined in the intrinsic region. Kerkhoff's experimental procedure involved using $BaCl_2$ protective cylinders which might have diffused into the KCl increasing t_1. In fact the temperature at which the knee occurred rose considerably as a result of electrolysis. The most recent determination (Haven, 1964) yielded a value of $t_1 = 0.46$ at 600°C in comparison with Kerkhoff's value of 0.71 at the same temperature. Haven gives very little detail except to say the measurement was in the intrinsic region and apparently no aliovalent protective crystals were used; for this reason it is probably a more reliable value. Qualitatively these results are valuable. They show that $t_1 = 1$ in the extrinsic region, confirming an aspect of the interpretation of conductance data. In addition Faraday's law is obeyed indicating that the conduction is purely ionic.

Etzel and Maurer (1950) interpreted their conductivity data for the system NaCl + $CdCl_2$ by means of a least squares fit to equation 1.07.21. From the coefficients of σ and σ^2 they were able to determine the cation vacancy mobility μ_1 and the association constant K_2 as functions

of temperature. These yielded $\Delta h_1 = 0.85$ eV and ζ (for the Cd-vacancy complex) = 0.24 eV at 403°C and 0.25 eV at 256°C. Lidiard (1957) re-interpreted Etzel and Maurer's data using 1.07.22. This yielded a better fit to the experimental results with an association energy of 0.34 eV. The improved fit suggests that long range coulombic interactions may be affecting the conductivity.

Rolfe (1964) has carried out a complete analysis of the conductance of KBr doped with K_2CO_3 and $CaCl_2$. The K_2CO_3 was found to be sufficiently soluble at high temperatures to produce anionic conductance in the extrinsic region. No attempt was made to free the calcium doped crystals of OH^-. The results were treated using the Stasiw and Teltow association theory outlined in 1.07. The mobility ratio ϕ was found by comparing the temperature dependence of the anionic and cationic extrinsic regions neglecting association. At high temperatures it was assumed association effects were negligible. The log ϕ versus 1/T plot was extrapolated to lower temperatures providing the necessary range of values. The parameters quoted by Rolfe are included in Table 4. By plotting log K_2 against 1/T Rolfe managed to obtain ζ in terms of an enthalpy 0.46 eV and an entropy 1.51×10^{-4} eV/deg.

This value is lower than that obtained by Gründig suggesting the criticisms of his treatment are correct. In fact, with the estimated correction, Gründig's value 0.48 eV is in excellent agreement with that of Rolfe. Rolfe concluded his results did not justify an attempt to interpret them using the more elaborate association theory including long range coulombic interactions.

TABLE 4

Experimental conductivity parameters

Material	h(eV)	$s(10^{-3}$ eV per deg.)	Δh_1(eV)	$\Delta s_1(10^{-3}$ eV per deg.)	Δh_2(eV)	Δs_2 (10^{-3} eV per deg.)
KBr + K_2CO_3 KBr + $CaBr_2$ (Rolfe,1964)	2.53	0.854	0.665		0.87	
KCl + $SrCl_2$ (Allnatt and Jacobs, 1962)	2.30	0.69	0.75	0.114	2.45	1.75

A similar treatment of data for the system KCl+$SrCl_2$ has been carried out by Allnatt and Jacobs (1962) (Table 4) and Jacobs and Maycock (1963,a). The mobility ratio ϕ was determined from a plot of log σT against 1/T. A tangent to this plot was drawn just above the knee and assumed to

represent the cation contribution. This procedure is not legitimate since the curvature in the intrinsic region is slight. It is possibly for this reason that the values of $\mathcal{J}$ which were obtained decreased with increasing temperature from 0.43 at 300°K to 0.2 eV at 900°K. Hydroxide impurity might have been an additional factor affecting this result. The KCl was treated at 500°C with HCl prior to crystal growth. This might not have removed all the hydroxide for although the crystals showed no 204 mμ absorption the Ca-OH complexes apparently do not absorb in this region. Additional evidence for the presence of OH^- comes from the plot of σ against c. The isotherms of both Maycock and Allnatt cut the concentration axis above the origin, suggesting some of the Sr^{2+} was complexed.

A combination of DC conductivity and dielectric loss measurements have been made on a quenched crystal of KCl doped with $CaCl_2$ annealing at 144°C (Nimomiya, 1960). The number of vacancy pairs was found to be proportional to the number of free vacancies raised to the power 1.92. A value of 2 would be expected on a kinetic basis since the number of free calcium ions is equal to the number of free vacancies. This is true in the presence of OH^- or precipitate.

The effect of pressure up to 9000 Kg/cm^2 upon the conductivity of $KCl+SrCl_2$ and $NaCl + CaCl_2$ has been studied by Pierce (1961). The activation enthalpy for motion of cation vacancies Δh_1 may be regarded as comprising an internal energy U_1 and a $P\Delta V_1$ term. The pressure dependence enables an estimate to be made of the activation volume ΔV_1. For cation vacancies in KCl $\Delta V_1 = 7.0$ cc/mole, in NaCl $\Delta V_1 = 7.7$ cc/mole. Pierce points out that there is an uncertainty in the interpretation since the pressure dependence of the association energy is not known.

Dreyfus and Nowick (1962) have replotted conductivity data for KCl and NaCl from a number of sources. They obtain the best values for the slopes in the intrinsic and high temperature extrinsic regions of a log σT versus $1/T$ plot (Table 3). Thus their values of Δh_1 are obtained neglecting association which can be important at the highest temperatures in the extrinsic region. Their interpretation of the intrinsic region ignores the possibility of anion conductance.

An excess conductivity of KCl and KBr subjected to plastic deformation (Camagni and Manara, 1965) has been interpreted as possibly arising from interstitial anions. The extremely low activation energy for motion, 0.35 eV

in both salts is compared with Tharmalingam's calculated energies for the interstitialcy mechanism (Table 1). This mechanism involves displacement of a lattice ion by an interstitial ion.

Morrison et al. (1965) have conducted anion diffusion experiments on NaCl using an isotopic exchange method. They conclude that vacancy pairs contribute to diffusion in both the intrinsic and extrinsic regions. An analysis of the intrinsic region, as defined by conductance measurements, was made in terms of two exponentials. One of the terms, the diffusion coefficient arising from anion vacancies was 1.1 $e^{-1.92/kT} cm^2/sec.$, the other, for vacancy pair diffusion, was 363 $e^{-2.37/kT} cm^2/sec.$ Morrison points out that the presence of vacancy pair diffusion has obscured the correct interpretation of most of the previous experimental data, including that for KCl (Barr et al., 1960). According to the Nernst-Einstein relation (1.07.24) the activation energy for diffusion by anions in the intrinsic region is $\Delta h_2 + \frac{1}{2}h$ (1.07.15). Using Etzel and Maurer's (1950) result for h from conductance measurements, Morrison obtains a value of 0.9 eV for Δh_2. This may be compared with the calculated value of 1.11 eV (Table 1). 2.37 eV is also in fair agreement with the calculated value of the activation enthalpy for an

anion jumping into a pair, 2.54 eV and a cation jumping into a pair, 2.73 eV (Tharmalingam and Lidiard, 1961). A similar analysis of diffusion data in conjunction with conductance measurements would enable the Nernst-Einstein relation to be tested for KCl. Laurent and Bernard (1957) attempted to measure cation diffusion coefficients by the same technique but there are experimental difficulties and their value (Table 3) is extremely low.

Values for the impurity vacancy association energy may be derived from the concentration and temperature dependence of the diffusion coefficient for the impurity (Lidiard, 1957). Keneshea and Fredericks (1965) have studied the diffusion of Cd^{2+} in KCl using tracer techniques. They obtain a value of 0.51 eV for the cadmium-vacancy association energy, this is somewhat higher than the calculated value of 0.32 (Table 2). The association energy for the Pb^{2+}-vacancy complex, found using the same method (Keneshea and Fredericks, 1963) varied between 0.58 eV at 373°C and 0.41 eV at 500°C.

1.09 Polarization phenomena.

When a D.C. electric field is applied to a crystal, a number of charge separation processes can occur in the time interval before the inertia of the ions allows them to flow through the lattice giving rise to the conductance

described in the last section. At even longer times the possibility of a macroscopic polarisation arises if the charge carriers, namely the vacancies and ions, are unable to discharge at the electrodes. This latter process is called space charge polarisation. Individual mechanisms can be identified by studying the time dependence of the current resulting from application of a D.C. field (e.g. Dreyfus, 1961). Alternatively, A.C. fields may be used when the admittance of the crystal is studied as a function of frequency. Since an extensive review of early work on D.C. polarisation has been given by Allnatt (1959) only the more recent results are considered here.

An impurity-vacancy complex constitutes an electric dipole capable of adopting different orientations. In the absence of a field reorientation can be either by exchange of the M^{2+} ion and the vacancy with a probability w_2 per unit time or by the vacancy jumping from one nearest neighbour cation site to another with a probability w_1. In the presence of an electric field these probabilities will be modified as described in 1.07. Equations may be derived for the rates of change of each group of equivalent orientations with respect to the field. The steady state solution of these for an A.C. applied field represented by $E = E_0 e^{i\omega t}$, enables the complex polarisation per unit

volume of the crystal to be calculated (Lidiard, 1957; 1954b). This polarisation P is given by

$$1.09.1 \qquad P = \frac{2a^2e^2x_kNE_o\exp(i\omega t)}{3kT[1 + i\omega/2(w_1+w_2)]}$$

where a is the anion-cation separation and x_kN the number of complexes per unit volume. The current density due to the complexes will be

$$1.09.2 \qquad J_1 = \frac{dP}{dt} = \frac{2a^2e^2x_kNE_o\exp(i\omega t)[i\omega + \omega^2/2(w_1+w_2)]}{3kT[1 + \omega^2/4(w_1+w_2)^2]}$$

In addition there will be a current density J_2 arising from the free vacancies and the displacement current.

$$1.09.3 \qquad J_2 = \sigma E_o\exp(i\omega t) + (i\omega\epsilon/4\pi)E_o\exp(i\omega t)$$

where ϵ is the static dielectric constant of the crystal. The complex dielectric constant $(\epsilon_1 - i\epsilon_2)$ (Fröhlich, 1958) may be identified by equating the total current density to the formal expression for the current density.

$$1.09.4 \qquad J_1 + J_2 = (i\omega/4\pi)[\epsilon_1 - i\epsilon_2]E_o\exp(i\omega t)$$

Thus

$$1.09.5 \qquad \epsilon_1 = \epsilon + \frac{8a^2e^2x_kN\pi}{3kT[1 + \omega^2/4(w_1+w_2)^2]}$$

1.09.6 $$\epsilon_2 = (4\pi\sigma/\omega) + \frac{8a^2e^2x_k N\pi}{3kT}\left[\frac{\omega/2(w_1 + w_2)}{1 + \omega^2/4(w_1+w_2)^2}\right]$$

The contribution of the dipoles to ϵ_1 is negligible so the dielectric loss angle δ is given by

1.09.7

$$\tan\delta = (\epsilon_2/\epsilon_1) = (4\pi\sigma/\omega\epsilon) + \frac{8\pi a^2e^2x_k N\omega\tau}{3\epsilon kT(1+\omega^2\tau^2)}$$

where $\tau = 1/2(w_1 + w_2)$.

When the contribution from the vacancies $4\pi\sigma/\omega\epsilon$ is subtracted, the expression for $\tan\delta$ has identical frequency dependence to that for a Debye loss characterised by a single relaxation time τ.

The results of extensive measurements of $\tan\delta$ for a number of alkali halides have been given by Dryden and Meakins (1957). In all cases the value of ω at the maximum absorption frequency, characterised by $\omega = 1/\tau$, could be expressed in terms of the temperature as

$$\omega_{max} = 2\pi A\exp(-\Delta E/kT)$$

Results for KCl were

KCl + $CaCl_2$	$\Delta E = 0.64$ eV	$A = 8 \times 10^{12}$/sec.
KCl + $SrCl_2$	$\Delta E = 0.67$ eV	
KCl + $BaCl_2$	$\Delta E = 0.70$ eV	

Clearly this dielectric loss can only be observed when there are a substantial number of complexes present. This restricts measurements to below about 100°C. The technique has been extended by Cook and Dryden (1960) and Dryden (1963) to study the kinetics of aggregation of dipoles in quenched crystals.

Dreyfus (1961) has studied the dielectric loss arising from impurity vacancy complexes, using D.C. techniques. A Debye loss should give rise to an exponential current decay on application of a D.C. field. Dreyfus observed such a decay in NaCl crystals doped with $MgCl_2$, $MnCl_2$, $CaCl_2$, $CdCl_2$ and $SrCl_2$ at temperatures below 0°C. From the temperature dependence of the relaxation time, he obtained activation energies for the motion of vacancies on sites adjacent to the impurities. These varied between 0.705 eV for Sr^{2+} and 0.661 eV for Mg^{2+}. A discussion is given of the theory for relaxations arising from next nearest neighbour and fourth nearest neighbour vacancies. It is concluded that the activation energy for Mg^{2+} corresponds to the motion of fourth nearest neighbour vacancies, whereas for all the other impurities, next nearest neighbour relaxations were being observed.

Kessler and Marini (1965) have observed a dielectric relaxation in alkali halides at temperatures between 400

and 100°C using a frequency of 1 kc/sec. The maximum was displaced to lower temperatures with increasing impurity content. The magnitude of tan δ for the relaxation process was found to be independent of impurity content but proportional to the crystal thickness. The latter observation suggests that the loss arises from space charge formation; however, no further explanation is given.

A Debye type of relaxation has also been found in KCl at temperatures above 650°C and in the frequency range 1 to 10 megacycles/sec. (Sastry and Srinivasen, 1963). The results were interpreted using the simple Debye theory (Fröhlich, 1958), in other words a single relaxation time was assumed. The real and imaginary parts of the dielectric constant are given by

$$1.09.8 \qquad \epsilon_1 = \epsilon_\infty + (\epsilon_s - \epsilon_\infty)/(1+\omega^2\tau^2)$$

$$1.09.9 \qquad \epsilon_2 = \frac{4\pi\sigma}{\omega} + \frac{(\epsilon_s - \epsilon_\infty)\omega\tau}{1+\omega^2\tau^2}$$

According to the Debye theory the difference between the low and high frequency limits of ϵ_1 is

$$1.09.10 \qquad \epsilon_s - \epsilon_\infty = \frac{4\pi n\mu^2}{3kT}$$

where n is the number of dipoles per unit volume and μ

their dipole moment. ϵ_1 and ϵ_2 were obtained from measurements of capacitance and conductance. The maximum value of ϵ_2 occurs when $\omega\tau = 1$, $\epsilon_s - \epsilon_\infty$ may be found by subtraction of the conductivity contribution from this maximum value. Sastry assumed the loss arose from vacancy pairs and obtained their apparent concentration by assigning them a dipole moment ea, where a is the anion-cation separation. The temperature dependence of n and τ were found to satisfy the equations

$$n = 7.4 \times 10^{27} e^{-\frac{1.34}{kT}} \text{ cm}^{-3}$$

$$\tau = 2.98 \times 10^{-13} e^{\frac{1.04}{kT}} \text{ sec.}$$

The calculated value (Tharmalingam and Lidiard, 1961) of the activation energy in KCl for an anion jumping into a vacancy pair is 1.15 eV and for a cation 1.30 eV. These are in fair agreement with the experimental value of 1.04 eV. There is also good agreement between the calculated energy to create a vacancy pair 1.28 eV and the enthalpy associated with n, 1.34 eV. However, the magnitude of n is implausibly large, at 775°C $n = 3.21 \times 10^{21} \text{cms}^{-3}$ or 20% of the concentration of ion pairs. A similar result has been found for KBr (Maurer, 1963). In order to account for the anomaly Boswarva and Franklin (1965) extended the simple

theory to include internal field corrections, but were still unable to account for the large value of n. There is independent evidence for the existance of vacancy pairs at these temperatures. This comes from the latest diffusion experiments, the details of which have been given already.

Sutter and Nowick (1963) have carried out D.C. polarisation measurements on NaCl in the temperature range 400° to 20°C. It was found that current time decay curves, on application of a potential and on its removal, could be superimposed. Ohm's law was obeyed for the entire decay curve using applied potentials between 20 and 200 volts. Sutter and Nowick conclude that since the superposition principle and Ohm's law are obeyed by the decay, the potential distribution within the crystal is linear. This suggests that the polarisation is not due to the formation of a space charge by blocking at the electrodes. The space charge polarisation theory of Jaffé (1933) predicts substantial non-linearity for the voltages used in these experiments. There is a possibility that the charge carriers are blocked at mosaic boundaries distributed throughout the crystal. On a macroscopic scale the potential distribution could then be linear. This interpretation requires the decay conductance and its steady

state value at infinite time to be related. Additional experiments made by Sutter and Nowick suggested they were completely unrelated.

An alternative explanation is that the polarisation arises from an alignment of dipoles. For a simple Debye process the conductance should decay exponentially with time whereas the time dependence found by Sutter and Nowick obeyed the relation

1.09.11 $$\sigma(t) - \sigma_{\infty} = at^{-n}$$

where $\sigma(t)$ is the conductivity at time interval t after application of the potential and σ_{∞} is the final steady state conductivity. No definite conclusions could be drawn but the authors proposed the dipoles could arise either from small regions of higher conductivity or from polarisation of charge clouds surrounding dislocations (Eshelby et al., 1958). If these interpretations are correct, the final steady state conductivity is the true conductivity of the vacancies. Parker (1954) has studied the same polarisation in NaCl and KCl. His results do not agree with this more recent work in that he found the rate of decay depended upon the applied voltage. Consequently Parker attempted to interpret his data using the space charge polarisation theory.

A polarisation found at temperatures above about 550°C in pure and doped KCl has been interpreted in terms of the space charge polarisation theory (Jacobs and Maycock, 1963b; Allnatt and Jacobs, 1961). A.C. measurements of the equivalent parallel combination of resistance and capacitance of the crystal were made at different frequencies. These were compared with the predictions of the A.C. space charge polarisation theory developed by Macdonald (1953) and Friauf (1954). The theory was originally proposed by Jaffé (1933). To take into acoount the non-linear potential distribution in the crystal a solution must be found for the equations of detailed balance. The concentration of charge carriers in a volume element of the crystal will be governed by diffusion, migration in the local electric field and by generation and recombination of the carriers.

For the case of neutral centres dissociating to give positive and negative charge carriers, the rate of change of the concentration of negative carriers will be given by

$$1.09.12 \qquad \frac{\partial n}{\partial t} = k_1 n_c - k_2 np$$

where n_c is the concentration of neutral centres, p the concentration of positive carriers and n the concentration of negative carriers. This is combined with the expressions obtained by considering the flux of carriers into a slab of unit cross section and thickness δx, arising from

diffusion and motion in the electric field $\mathbf{E}(x,t)$. The equations of detailed balance are,

1.09.13 $$\frac{\partial p}{\partial t} = k_1 n_c - k_2 np + D_p\left(\frac{\partial^2 p}{\partial x^2}\right) - \mu_p \frac{\partial}{\partial x}(pE)$$

1.09.14 $$\frac{\partial n}{\partial t} = k_1 n_c - k_2 np + D_n\left(\frac{\partial^2 n}{\partial x^2}\right) + \mu_n \frac{\partial}{\partial x}(nE)$$

and for the neutral centres

1.09.15 $$\frac{\partial n_c}{\partial t} = - k_1 n_c + k_2 np$$

where D_p, μ_p and D_n, μ_n are the diffusion coefficients and mobilities for positive and negative charge carriers respectively. These equations together with Poisson's equation,

1.09.16 $$\frac{\partial E}{\partial x} = (4\pi e/\epsilon)(p-n)$$

may be used to determine the carrier distributions for a given set of boundary conditions. One condition equates the applied potential to the total potential drop in the crystal. For a sinusoidal applied voltage this is

1.09.17 $$V_1 \exp(i\omega t) = \int_0^L E(x,t)\,dx$$

where L is the length of the crystal and ω the frequency.

Macdonald, who gives the most complete and accurate analysis, considered the case of completely blocked electrodes. This necessitates the second condition, of zero current at the electrodes expressed by

$$\left.\begin{aligned} 1.09.18 \qquad & \mu_p pE - D_p \frac{\partial p}{\partial x} = 0 \\ 1.09.19 \qquad & \mu_n nE + D_n \frac{\partial n}{\partial x} = 0 \end{aligned}\right\} \quad x = o, L$$

Approximate solutions to these equations have been found by linearising them, assuming that n, p, n_c and E are all of the form

$$1.09.20 \qquad n(x,t) = n_o(x) + n_1(x)e^{i\omega t}$$

When the additional assumption is made that $n_o(x) = p_o(x)$ it follows that $E_o = 0$ and n_o, p_o are independent of x. Macdonald's solution (1953) is extremely complicated and left in a complex form.

Jacobs and Maycock found that for the case of doped KCl, assuming the positive carriers M^{2+} were fixed and only the cation vacancies mobile, Macdonald's solution reduced to give a space charge capacitance:

$$1.09.21 \qquad C = \left(\frac{\pi kT}{\epsilon c_o}\right)^{\frac{1}{2}} \frac{4\sigma^2}{e\omega^2 L^2}$$

This is the solution for complete dissociation of the

neutral centres, i.e. impurity-vacancy complexes. For small dissociation C is merely reduced by a factor of $1/\sqrt{2}$.

For pure KCl Jacobs and Maycock found their data gave straight line plots of ωC against $1/\omega$ in agreement with 21. For doped KCl the plots were slightly curved. However, the magnitude of C as calculated from 21 for the doped crystals was greater than the experimental value by a factor of 2 to 4, the agreement being better at lower temperatures. The capacitance of the pure crystals was almost that expected when calculated for one carrier and small dissociation. A disturbing feature is that the measured capacitance of the pure crystals determined previously (Allnatt and Jacobs, 1961) was less by a factor of 2.

An experimental technique has been developed recently (Bucci and Fieschi, 1964) known as ionic thermoconductivity. A potential of several hundred volts is applied across a crystal at about $0^{\circ}C$. The crystal is cooled with the field present. At about $125^{\circ}K$ the field is removed and the temperature raised at $0.2^{\circ}K/sec$. Any dipoles present in the crystal will havebeen aligned by the field. As the temperature is raised these relax and a current flows. The measured current is plotted against the temperature.

Current peaks are obtained, the areas of which can be related to the concentration of a particular species, its dipole moment and relaxation time. Bucci and Fieschi identified a peak corresponding to strontium vacancy complexes, the diminution of this peak after X-irradiation has been correlated with colour centre work (Beltrami, Cappelletti and Fieschi, 1964). In later work by polarising at higher temperatures Bucci and Riva (1965) have identified two peaks as corresponding to the polarisation found by Sutter and Nowick (1963) and the space charge polarisation observed by Jacobs and Maycock (1963,b). The results are rather qualitative and no activation energies are given for the relaxation processes.

1.10 Conclusion.

The primary object of this research was to determine the association energy for the Sr^{2+}-vacancy complex. In order to do this strenuous efforts were to be made to eliminate the two factors which may have influenced previous determinations. These are the presence of OH^- and the very approximate nature of the data analysis. The use of an improved method of treating the results should yield a more accurate complete set of conductance parameters for KCl.

High-temperature A.C. polarisation effects were also to be studied with the intention of determining whether they arose from space charge polarisation. To further this end it was hoped that a close examination of the best available theory, that of Macdonald, might aid in rationalising some of the previously unexplained observations.

2. EXPERIMENTAL

2.01 Preparation of single crystals.

2.01.1 The crystal growing furnace.

The furnace (Fig.2,A) comprised a vertical silica tube of 2.5" nominal bore, wound in four sections and surrounded by firebricks, the whole being enclosed within a syndano box 38 x 39 x 46 cm. The tube of length 44 cm. was wound with 9 turns/inch of 18 S.W.G. Kanthal A1 wire, the resistances of the top and bottom windings were each 7 ohm and those of the upper and lower centre windings were each 12 ohm. The two top sections were connected in series and supplied by an 8 amp variac. The ratio of the current through these two sections was controlled by a 145 ohm variable resistance connected in parallel with the 12 ohm winding. Exactly the same arrangement was provided for the bottom two windings. The temperature of the furnace was controlled by electronic equipment described by Roberts (1951). The primaries of the two variacs were connected in parallel and the controller functioned by switching a resistance in or out of the primary circuit.

The temperature controller sensing element consisted of a platinum resistance thermometer comprising 1.5 metres

of 0.01 cm. diameter platinum wire, wound into a single spiral and inserted in a twin 2 mm. bore alumina tube. This arrangement made the thermometer virtually non-inductive. The temperature of the furnace was measured with a Pt/Pt-Rh thermocouple inserted from the top of the furnace tube.

The top of the furnace was sealed by a removable firebrick plug, drilled to accommodate the thermocouple tube and controller sensing element. To enable visual inspection the bottom of the tube was covered with a pyrex plate which entered the furnace tube and was held in place by a readily detachable sheet of syndano, the centre of which was drilled out 1 cm. less than the bore of the furnace tube. Two pyrex plates were used, one with a hole in the centre to accommodate the rod (Fig.2, D), used to support the crystal growth vessel, the other with no hole in it was used when heating KCl for the chlorination prior to growth.

By adjustment of the variacs and parallel resistances a gradient of 38°C/cm. was produced in the middle of the furnace. The settings were, top variac 100 V, resistance shunting the upper centre winding 93 ohm; bottom variac 30 V, resistance shunting the lower centre winding 45 ohm. The formation of this sharp freezing gradient, necessary

FIG 2

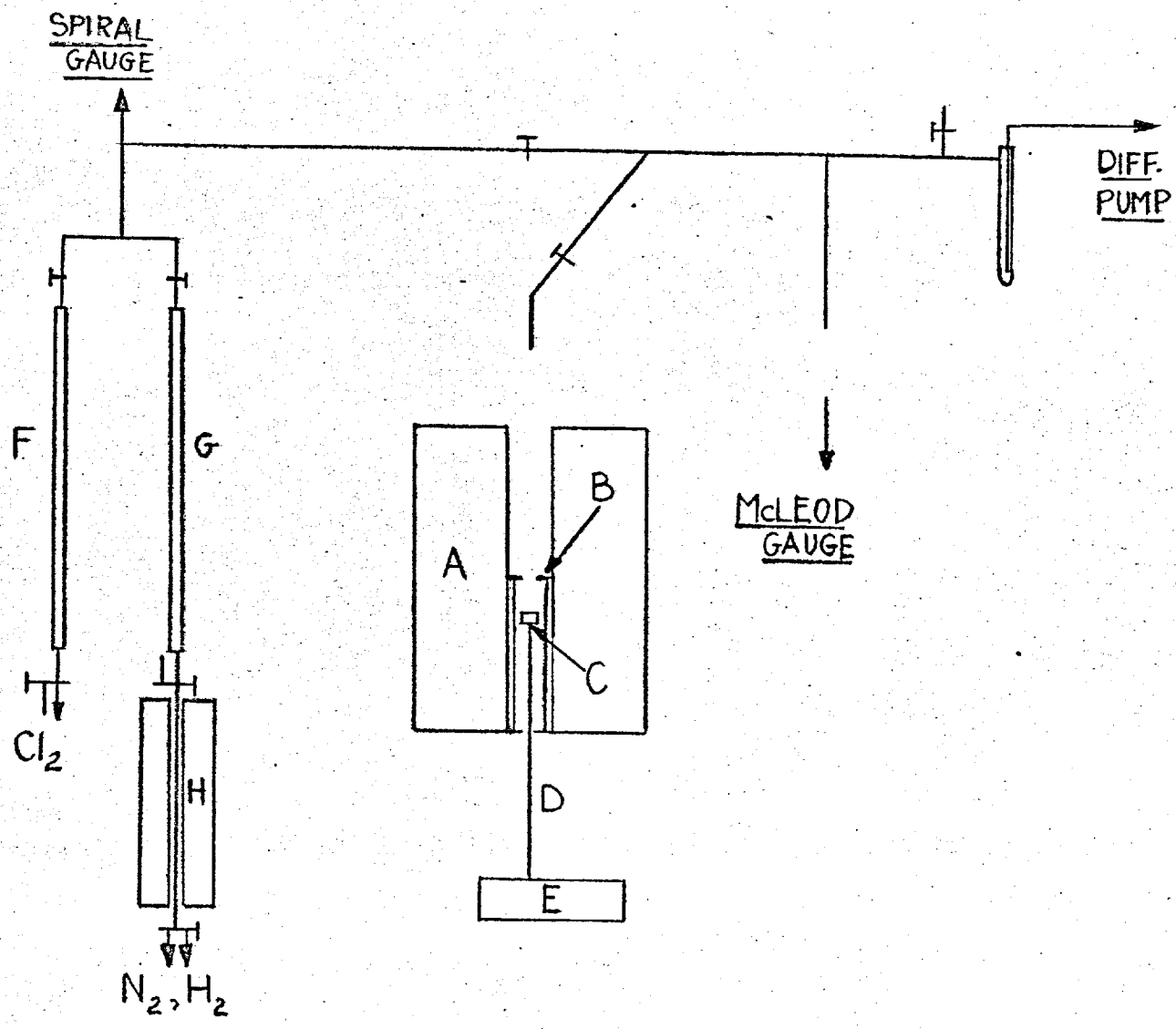

for crystal growth, was assisted by a platinum foil coated nichrome baffle (Fig.2, B), situated in the centre of the furnace. This was supported on a $2\frac{1}{8}$ inch nominal bore silica tube, slid into the main tube and resting on the pyrex plate described above.

2.01.2 Crystal growth.

For growth in silica the high purity quartz container shown in Fig.3A was used. This was 78 mm. long and 26 mm. internal diameter with a basal projection of length 15 mm. and internal diameter 2 mm. Most of the crystals were grown in specpure graphite crucibles (Fig.3B) supplied by Johnson Matthey or Morganite. Two grades of graphite were used, one designated EYC 110 (less than 5 ppm metallic impurities), the other EY 9 had a slightly higher impurity content. These were of overall length 153 mm. with an internal diameter of 24 mm. and a wall thickness of 3 mm. The base of the crucible was thicker to allow a hole of length 10.8 mm. and diameter 2 mm. to be bored in the bottom. When in use, the graphite crucible was sealed in a high purity quartz container, the top and bottom of which is shown in Fig.3C. The container top was 15 mm. long and the bottom 185 mm. with a bore of 31 mm. Before using, all the silica vessels were immersed for half-an-hour in a mixture of 1 part HF and 10 parts

FIG 3

SCALE OF A AND B, 1:1

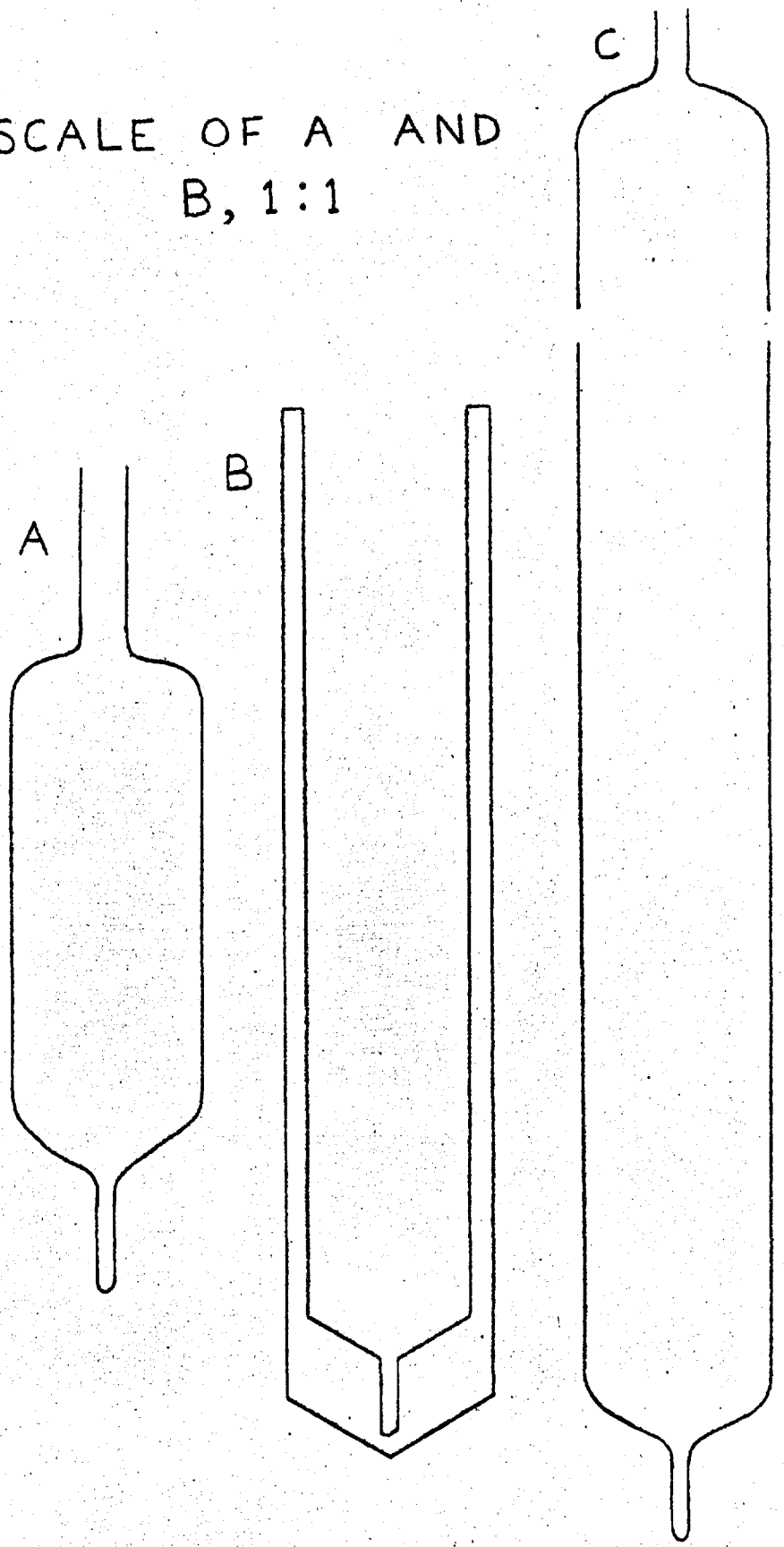

HNO_3, they were then rinsed with de-ionised water and finally immersed in it for at least one hour.

Before inserting the KCl, the graphite crucibles were cleaned in the following way. The crucible was sealed inside the quartz container which was attached to the vacuum line via a B10 quartz socket so that it was positioned inside the furnace (Fig.2). (All the joints and taps on the vacuum line were greased with KEL F, a halogenated hydrocarbon grease supplied by the Minnesota Mining and Manufacturing Co. This was fairly resistant to attack by Cl_2.) The baffle and support tube were removed from the furnace and the container evacuated using an Edwards rotary oil pump and a mercury diffusion pump with liquid nitrogen traps. The crucible and container were heated to 900°C under vacuum when one atmosphere of Cl_2, measured with a spiral gauge, was admitted through the drying tower (3 parts $Ba(ClO_4)_2$ + 1 part $Mg(ClO_4)_2$) (Fig.2,F). The dried Cl_2 was passed through porous glass frits, just above the drying tower, to prevent carriage of the drying agent to the crucible. After about 2 hours the Cl_2 was flushed out of the line with dry O_2-free N_2. The N_2 was passed over reduced Cu at 700°C (Fig.2,H), then through a drying tower (Fig.2,G) and a porous frit. The container was re-evacuated for an hour, the furnace

switched off and the vacuum let down with the purified N_2. It was hoped that in this way metallic impurities in the graphite would be removed as volatile chlorides.

On cooling the crucible container was detached from the vacuum line and the graphite crucible filled with 50 g. of KCl, using a long funnel to ensure the salt entered the crucible. (Specpure KCl was supplied by the Koch Light Co.) The container was rejoined to the line and very slowly heated to 560°C under vacuum to allow H_2O to be pumped off the KCl. At this temperature one atmosphere of Cl_2 was admitted and the temperature raised to 800°C, well above the MP of KCl, 770°C. The molten KCl was kept under Cl_2 for about 2 hours to destroy anionic impurities. Finally the furnace was switched off and when the KCl had solidified the Cl_2 was flushed out with purified N_2 and the container re-evacuated. On cooling it was sealed off under vacuum ready for crystal growth.

For growth the sealed container was cemented with alumina onto a nickel block of overall length 3 cm. and diameter 3 cm. The block had a conical impression in the top with a hole in the centre to accept the basal projection of the crucible container. A stainless steel rod (Fig.2,D) 6.5 mm. in diameter was attached to the block and the lower end held in the chuck of a gearbox

(Fig.2,E). The container was positioned above the baffle and the furnace switched on at the settings in 2.01.1 and left overnight to allow thermal equilibrium to be achieved. After ensuring the baffle temperature was 770°C the thermocouple was removed since it acted as a considerable heat sink and the gearbox switched on. This lowered the container at a rate of 2 mm./hour. Finally, when the container was well below the baffle, the furnace was switched off and allowed to cool slowly. The crystal container was removed and smashed with a hammer allowing the graphite crucible, containing the crystal, to be removed intact. When growing directly in silica, the same procedure was used to chlorinate the KCl and grow the crystals.

Considerable time was spent in an attempt to purify KCl for crystal growth. An apparatus was constructed from high purity quartz which was supported inside the furnace. This consisted of two chambers, an upper and a lower one, each separately connected to the vacuum line and separated by a quartz frit. KCl was melted in the upper chamber and prevented from passing through the frit by maintaining a positive pressure of Cl_2 or N_2 in the lower chamber. The KCl was chlorinated by allowing Cl_2 to pass through the frit and bubble through the molten salt. The

Cl_2 was flushed out with N_2 and metallic potassium introduced to the upper chamber through a capillary. It was hoped this would dissolve in the KCl and displace divalent impurities which would form a surface slag. The KCl was then filtered through the frit into the lower chamber, retaining the slag and some of the melt in the upper chamber. The lower chamber was shaped in the form of a crystal growth vessel and could have been evacuated and drawn off ready for crystal growth. However, the potassium would not dissolve in the melt at the pressures which it was possible to attain so this method was abandoned.

2.02 Analysis of crystals.

The crystals doped with strontium chloride were analysed in the manner described by Allnatt (1959). To avoid errors arising from concentration gradients in the crystal boule the actual specimens used for conductivity measurements were analysed. The instrument used for the analysis was a Philips X-ray diffractometer type PW 1051, fitted with a sodium chloride analysing crystal. Concentration standards containing 60, 50, 30, 20, 10, 5 and 0×10^{-5} mole fraction of strontium were used. These were prepared by dissolving known weights of $SrCl_2$ and KCl in distilled water, evaporating to dryness over a steam bath and finally drying at $100^{\circ}C$. The specimens to be analysed

and the standards were powdered in an agate mortar before use. One of the standards was evenly distributed over a thin mylar window 2 cm. square and mounted in the diffractometer. Ten successive one minute counts of the fluorescence of the strontium K_α line ($2\theta = 15.09^\circ$) were made. These were followed by ten one minute counts of the background ($2\theta = 16.00^\circ$). The excitation was from a tungsten target with a tube potential of 40 kv and a filament current of 20 ma. This counting procedure was repeated for all the standards and the unknowns.

A graph was plotted of the mean of each set of ten counts for the standards against their strontium concentrations. The concentrations of strontium in the conductivity specimens were found from this graph. Since considerable variations were observed in the one minute counts for some of the specimens, the entire counting procedure was repeated together with a third determination for the two lowest doped samples. The counts (less the background) for the unknowns and their corresponding concentrations determined from the appropriate calibration graph are collected in Table 5.

TABLE 5

Strontium analysis of the doped conductivity specimens

Run No.	Mean of Counts/ minute			Mole fraction of strontium x 10^{-5}			Average mole fraction x 10^{-5}
8	335	233	264	12.8	9.7	11.0	11.1
14	414	376	423	15.9	15.5	17.5	16.3
13	500	576		19.3	23.8		21.5
15	724	538		27.7	22.2		25.0
11	696	673		26.5	27.7		27.1
12	869	1215		33.3	50.0		41.7

Although great care was taken with all the analyses, the reproducibility was not as good as that found by Allnatt (1959).

2.03 The conductivity cell.

Pieces of single crystal about 3 mm. thick and 8 mm. square were cleaved out of the grown crystal and their dimensions measured. These were mounted in the support shown in Fig.4 and originally designed by Allnatt (1959). The electrodes, cut out of platinum foil, were 18 mm. in diameter with a piece of foil left projecting for making a contact. The tip of a 13% Pt-Rh thermocouple wire was

spot welded on to the centre of the back of each electrode and a thermopure Pt wire spot welded on to the foil projection. Circular pieces of mica 2 mm. in diameter, with radial cuts in them, were slipped between the foil and the Pt-Rh wire. These acted as insulators ensuring the Pt-Rh wire only contacted the Pt foil at its centre. The crystal was placed between two such electrodes and the whole sandwiched between two alumina discs A, 20 mm. diameter and 4 mm. thick with radial grooves cut in them to accommodate the Pt-Rh leads. This arrangement was held together between two spectrosil plates B, (20 x 49 x 3 mm.) under the light pressure supplied by the tungsten springs D (28 mm. long). The pressure was adjusted by the screw F which was threaded into one of the nickel plates E and made finger tight. The support was freely suspended from two tungsten rods G, sealed into a silica head which was attached to a vacuum line. Two sets of thermocouple wires (Pt, 13% Pt-Rh) were also sealed into the head with soda glass. Inside the cell these were spot welded on to the electrode leads and surrounded by silica tubes to prevent shorting. Outside the cell they were enclosed in shielded polythene insulators and the ends dipped into four mercury cups. The supporting framework was enclosed in a jacket comprising a high purity

FIG 4

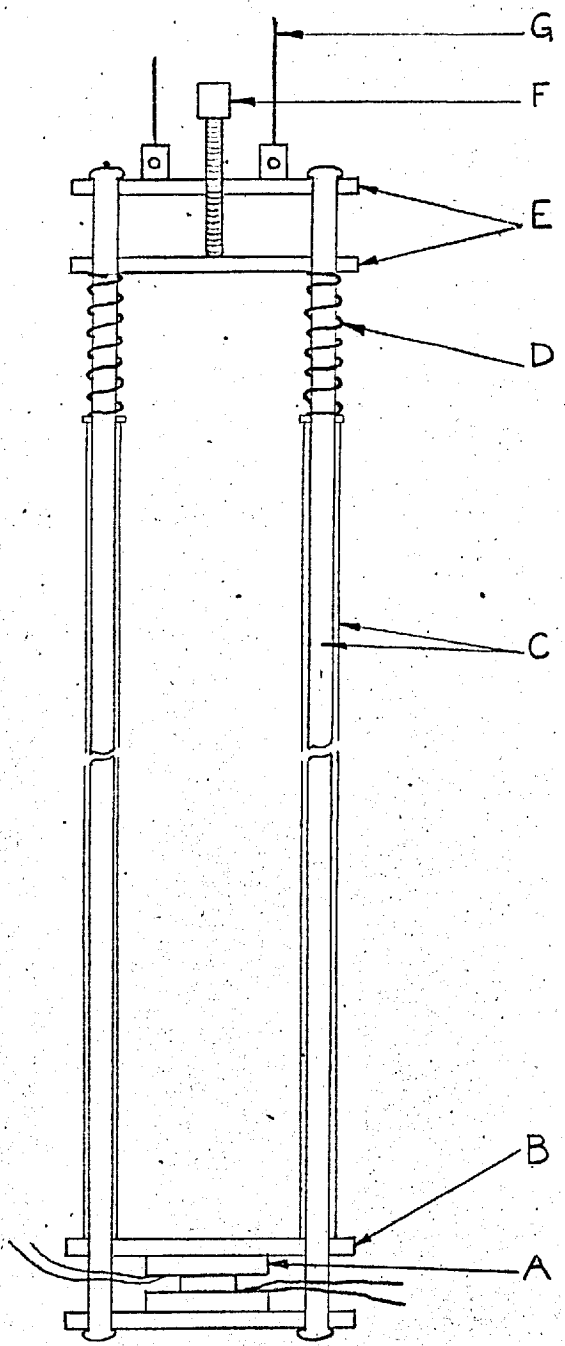

quartz tube, 55 mm. nominal bore and 460 mm. long with a B55 quartz socket on the end. This was attached to a B55 cone on the silica head. Picene was used to provide a vacuum tight seal. The bottom of the jacket was narrowed and attached via a B10 quartz cone and a tap to a bubbler containing di-n-butyl phthalate. The jacket was surrounded by an earthed nickel shield and the furnace lifted into position round the tube and supported by a dexion stand. The top and bottom of the jacket lay outside the furnace and were water cooled to prevent picene from running out of the joints. The cooling tubes also prevented overheating of the support springs D, situated just below the B55 joint.

The only change made in the design used by Allnatt was an increase in length of the high purity quartz rods and tubes C. These were extended to make the overall length of the support 38 cm. A corresponding increase was made in the length of the cell jacket. This enabled higher temperatures to be used without any danger of picene running out of the upper joint.

Great care was taken to ensure the interior of the conductivity cell was kept clean and the entire electrode assembly was put together with nickel tweezers. The alumina discs A, providing the main insulation, were

boiled three times in aqua regia for periods of several hours, and finally boiled for similar lengths of time in three lots of deionised water. The jacket was rinsed out with HF and soaked in deionised water. All the thermocouple leads in the cell were rinsed and flamed off. Before each run the entire cleaning procedure was repeated and new electrodes were constructed.

The vacuum line was similar to that used for crystal growth. The cell could be evacuated to 10^{-6} mm. Hg. White spot oxygen-free nitrogen (provided by the British Oxygen Co.) could be passed through a drying tower of $Ba(ClO_4)_2$ + $Mg(ClO_4)_2$, over reduced copper at 700°C, through a porous frit and into the head of the conductivity cell via a cardice trap. Continued passage of the nitrogen could be achieved by opening the tap at the bottom of the cell and allowing the nitrogen to flow out through the bubbler.

The furnace was a silica tube 12.3" long and nominal bore 3" wound in three sections with 2.49 ohm/yd. nichrome wire. The two end sections were of 28 turns at 8/inch and the middle section was 24 turns at 7 turns/inch. The three sections were connected in series and supplied by an 8 amp variac. The current through each section could be controlled by three variable resistances, each

connected in parallel with a winding. The tube was mounted in a syndano box filled with vermiculite and surrounded by earthed aluminium foil to provide a poor emission surface and reduce 50 cycle "pick-up" by the A.C. bridge.

The temperature regulator was the same as that described in 2.01.1 but it was found that a far more stable temperature could be achieved by winding the platinum resistance thermometer directly on to the furnace tube beneath the heater windings. The thermometer was non-inductively wound and insulation from the furnace windings was provided by mica sheets, held in place by asbestos paper. With this arrangement the regulator responded very rapidly to variations in temperature near the heater windings. Asbestos wool plugs were inserted at the top and bottom of the furnace tube to provide the insulation necessary for this arrangement of the temperature regulator sensing element. The temperature could be held constant to within 0.2 deg. at 680°C for periods up to 6 min., which is ample time for taking a measurement of temperature and resistance. For periods of 40 min. the temperature was stable to within 1°C. The long term stability was useful for measuring frequency dependence of capacitance and better than that achieved by Allnatt (1959) and Maycock (1962) who used the sensing element described in 2.01.1.

2.04 The A.C. bridge.

Conductance and capacitance measurements were made using the A.C. bridge shown in Fig.5. The bridge components are listed in the accompanying description of Fig.5. The output from the bridge was applied to a battery driven transistor amplifier A. This type of amplifier minimises A.C. "pick-up". The parallel-T filter F cut out most of the 50 cycle "pick-up" before the signal was applied to the y plates of the oscilloscope. A signal of the same frequency and phase as the input was applied to the x plates. The balance condition when the y component is zero may be expressed as

$$R(\text{crystal}) = \alpha R_1$$

$$C(\text{crystal}) = (C_f + C_1 + C_2 - \alpha C_c)/\alpha$$

where R and C are the crystal's equivalent combination of resistance and capacitance, neglecting lead capacitances and α is the bridge ratio.

All the bridge connections were made using coaxial cable with the sheath earthed and all the components were shielded. As described in 2.02 the conductivity cell and furnace were clad with earthed shields. In addition all the metallic components near the cell were earthed. The input was via a 1:1 shielded transformer and the y plates of the oscilloscope were at a floating potential.

FIG 5

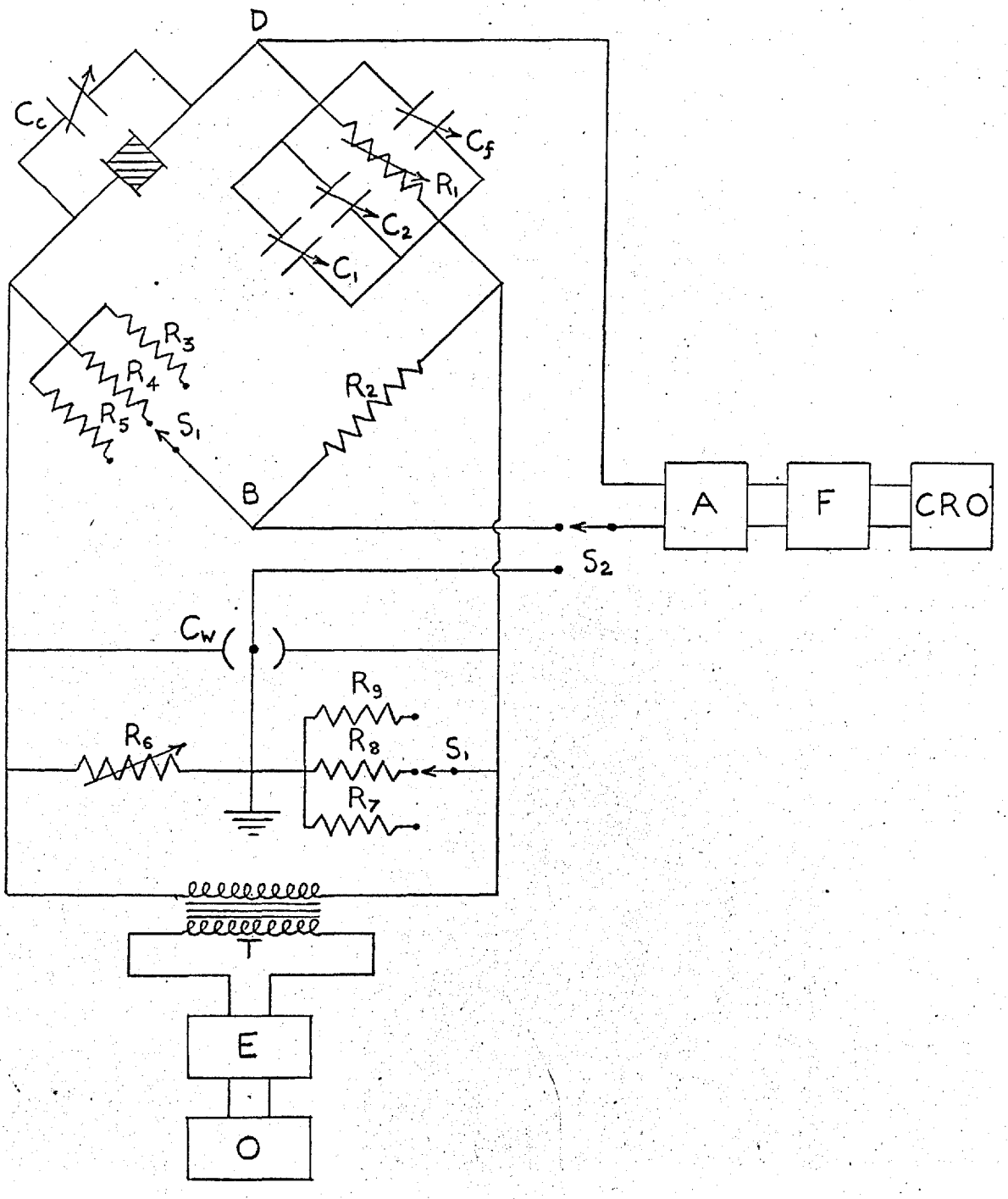

Component values - Fig.5.

All bridge resistances were precision Sullivan non-inductively wound except the Tinsley decade box.

R_1	Sullivan decade box (11,111.1 ohm) + Tinsley low inductance decade box (5278 L.F.5) 1.11 x 10^7 ohm.		
R_2	1 K	R_3	100 K
R_4	10 K	R_5	1 K
R_6	Pye decade box (11, 111 ohm).		
R_7	10 K	R_8	1 K
R_9	100 ohm		
S_1, S_2	Yaxley switches (ceramic base).		
O	Advance oscillator (J1).		
A	Amplifier.		
F	Filter (parallel-T).		
T	Sullivan balanced and screened transformer.		
E	Sullivan decade attenuator (600 ohm) (T network).		
C_f	Sullivan air condenser (C.859/S), 61 pF.		
C_c	Sullivan air condenser (C.855/S), 390 pF.		
C_1	Sullivan mica decade condenser (C.2099), 1F.		
C_2	Sullivan air condenser (C.500D), 1290 pF.		

The shielding reduced mutual capacitative and inductive interaction and minimised A.C. "pick-up".

To minimise the effect of stray capacitances to earth a Wagner earth was incorporated in the bridge circuit. By simultaneously balancing the bridge (using R_1 and C_2) and balancing point D of the bridge with the Wagner earth (throwing S_2 and using C_w and R_6), a balance condition was systematically approached such that points B and D though not directly connected to earth were at earth potential. All the condensers were shielded with the low potential side, point D on the bridge, connected to the screen, thus at balance all the screens were at earth potential.

The frequency of the signal applied to the bridge could be varied between 125 cps and 50,000 cps. Below 125 cps the bridge was unusable due to signal reduction by the parallel-T filter. The ratio arm switch S_1 allowed one of three ratios, 1:1, 1:10, 1:100, to be selected. An attenuator E enabled a range of discrete voltages to be applied to the bridge from 0.0045 V to 45 V. For resistances up to 10^7 ohm, the measurements were made at 1 kc/sec; for resistances above this a 250 cps frequency was employed. For all capacitance measurements (except when voltage dependence was being studied) and resistances up to 10^6 ohm 1.42 V were applied across the bridge.

For resistances between 10^7 and 10^8 ohm, 2.53 V was used and for higher resistances, 45 V.

The bridge was checked against standard resistances and capacitances. Resistances up to 10^5 ohm were measured using the 1:1 ratio, the accuracy was 0.05% from 250 to 10,000 cps and less than 0.2% at 50 kc/sec. For resistances between 10^5 and 10^6 ohm measured on the 1:10 ratio arms, the accuracy was less than 0.4% below 1 kc/sec., 1% at 10 kc/sec., but dropped to 39% at 50 kc/sec. For resistances between 10^6 and 10^7 ohm on the 1:100 ratio arms the accuracy was 0.4% below 1 kc/sec. but dropped to 27% at 10 kc/sec. To extend the range of measurement up to 10^9 ohm a low inductance decade resistance of 10^7 ohm was connected in series with R_1. This resistance was of poorer quality than R_1 but by working at 45 V and 250 cps 1% accuracy was obtained on the 1:100 ratio arms.

Capacitance was only measured using the 1:1 ratio arms since for resistances above 10^5 ohm the space charge capacitance was rather small. Absolute values of capacitance above 100 pf could be measured to within 1% using applied potentials of 1.4 V but at 0.08 V the accuracy dropped to about 10%. However, since the space charge capacitance is the difference of capacitance measured at a given frequency and the geometrical capacitance (i.e. that measured at a high frequency), the accuracy

of measurement is only dependent upon the incremental accuracy of the capacitances and the frequency independence of the measurement. The frequency dependence was checked using standard resistances of typical values from 10^3 to 10^5 ohm and the variation from 250 cps to 1 kc/sec. for capacitances greater than 100 pf was less than 0.05% rising to 0.5% between 1 kc/sec and 50 kc/sec. The accuracy decreased for applied potentials less than 1.4 V.

The bridge was found to be sufficiently accurate for most of the errors to arise from temperature control. It was for this reason that the modification of the temperature regulator (2.03) was made.

2.05 Experimental procedure.

The crystal was mounted in the conductivity cell as described in 2.03. The cell was evacuated and the temperature slowly raised to 250°C to pump off moisture and allow it to condense in liquid nitrogen traps. At this temperature the purified nitrogen was slowly admitted. When the pressure reached one atmosphere the tap at the bottom of the conductivity cell was opened allowing a gentle stream of nitrogen to flow out through the bubbler. The temperature was raised to 680°C and the furnace resistors adjusted to obtain zero temperature gradient between the thermocouple-electrodes on either side of the

crystal. The crystal was annealed at this temperature for several days until its resistance dropped to a constant value (pre-anneal measurements were taken for some crystals but this is made clear where the results are presented). Resistance and capacitance at 1 kc/sec. and capacitance at 300 cps were measured as the temperature was decreased. The regulator was set to a particular value and when the temperature had stabilised the thermocouple leads from the ice junction were inserted in the mercury cups near the cell head. The temperature was measured, the thermocouple leads removed and replaced by the shielded leads from the A.C. bridge, allowing the resistance and capacitance at 1 kc/sec. to be measured. This was repeated several times in quick succession until two or more identical (resistance to within 0.2%) consecutive pairs of readings were obtained. These were averaged to obtain a final value. The capacitance at 300 cps was then measured, before lowering the temperature for the next set of readings. When these measurements had been completed on a doped crystal the temperature was raised to 680°C again. The capacitance and resistance were then measured as a function of frequency (and in some cases voltage) at several fixed temperatures. At the end of a run the dimensions of the crystal were measured again.

The frequency scale on the Advance oscillator was rather coarse and for the first hour or so after switching on, the output frequencies did not correspond exactly with the scale reading. To overcome these two sources of error, use was made of the small but inevitable 50 cycle 'pick-up' which appeared on the oscilloscope. Frequencies were chosen which were simple multiples of 50 cps. These were then located precisely by turning the frequency selector until the superimposed 50 cycle ripple became stationary. It was found that this procedure (used to obtain all the frequency dependence data recorded here) considerably reduced the scatter in a plot of capacitance against frequency.

3. RESULTS

3.01 Conductivity measurements on 'pure' crystals in the intrinsic region.

Fig.6 shows the reproducibility achieved in the intrinsic region of the log σT versus 1/T plots for a series of crystals. The curves are designated by their run numbers. Table 6 gives details of the crystals used.

TABLE 6.

Run No.	KCl	Crucible Material
1	A.R. twice recryst.	spectrosil
4	Light's specpure	graphite (Morganite EY9)
5	Light's specpure	graphite (Morganite EY9)
6	Light's specpure	graphite (Morganite EY9)
9	38 times zone refined in HCl	silica
10	Light's specpure	graphite (Johnson Matthey EYC 110)

The material for all the crystals except that for run 9 was chlorinated in the molten state. The crystal used for run 9 was cleaved from a section of a zone refined ingot donated by the U.S. Naval Research Laboratory.

FIG 6

CONDUCTIVITY OF PURE KCl

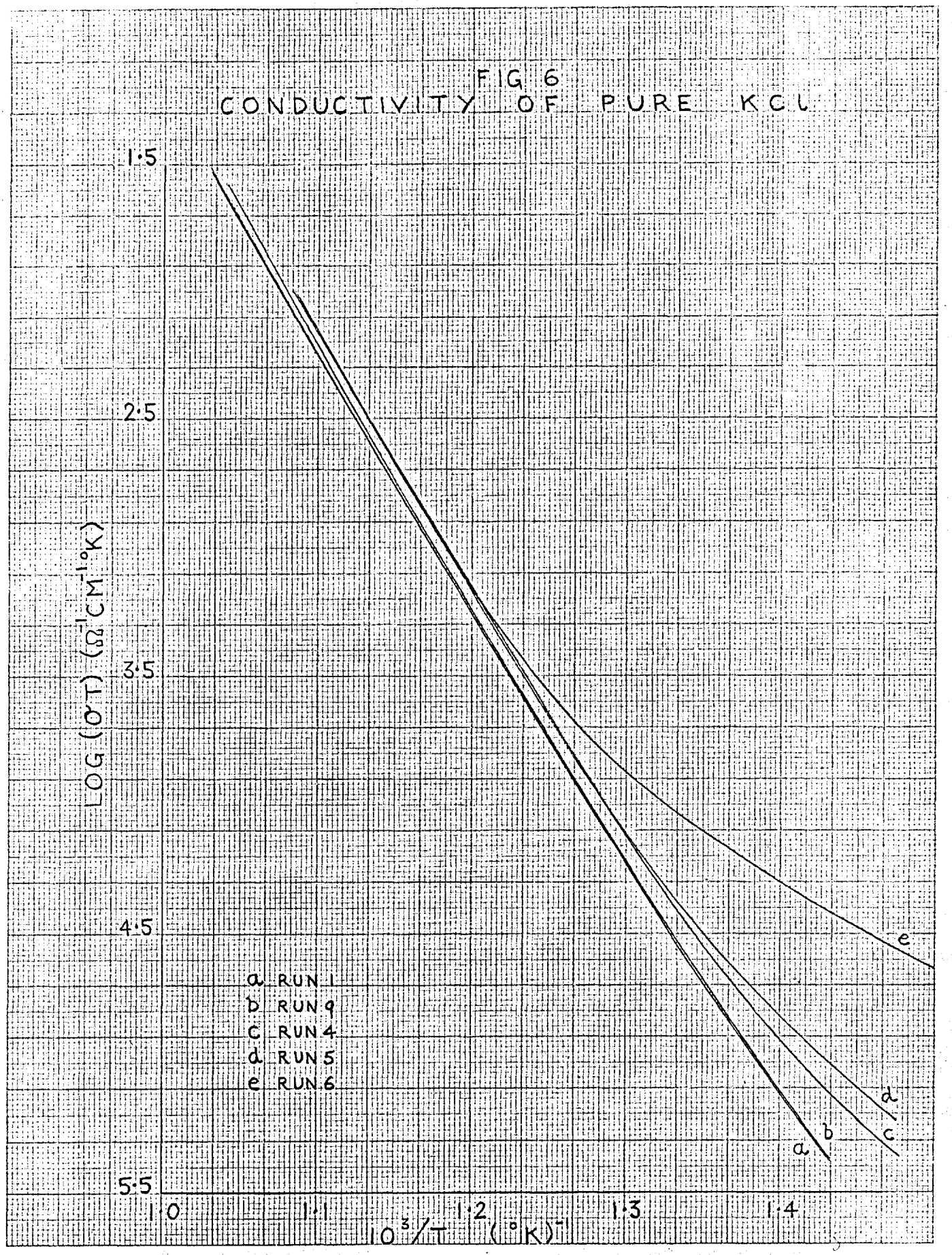

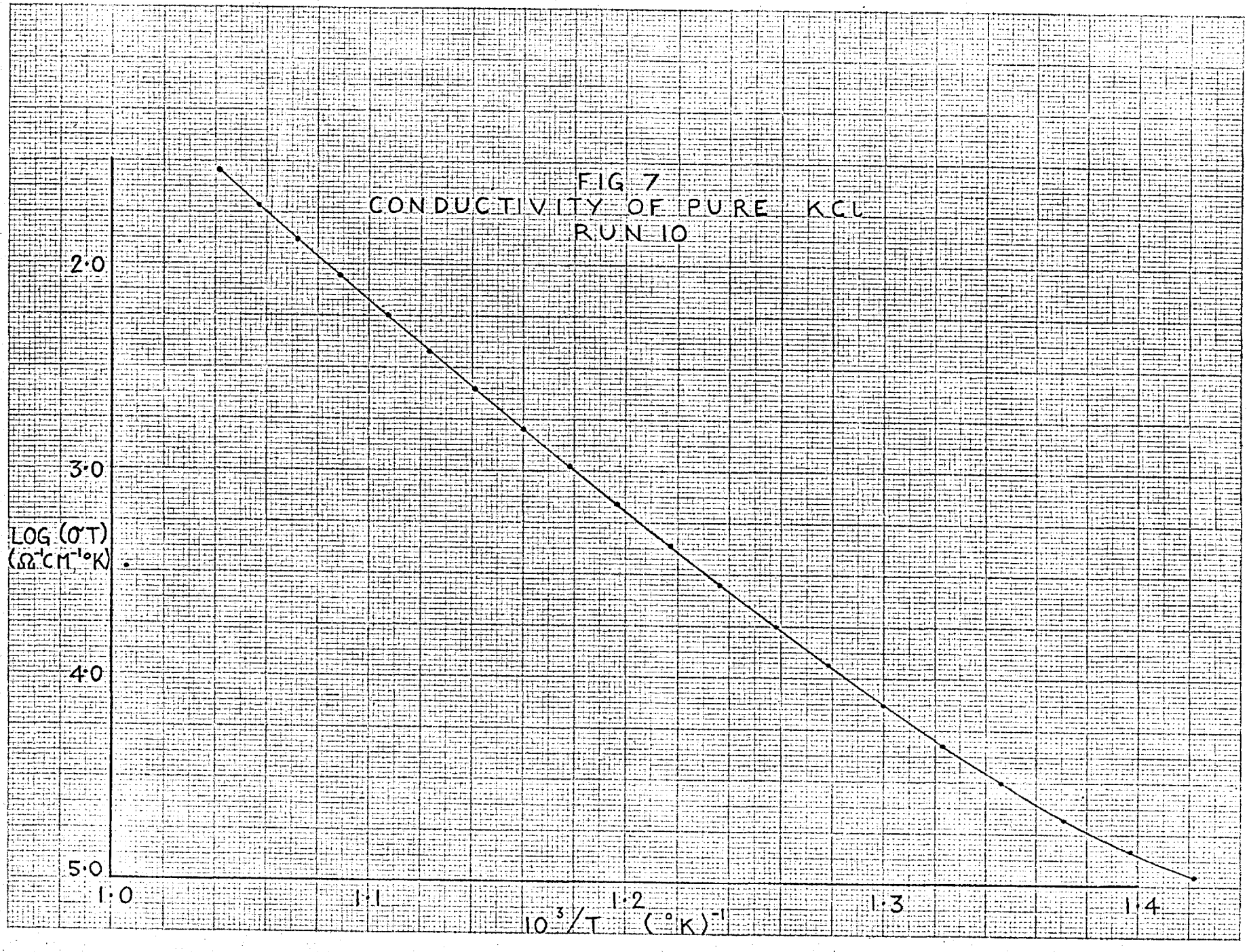
FIG 7
CONDUCTIVITY OF PURE KCl
RUN 10
2·0
3·0
4·0
5·0
LOG (σT)
(Ω⁻¹CM⁻¹°K)
1·0
1·1
1·2
1·3
1·4
10³/T (°K)⁻¹

Before commencing measurements all the crystals were annealed in the conductivity cell at 650 to 680°C until the resistance at a fixed temperature was reproducible to within 1%. The procedure took several days during which the resistance always dropped. This may be interpreted in terms of two processes resulting from plastic flow of the crystal under the spring pressure holding the electrodes in place. Electrical contact with the electrode will be improved by a levelling out of steps on the crystal surface. Also, the crystal will be slightly distorted in a way such as to reduce the thickness and increase the area. Both of these are cooperative in increasing the apparent conductivity.

TABLE 7

Run	Before run		Log (σT) using l/A before run	After run		Log (σT) using l/A after run
	l cm	A cm^2		l cm	A cm^2	
4	0.2905	0.9407	-2.170	0.2892	0.9440	-2.173
5	0.3393	0.7650	-2.192	0.3305	0.7083	-2.170
6	0.3775	0.6326	-2.119	0.3603	0.6728	-2.166

Table 7 shows conductivity values calculated at $10^3/T = 1.1/°K$ using crystal dimensions before and after the run. Clearly there is considerably more scatter in log σT using the pre-anneal dimensions. All the

conductivity values quoted here, other than those in Table 7 were calculated using dimensions taken after the run. There is the further complication of sublimation. This is apparent from some of the dimensional changes and the sublimate of KCl in the cool part of the conductivity cell. However, the reproducibility after annealing suggests that it is not sufficiently rapid to affect the dimensions during the short time spent at high temperatures, once the run was commenced. The same annealing procedure was used for doped crystals. These also showed an asymptotic drop in resistance, to which a contributory factor may have been slow dissolution of impurities.

The curvature in the intrinsic region is clearly exhibited in Fig.7. Hence no attempt has been made to measure a gradient for these plots.

3.02 Conductivity measurements in the extrinsic region of 'pure' crystals.

When the nitrogen stream through the conductivity cell was replaced by oxygen, the conductance in the extrinsic region for run 5 decreased by a factor of 3 after passing oxygen at 616^{o}C for 22 hours. To investigate this effect further, a modification to the vacuum line was made so as to enable gas to be either passed directly into the conductivity cell from a cylinder or to be bubbled through

de-ionized water before entering the cell. Fig.8 shows the extrinsic plots for run 6 after being subjected to the sequence in Table 8. Although numerous conductance measurements were made in the intrinsic region throughout the whole time the crystal was exposed to oxygen and water vapour, absolutely no change was noted from that measured previously in an atmosphere of dry oxygen-free nitrogen. On removing the crystal it was found to be etched on the sides where it was directly exposed to the surrounding atmosphere. This etching made the surface of the sides appear whitish and considerably reduced the transparency of the crystal when viewed through them.

TABLE 8.

Points on graph	Treatment.
•	Dry O_2-free nitrogen
⊙	16 hours 'white spot' N_2 at 620°C + 19 hours at 460°C.
■	+ 65 hours 'white spot' N_2 at 608°C.
▲	+ 14 hours wet N_2 at 608°C.
⊙	+ 136 hours wet N_2 at 608°C.
⊡	+ 38 hours wet O_2 at 608°C.
◬	+ 18 hours wet O_2 at 608°C.

FIG 8
RUN 6, REDUCTION IN EXTRINSIC CONDUCTIVITY BY WATER VAPOUR AND OXYGEN (SEE TEXT)

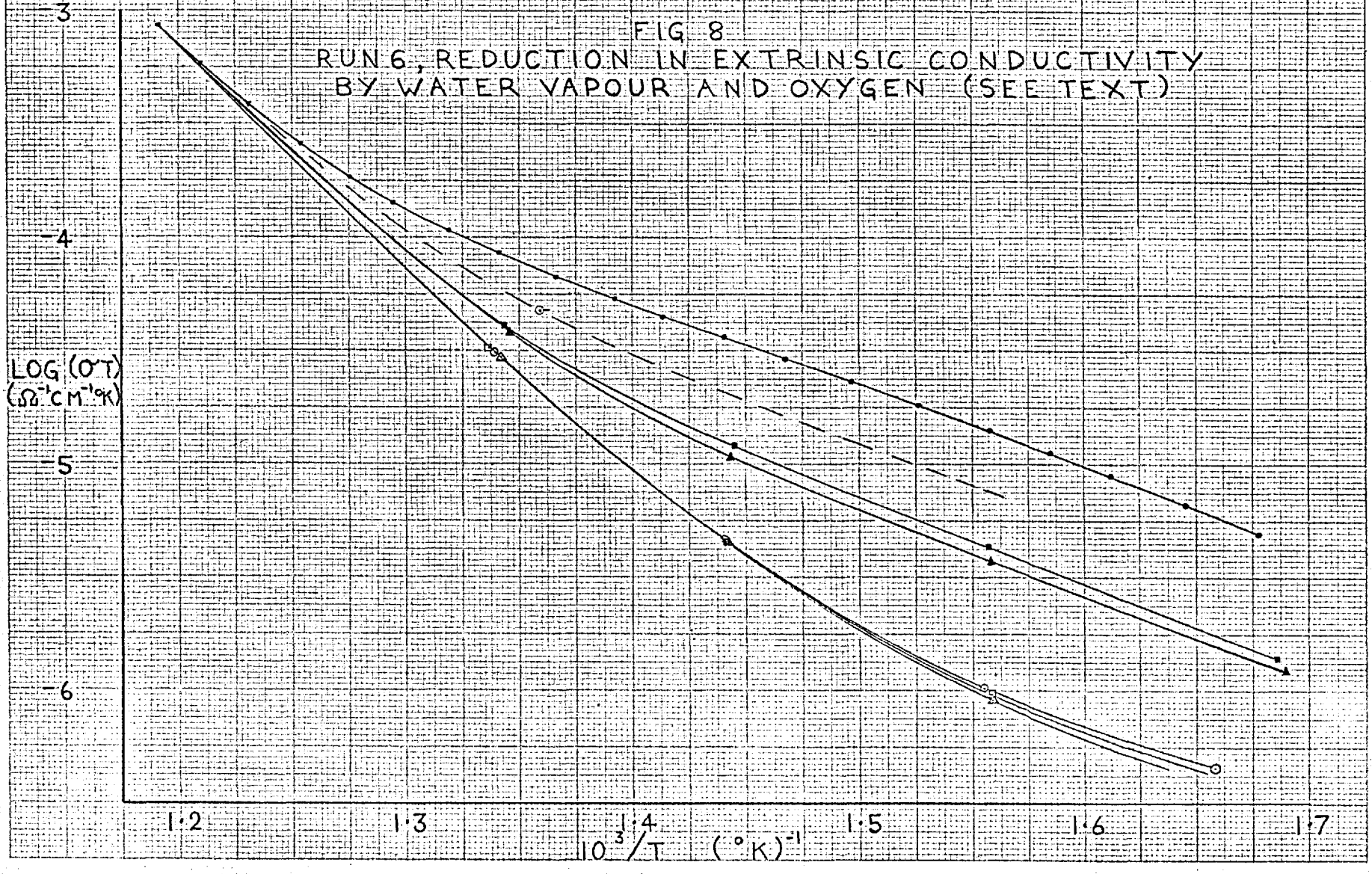

FIG 9
CONDUCTIVITY CHANGE AT 645·1°K, RUN 6

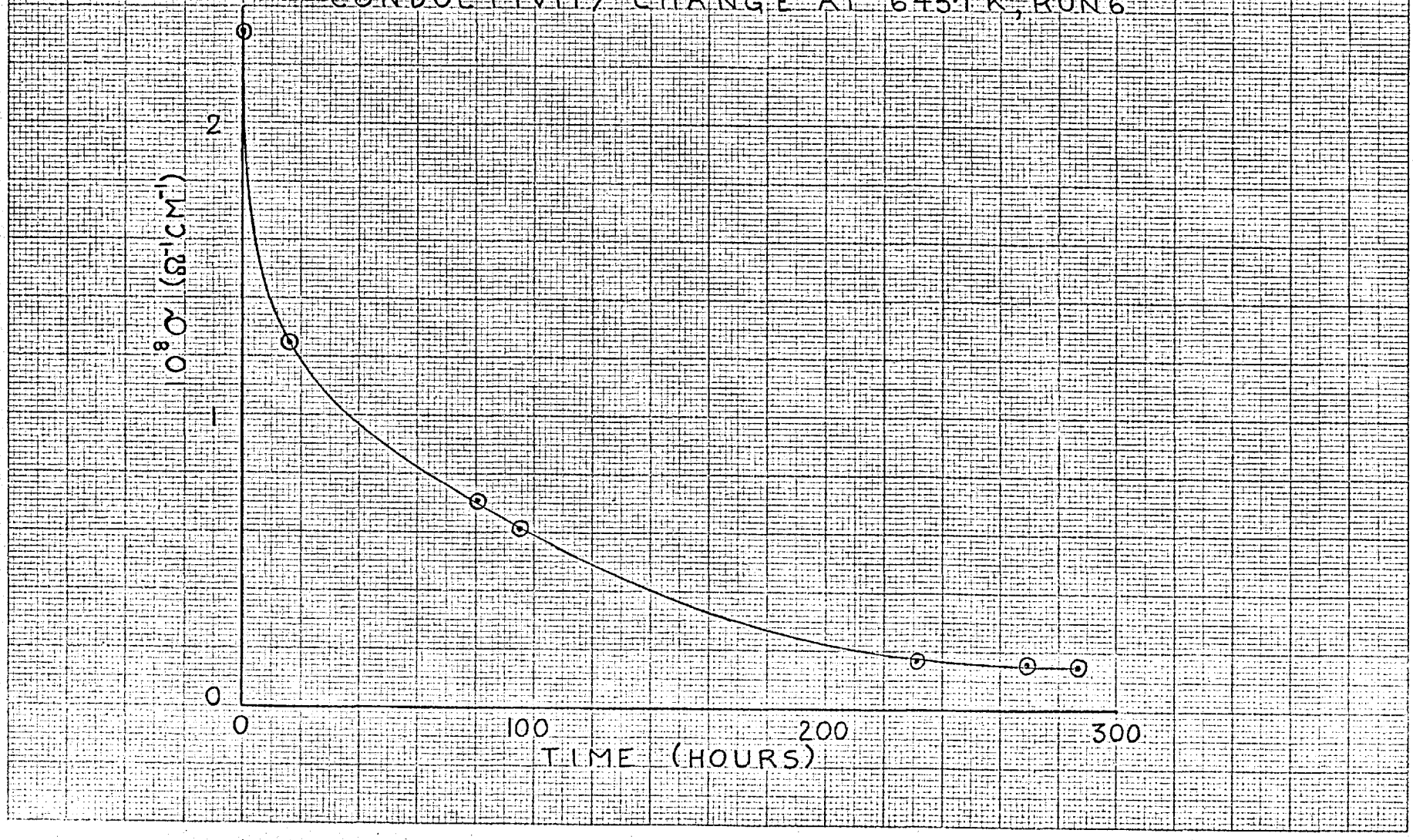

In Fig.9 the conductivity at $10^3/T = 1.6/^oK$ is plotted as a function of time spent at the highest temperature.

The slope of a tangent of the log σT versus $1/T$ plot for run 6 taken at the highest temperature in the extrinsic region is $-\frac{0.70\ eV}{k}$. This is noticeably lower than most of the previous values for Δh_1 (Table 3).

Calcium analyses and estimates of other impurities were made for some of the crystals used for conductivity measurements. The results are given in Table 9 together with an analysis of twice recrystallised A.R. material, the same batch used for growing crystals used in runs 1 and 3. The analyses were made by atomic absorption photometry and carried out by Dr. R. Black of the U.S. Naval Research Laboratory.

TABLE 9.

Results of analyses for trace impurities.

Impurity	A.R.	Run 3	Run 1	Runs 4, 5 and 6.
Ca	2 ppm	4^+ ppm	3.5 ppm	3^- ppm
Ag (relative values)	1	2	3	
Al	very low	trace	considerable	
Na	none	none	trace	
Si	none	none	none	
Ni	trace	trace	trace	
Cu	none	none	trace	

The samples are labelled by run numbers appropriate to conductance cleaves taken from the same crystal. Since the concentrations approach the lower limit of the analytical technique the numerical results are ± 1 ppm but the order is probably correct. The increased Ca, Al and Ag content of the crystals used for runs 1 and 3 over that of the starting material indicate that impurities have been leached out of the growth vessel. This result is qualitatively confirmed by the conductivity measurements. Run 10 showed the lowest conductivity in the extrinsic region and the crystal was grown in what was stated to be the purest graphite, J.M.EYC 110 containing less than 5 ppm metallic impurities. This purity is achieved in part by fluorination of the crucible at 2500°C after the machining is completed. At the other extreme the extrinsic region for run 3 extended to $10^3/T = 1.05/^{\circ}K$. The crystal for this run was grown in a Morganite EY9A graphite crucible which had not been purified after machining. The extrinsic conductivity of run 6 lay between these two extremes in agreement with the purity of the EY9 graphite crucible, which although fluorinated, is not stated to have as high a purity as EYC 110.

U.V. spectra of the 'pure' crystals before and after conductance measurements, including the O_2 treated specimen

from run 6, showed no absorption down to 190 mμ. This indicates the absence of OH^- and also substantial amounts of cationic impurities such as lead and thallium. There remains the possibility that impurity-OH^- complexes were present in the crystals. Etzel and Patterson (1958) found these could only be detected by the OH stretch frequency in the infra red. Unfortunately the conductivity specimens were too thin for I.R. measurements. The OH absorption, being very weak, requires extremely thick crystals for its detection.

Tables 10, 11 and 12 list the conductivity data for runs 6, 9 and 10. The extrinsic region of run 6 was used to estimate the background concentration of impurities for one of the doped crystals, run 8, grown in a similar crucible and using the same batch of Light's specpure KCl. Similarly run 10 yields the background for the doped runs 11, 12, 13, 14 and 15, using a different batch of KCl and the purest graphite crucibles. The data from run 9, which has a long intrinsic region was used together with that from runs 6 and 10 for a fitting procedure to obtain the conductivity parameters.

TABLE 10

Run 6

$10^3/T$	-log σT	$10^3/T$	-log σT	$10^3/T$	-log σT
1.0833	2.0007	1.2950	3.8516	1.5848	4.9498
1.0999	2.1676	1.3188	3.9710	1.6122	5.0515
1.1175	2.3436	1.3411	4.0709	1.6453	5.1773
1.1350	2.5180	1.3663	4.1760	1.6785	5.3030
1.1538	2.7101	1.3924	4.2672	1.7153	5.4376
1.1718	2.8843	1.4135	4.3494	1.7569	5.6164
1.1911	3.0707	1.4405	4.4409	1.7887	5.7346
1.2097	3.2411	1.4672	4.5367	1.8292	5.8943
1.2305	3.4129	1.4968	4.6387	1.8741	6.0755
1.2532	3.5854	1.5258	4.7396	1.9169	6.2571
1.2754	3.7341	1.5572	4.8488	1.9690	6.4740

TABLE 11

Run 9

$10^3/T$	-log σT	$10^3/T$	-log σT	$10^3/T$	-log σT
1.0411	1.5831	1.1979	3.2223	1.3552	4.7283
1.0568	1.7515	1.2151	3.4012	1.3790	4.9341
1.0721	1.9207	1.2372	3.6121	1.4053	5.1492
1.0893	2.0999	1.2552	3.7829	1.4331	5.3676
1.1057	2.2746	1.2654	3.8899	1.4614	5.5999
1.1221	2.4548	1.2862	4.0804	1.4926	5.8266
1.1401	2.6388	1.3082	4.2838	1.5207	6.0137
1.1605	2.8455	1.3312	4.5058	1.5540	6.2177
1.1789	3.0339				

TABLE 12

Run 10

$10^3/T$	-log σT	$10^3/T$	-log σT	$10^3/T$	-log σT
1.0413	1.5426	1.2173	3.3562	1.4225	4.9546
1.0568	1.7094	1.2366	3.5500	1.4487	5.0656
1.0721	1.8760	1.2585	3.7479	1.4782	5.1728
1.0890	2.0501	1.2791	3.9296	1.5054	5.2734
1.1076	2.2445	1.2999	4.1307	1.5354	5.3665
1.1234	2.4179	1.3235	4.3255	1.5679	5.4768
1.1413	2.6000	1.3461	4.5031	1.6093	5.6137
1.1599	2.7897	1.3712	4.6823	1.6478	5.7374
1.1786	2.9734	1.3973	4.8290	1.6639	5.7921
1.1973	3.1601				

3.03 Conductivity of Sr^{2+} doped crystals.

Typical plots of log σT versus $1/T$ are shown in Fig.10 for runs 12 and 14. Graphs for the other runs were similar to these. The curvature due to association as described in section 1.07 is clearly demonstrated by the increasing divergence from the dotted tangents. Points taken at the highest temperatures for run 14 just show the beginning of an upward curvature into the intrinsic region. The range of measurements was restricted on the high temperature side by the onset of sublimation and at low temperatures by precipitation of the Sr^{2+}. The criterion used to ensure that precipitation was not occurring was reproducibility of conductance after 16 hours at a particular temperature. It would have been desirable to extend the range of doping. However, the inaccuracy of the Sr^{2+} analysis prevents the measurement of concentrations lower than those used here and with higher concentrations precipitation considerably limits the temperature range of the measurements.

Fig.11 is a plot of Sr^{2+} concentration against conductivity at $10^3/T = 1.1/^oK$ for all the doped crystals. Each point on the graph is labelled by its run number. The plot includes run 15 for which carbon electrodes were used, the details of which will be given in 3.04. It is

FIG 10

CONDUCTIVITY OF DOPED KCL

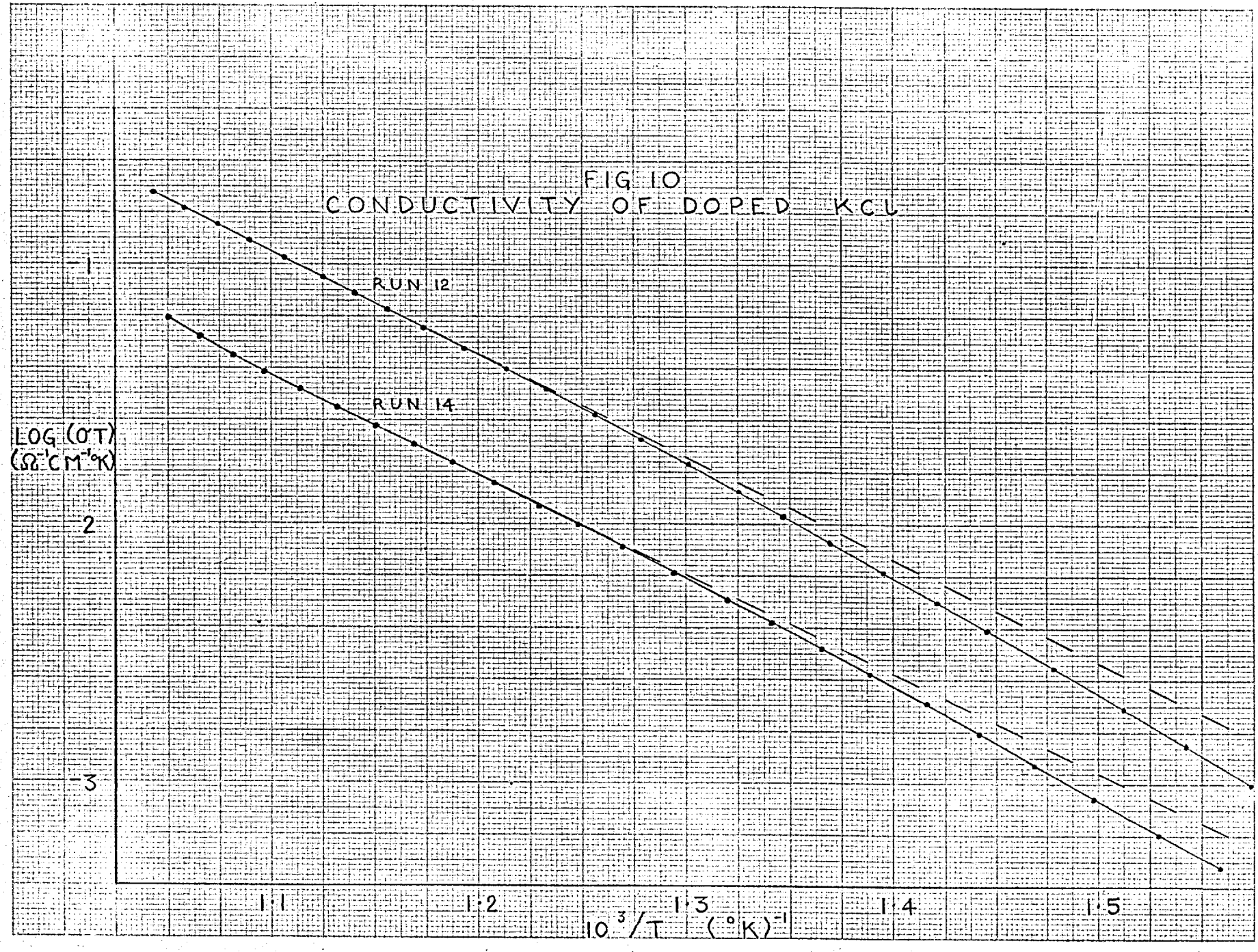

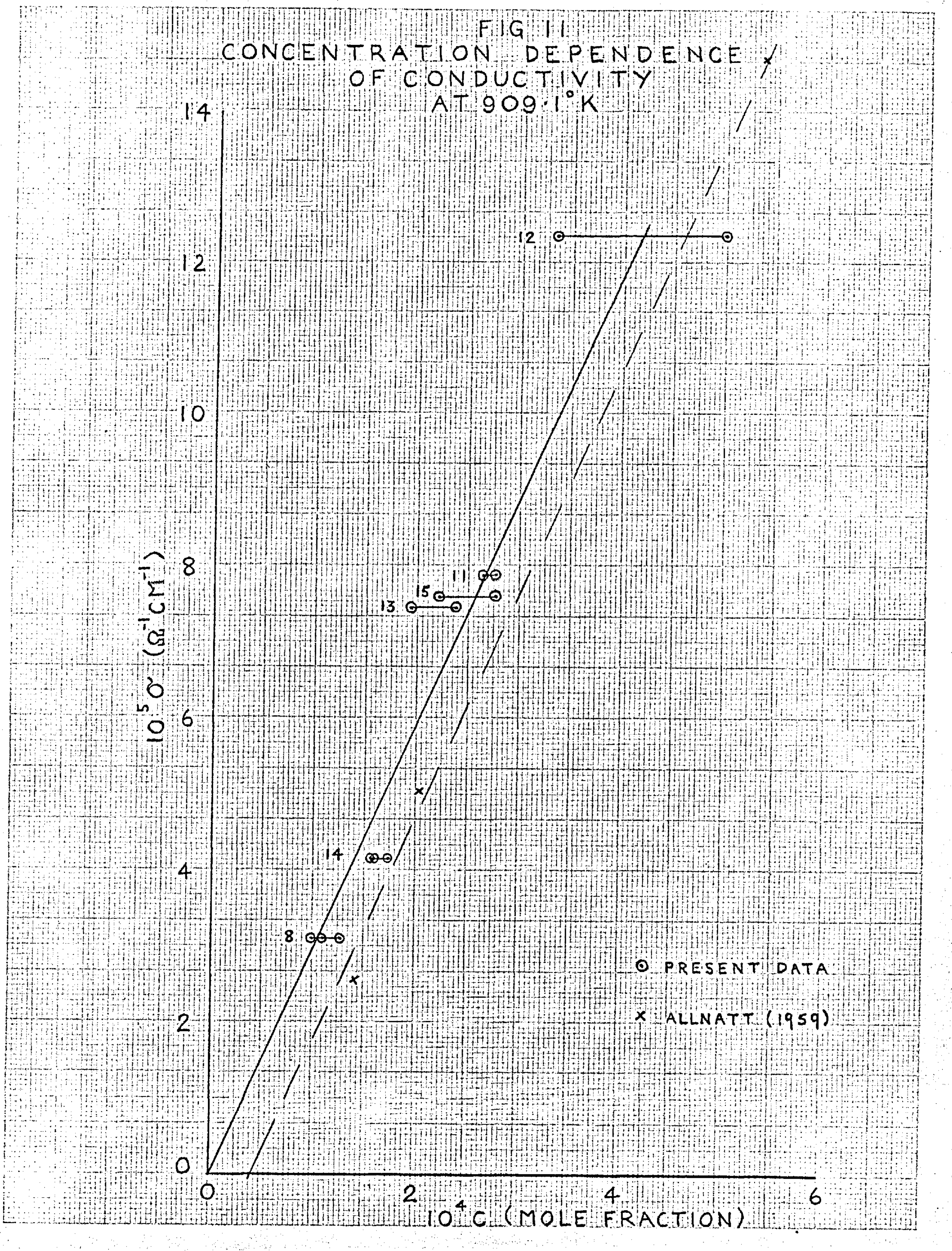
FIG 11
CONCENTRATION DEPENDENCE
OF CONDUCTIVITY
AT 909·1°K
14
12
10
8
6
4
2
0
$10^5 \sigma$ (Ω^{-1} CM^{-1})
0
2
4
6
10^4 C (MOLE FRACTION)
12
11
15
13
14
8
⊙ PRESENT DATA
× ALLNATT (1959)

clear, however, that at this temperature there is no detectable difference between the measured conductivity using carbon electrodes and that using platinum electrodes. All the concentration determinations for the conductivity specimens are plotted and the points for each run are linked by a line to indicate the errors involved in the analysis. Clearly the method used to measure the concentration was not very satisfactory and probably introduced errors far greater than those arising from the measurement of specific conductivity. A straight line has been drawn through all the points since their scatter does not justify any attempt at drawing a curve. In any case at this temperature the curvature due to association would be slight. The fact that a straight line through the origin fits the data, is good evidence for the effective removal of OH^- or any other anions which might complex with the Sr^{2+}. Ideally the line should cut the conductivity axis at a point corresponding to the conductivity of the unavoidable impurities, but since the mole fraction of these is $\sim 10^{-6}$ this intercept would be negligible on the scale in Fig.11

TABLE 13

Run 8

$10^3/T$	-log σT	$10^3/T$	-log σT	$10^3/T$	-log σT
1.0693	1.4301	1.2338	2.0758	1.4189	2.8532
1.0849	1.4928	1.2547	2.1585	1.4462	2.9721
1.1024	1.5612	1.2746	2.2453	1.4745	3.0976
1.1192	1.6276	1.2962	2.3347	1.5034	3.2286
1.1374	1.6971	1.3195	2.4295	1.5324	3.3569
1.1554	1.7657	1.3429	2.5269	1.5645	3.4990
1.1743	1.8391	1.3680	2.6343	1.6029	3.6683
1.1921	1.9129	1.3934	2.7398	1.6343	3.8134
1.2127	1.9931				

TABLE 14

Run 11

$10^3/T$	-log σT	$10^3/T$	-log σT	$10^3/T$	-log σT
1.0423	0.9148	1.2216	1.6233	1.4546	2.6154
1.0606	0.9899	1.2427	1.7071	1.4915	2.7838
1.0767	1.0554	1.2625	1.7882	1.4839	2.7549
1.0927	1.1176	1.2844	1.8792	1.5108	2.8786
1.1083	1.1784	1.3074	1.9811	1.5402	3.0087
1.1246	1.2430	1.3275	2.0633	1.5724	3.1594
1.1414	1.3094	1.3519	2.1686	1.6024	3.2987
1.1621	1.3875	1.3746	2.2691	1.6383	3.4714
1.1815	1.4648	1.4012	2.3767	1.6816	3.6763
1.2011	1.5413	1.4262	2.4917		

TABLE 15

Run 12

$10^3/T$	-log σT	$10^3/T$	-log σT	$10^3/T$	-log σT
1.0431	0.7232	1.1943	1.3241	1.3959	2.1849
1.0583	0.7839	1.2144	1.4054	1.4215	2.2986
1.0740	0.8464	1.2328	1.4823	1.4462	2.4102
1.0901	0.9101	1.2565	1.5801	1.4782	2.5540
1.1070	0.9752	1.2793	1.6767	1.5127	2.7138
1.1253	1.0460	1.3016	1.7726	1.5425	2.8487
1.1407	1.1112	1.3258	1.8738	1.5741	3.0023
1.1572	1.1758	1.3472	1.9747	1.6042	3.1465
1.1739	1.2432	1.3699	2.0731		

TABLE 16

Run 13

$10^3/T$	-log σT	$10^3/T$	-log σT	$10^3/T$	-log σT
1.0465	0.9535	1.2212	1.6433	1.4321	2.5417
1.0613	1.0154	1.2401	1.7224	1.4595	2.6609
1.0746	1.0697	1.2622	1.8112	1.4884	2.7927
1.0915	1.1365	1.2850	1.9048	1.5163	2.9192
1.1095	1.2058	1.3074	1.9999	1.5468	3.0561
1.1272	1.2735	1.3312	2.1006	1.5773	3.2007
1.1442	1.3404	1.3560	2.2069	1.6096	3.3517
1.1630	1.4167	1.3824	2.3259	1.6418	3.5027
1.1819	1.4916	1.4067	2.4297	1.6743	3.6562
1.2015	1.5671				

TABLE 17

Run 14

$10^3/T$	-log σT	$10^3/T$	-log σT	$10^3/T$	-log σT
1.0501	1.2081	1.2296	1.9321	1.4689	2.9301
1.0658	1.2811	1.2482	2.0040	1.4979	3.0580
1.0823	1.3536	1.2700	2.0915	1.5296	3.1955
1.0975	1.4154	1.2950	2.1930	1.5587	3.3234
1.1147	1.4830	1.3203	2.2927	1.5924	3.4800
1.1323	1.5503	1.3420	2.3808	1.6232	3.6260
1.1510	1.6220	1.3654	2.4795	1.6623	3.8083
1.1693	1.6925	1.3895	2.5797	1.7016	3.9900
1.1877	1.7645	1.4161	2.6930	1.7347	4.1483
1.2082	1.8438	1.4416	2.8130	1.7712	4.3342

For comparison the data obtained by Allnatt (1959) has also been plotted. A line through these points parallel to that through the present data cuts the concentration axis at $c = 4.2 \times 10^{-5}$. This may indicate that Allnatt had not effectively removed OH^- and an approximately constant concentration of this was creating an inactive concentration ($\sim 4.2 \times 10^{-5}$) of Sr^{2+} in all his crystals.

Values of log σT versus $10^3/T$ for the five runs which were analysed are collected in Tables 13-17.

3.04 Capacity measurements.

Extensive measurements were made on some of the doped crystals in order to determine the capacitance as a function of frequency of the A.C. applied field, temperature and Sr^{2+} concentration. Macdonald's space charge polarisation theory (1.09) is the most complete but his equations are very general and cumbersome; the solution was therefore re-derived and simplified for the case of KCl in the required temperature and frequency regions yielding a space charge capacitance per unit area, C_p, given by

3.04.1

$$C_p = \left(\frac{\pi kT}{\epsilon c_o}\right)^{\frac{1}{2}} \frac{4\sigma^2}{\omega^2 L^2 e} \left[1 + \frac{\pi kT}{\epsilon c_o} \frac{16\sigma^2}{\omega^2 L^2 e^2}\right]^{-1}$$

where ϵ is the low frequency dielectric constant, L the

length of the crystal and c_o the number of Sr^{2+} ions per unit volume. The data are illustrated by plotting them according to this equation, neglecting the second term in the square brackets which is small compared with unity. When this is done the expression is the same as that used by Jacobs and Maycock (1963,b) and referred to in 1.09.

From 1.07.17, when association is neglected, $\sigma(T) \propto (1/T)e^{-\Delta h_1/kT}$ thus plots of log $(C_p T^{3/2})$ versus $1/T$ should be straight lines of slope $2\Delta h_1/k$. Fig.12 shows this presentation of the data for run 12, the two lines are for capacitances measured at 1000 and 300 c/sec. Equally good straight lines were obtained for all the runs; the slight divergence at low temperatures could be due to errors in measuring the geometric capacitance. The geometric capacitance was measured at high frequencies $\sim$ 50 kc/sec. and subtracted from the low frequency capacitance to obtain C which is then equivalent to C_p. In Table 18 Δh_1 values taken from these graphs are compared with those obtained from the conductivity data over the same temperature region. Clearly these are not strictly Δh_1 values since they will be affected by association but they should be in error by the same amount for both the conductivity and capacitance in the same temperature region.

FIG 12
TEMPERATURE DEPENDENCE OF
CAPACITANCE FOR RUN 12

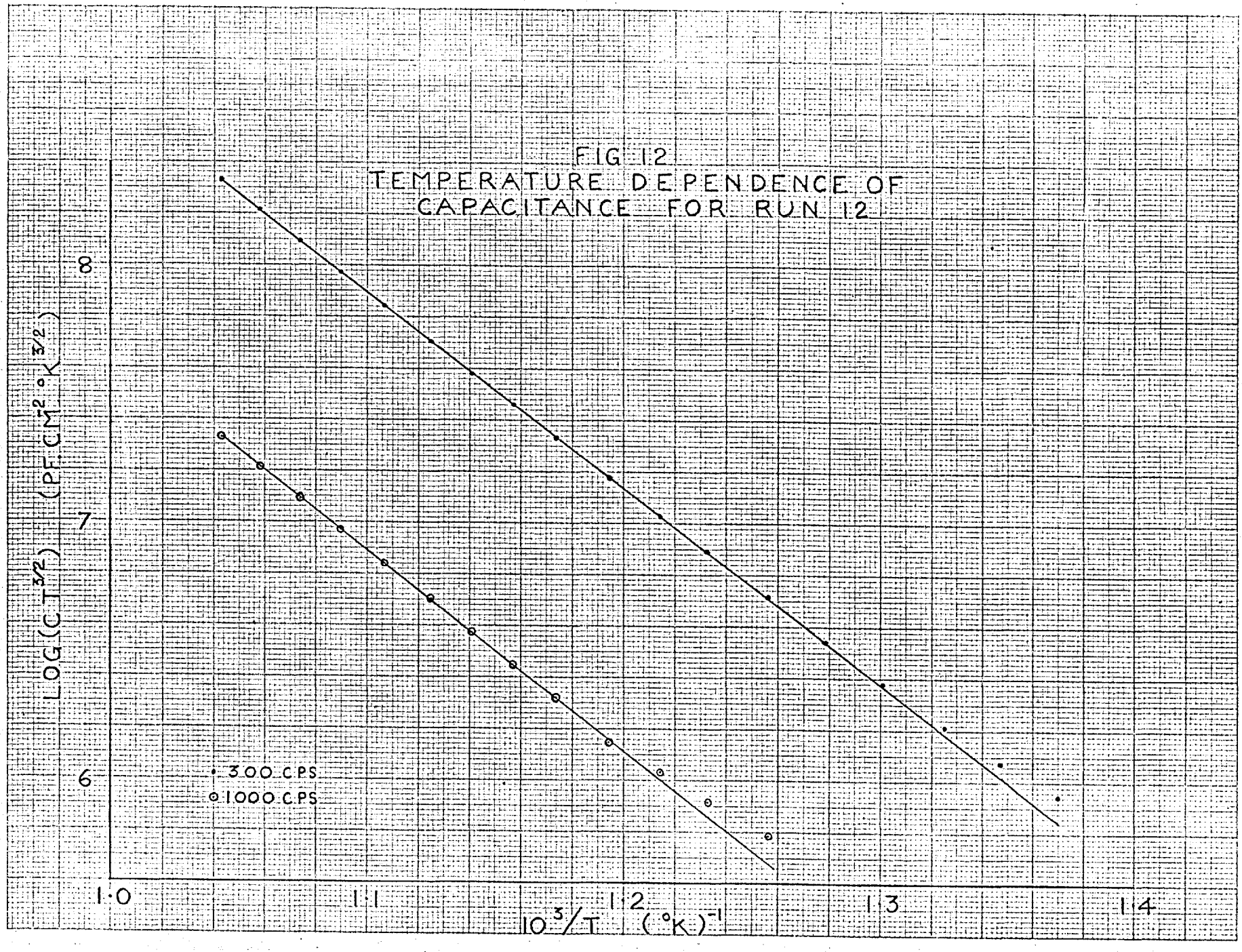

TABLE 18

Run	Δh_1 from gradient of log $(CT^{3/2})$ vs 1/T		Δh_1 from gradient of log(σT) vs 1/T
	300 c/sec.	1000 c/sec.	
11	0.737 eV	0.725 eV	0.776 eV
12	0.753 eV	0.769 eV	0.786 eV
13	0.736 eV	0.742 eV	0.776 eV
14	0.733 eV		0.772 eV

From 3.04.1, neglecting association $L^2C_p \propto c_o^{3/2}$ at a constant temperature. Since $\sigma = c_o e\mu$, a plot of log L^2C_p versus log σ should be a straight line of slope 1.5. Fig.13 shows points obtained from five runs at $10^3/T = 1.1/^oK$, each point being labelled by its run number. Graphite electrodes were used for run 15; these were two discs of specpure graphite, 3 mm. thick and 13 mm. in diameter, positioned between the crystal and the platinum electrodes. The graphite was Johnson Matthey grade 1 material J.M.21/91 containing less than 5 ppm impurities. Measurements on this crystal were confined to frequency dependence of the capacitance and a few conductivity and capacity measurements at selected temperatures. However, the same annealing procedure was performed before making the final measurements. In all cases where it was

FIG 13
VARIATION OF CAPACITANCE WITH CONDUCTIVITY

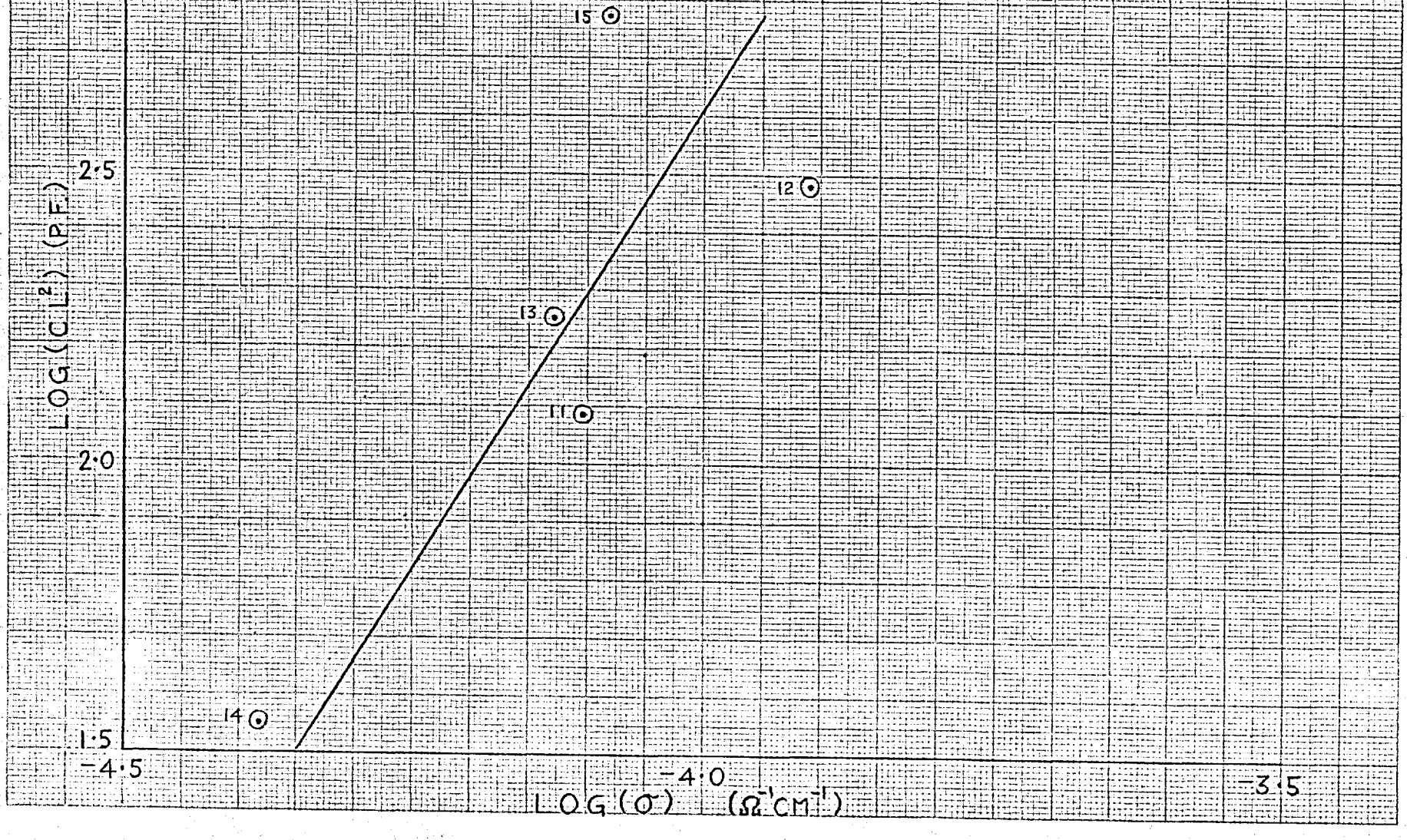

observed the capacitance fell during the high temperature anneal. For runs 12 and 15 the capacitance at 1500 c.p.s. dropped by a factor of about 3. With such large changes occurring any plot comparing magnitudes of C for various crystals might be expected to show scatter as in Fig.13. The results in this figure show a trend in the right direction but the slope of the line is 3.17.

The approximate form of 3.04.1 predicts the frequency dependence of C_p at a fixed temperature to be of the form $\omega C_p \propto 1/\omega$. Fig.14 shows the results for run 12 at a series of temperatures. The plots are almost straight lines but show definite curvature; an extrapolation of the high frequency points appears to go through the origin as required.

Several attempts were made to determine whether the capacitance being studied here showed any variation with the applied A.C. voltage. Within the experimental error, however, no voltage dependence of the capacitance was observed for applied potentials between 0.04 and 45 volts. As each measurement of capacitance as a function of frequency was accompanied by a resistance measurement, this amounted to a very thorough search for frequency dependence of resistance. Where platinum electrodes were

FIG 14

FREQUENCY DEPENDENCE OF CAPACITANCE FOR RUN 12 (L=0·326 CM)

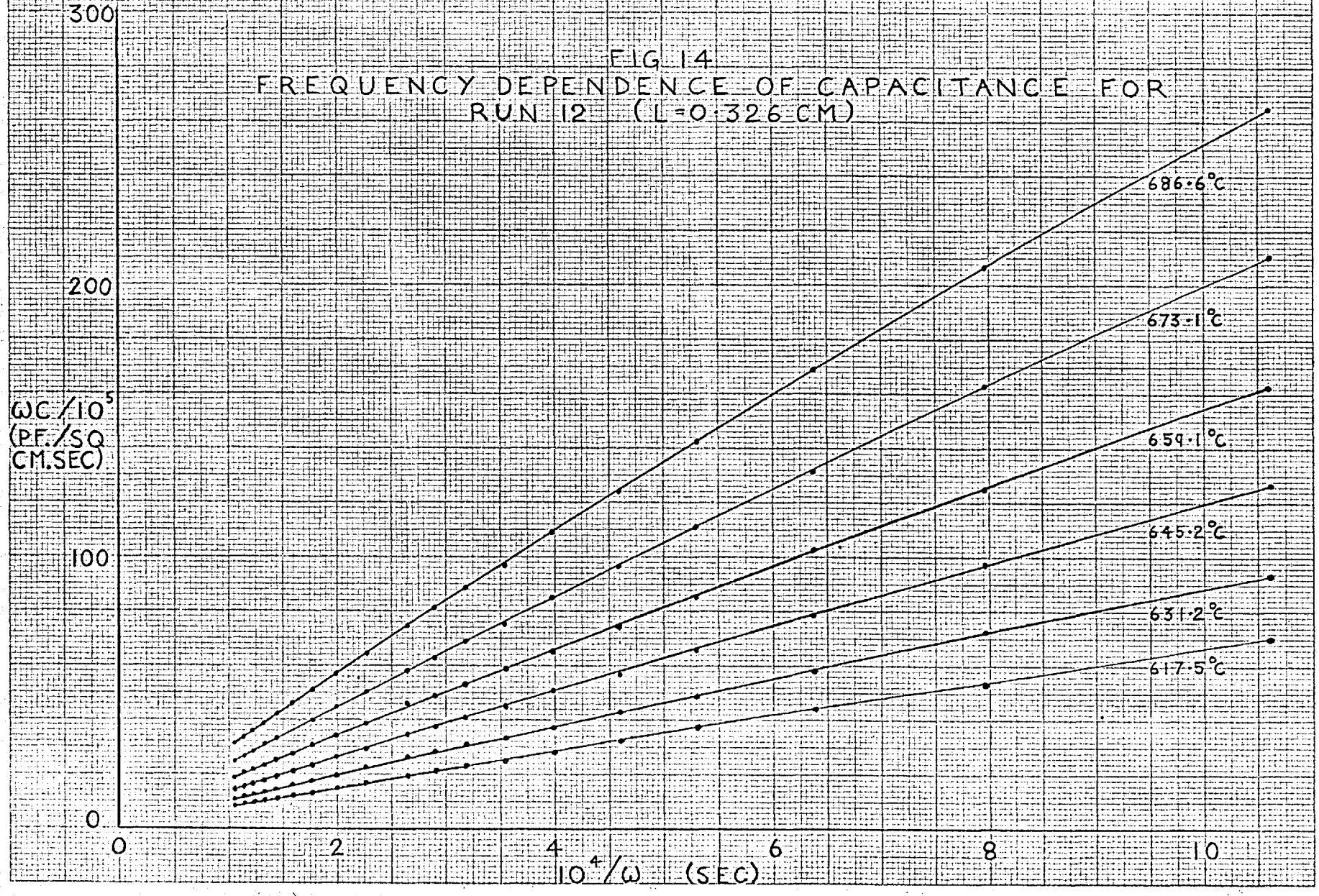

FIG 15
FREQUENCY DEPENDENCE OF CONDUCTANCE FOR RUN 15 ($L = 0.349$ CM, $A = 0.496$ CM^2, R AT $f = 1500$ CPS IS $2.460 \times 10^{-4}\Omega$ AT 557°C AND $1.277 \times 10^{-4}\Omega$ AT 612°C

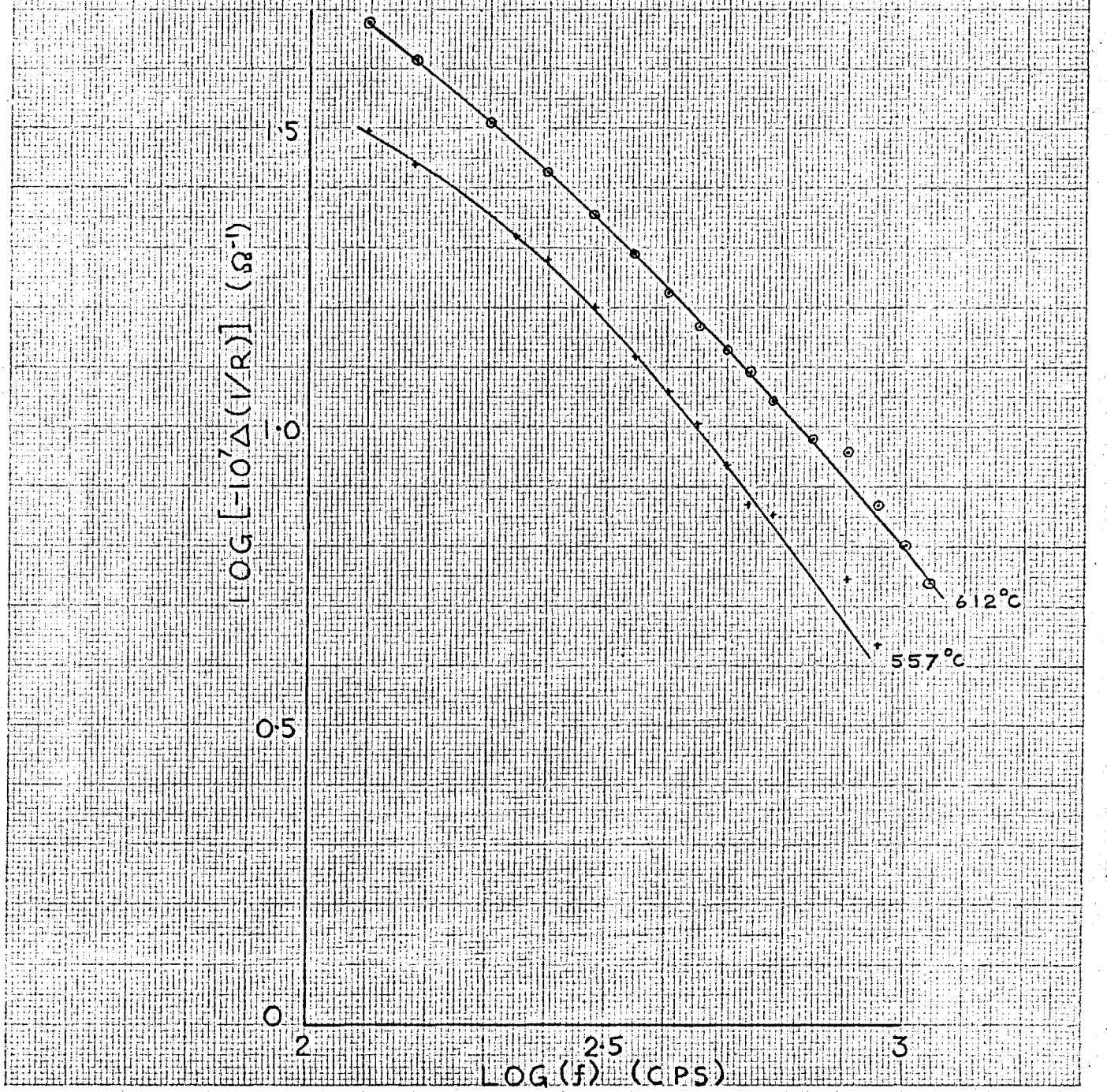

used, the resistance of the doped crystals increased by about 1% in going from 1500 to 125 c/sec. Although this change was too small to be studied it was definitely present. However, when graphite electrodes were used (run 15) a variation over the same frequency range of about 10% was observed prior to annealing. This is still rather small but the results are plotted in Fig.15 as log $\Delta(1/R)$ against log f where $\Delta(1/R)$ is the increase in conductance at a particular frequency f, over that measured at 1500 c/sec. After annealing the variation in resistance from 1500 to 125 c/sec. dropped to about 3%.

4. DISCUSSION

4.01 General comments.

Fig.6 shows the very good agreement in the intrinsic regions of the conductivity measurements from runs 4, 5 and 6. This reproducibility is also apparent from the conductivity values at $10^3/T = 1.1/^oK$ (Table 7) where the variation in σ is only 2%. The crystals for these three runs were grown in carbon (Table 6). The two crystals grown in silica, runs 1 and 9, have a noticeably lower conductivity, the difference being far greater than the experimental error in an individual measurement. It is, however, possible that such an error could arise from a poor contact between the crystal and the electrodes. There may be some significance in the fact that there is better agreement among crystals grown in crucibles made of the same material but it is not possible to come to any definite conclusions. Very great care was taken to ensure that good contact with the electrodes was achieved on the doped crystals. On the basis of these earlier runs on pure KCl it was felt that it was probably better to apply sufficient pressure to the electrodes to cause a little distortion of the crystal, rather than run the risk of a poor contact.

Graphite was chosen as a crucible material for all the crystals except that used in run 1 for it was found that a far greater degree of crystal perfection was obtained than for crystals grown in silica. Although no dislocation counts were made, silica grown crystals often had curved cleavage planes and multi-faceted surfaces, both of which were absent in the crystals grown in graphite. A further reason for using these crucibles was that it would be thermodynamically more favourable for the chlorine to oxidise anionic impurities in the presence of carbon. The two disadvantages of graphite are its greater impurity content over that of silica and a tendency for the crystals to twin as a result of nucleation on the relatively rough crucible walls. For the doping levels used, the impurities in the purest graphite available (Johnson Matthey EYC 110) were insignificant.

The curvature in the intrinsic region (Fig.7) cannot be represented by an expression such as 1.07.15, containing only one exponential term. Furthermore it is unlikely that this curvature is an experimental artefact since it has been noted previously (Allnatt and Jacobs, 1962; Gründig, 1965). The simplest interpretation of this is in terms of anion and cation vacancies with sufficiently similar mobilities to necessitate the retention of the two

exponentials in 1.07.13. The mobilities must be slightly different in order that the approximation 1.07.15 should not hold. Allnatt and Jacobs assumed that a tangent to the low temperature end of the intrinsic region represented the contribution of the cations. As outlined in 1.08 Grûndig obtained $|\Delta h_1 - \Delta h_2| = 0.22$ eV by simply taking the difference of high and low temperature slopes of the intrinsic region. This technique of drawing tangents is open to criticism (Rolfe, 1964). Since the curvature is relatively slight, there is no genuine criterion as to where tangents should be drawn to represent a given physical situation. The inaccuracies inherent in this method are shown by the complete lack of agreement between $|\Delta h_1 - \Delta h_2|$ obtained by Grûndig and the same quantity derived from the results of Allnatt and Jacobs, namely 1.70 eV (Table 4).

In this work (4.02) the results have been analysed according to the complete expression 1.07.12 in conjunction with values of x_1 and x_2 derived from 1.06.7 and 1.06.2.

The dramatic fall in extrinsic conductivity after exposure of the crystal to water vapour and oxygen (Figs.8 and 9) has not been reported before. Unfortunately, in these experiments the results show that sufficient care was not taken to introduce definable atmospheres and

identify their individual effects. Thus the drop in conductance after exposure to 'white spot' nitrogen might be due to traces of water or oxygen or a combination of the two. In a normal conductance run both of these impurities are removed from the nitrogen before allowing it to enter the cell.

There are two obvious interpretations of the effect of oxygen and/or water vapour. Either there is diffusion of some species from the gas phase into the crystal bulk which prevents impurities from contributing to the conductivity, or the crystal surface adjacent to the electrodes is attacked producing an interfacial resistance. The latter explanation is unlikely since it would require strict limitations on the conductance of the layer as a function of temperature. The layer conductance would be required to have the same type of temperature dependence as KCl in the extrinsic region but be lower in magnitude (Fig.8), whereas at high temperatures it would have to be much larger than the bulk conductance of KCl in order to explain the constancy of conductivity in the intrinsic region.

On the basis of results outlined in 1.08 the depression of extrinsic conductivity might arise from complexing of

the impurities with OH^- diffusing into the crystal. The OH^- may be formed on a crystal surface thus

4.01.1 $$H_2O + Cl^- \rightleftarrows OH^- + HCl$$

One objection to this is the lack of an OH^- absorption band at 204 mμ; for although impurity-OH^- complexes show no such absorption, there would have to be a substantial proportion of substitutional OH^- to impurities, before diffusion processes enabled complexing of 93% of the impurities (Fig.9). In support of this, although reaction 1 probably occurs in the melt in the presence of oxygen (Patterson, 1962), there have been no reports of the introduction of OH^- by simply heating a crystal in an atmosphere of water vapour and oxygen. A reaction between molten NaCl and dry oxygen with the liberation of chlorine has been observed by Otterson (1960). Two possible processes are

1.04.2 $$O_2 + Cl^- \longrightarrow O_2^- + \tfrac{1}{2}Cl_2$$

1.04.3 $$\tfrac{1}{2}O_2 + 2Cl^- \longrightarrow O^{2-} + Cl_2$$

The evidence for 2 has already been given (1.08) but there is no obvious reason why O_2^- should reduce the extrinsic conductivity. However, O^{2-} could combine with M^{2+} to form a complex occupying two lattice sites with the loss

of a vacancy. The only evidence for O^{2-} in alkali halides comes from Watkins (1959) who attributed an e.s.r. spectrum in Mn^{2+} doped KCl, NaCl and LiCl to a manganese ion adjacent to an ion such as S^{2-} or O^{2-}. There is a further possibility, namely that H_2O may be diffusing directly into the KCl. Such a process has been studied recently by Penley and Witte (1964) and Gründig et al. (1965). If H_2O diffused through the KCl only reacting with some M^{2+} ions to form $M(OH)_2$ or MO this would account for the lack of an OH^- band at 204 mμ. Such a scheme would not be unreasonable on chemical grounds.

The work of Kummer and Youngs (1962) suggests there is a tendency for Ca^{2+} in NaCl to concentrate in regions near the surface. However, the results were obtained using what was likely to be polycrystalline NaCl or at best very imperfect crystals. This combined with the high doping levels used makes it possible that $CaCl_2$ may have been precipitating over the large surface area exposed to the acetone which they used to leach out surface $CaCl_2$. It would be interesting to carry this work a stage further as some interest has been shown in the theoretical interpretation of the result (Allnatt, 1964). Since X-ray fluorescence arises from a thin region near to the surface exposed to the X-ray beam it might be possible to assess

surface concentrations of e.g. Sr^{2+} in large single crystals of KCl. To obtain a better understanding of the present work an experiment could be devised in which the conductance of a large single crystal of KCl doped with $SrCl_2$ was measured before and after exposure to oxygen and water vapour. All the outer surfaces of this crystal could then be cleaved off and the conductance of the interior portion remeasured. If the extrinsic conductivity of the centre section showed a similar drop to that of the crystal as a whole, Sr^{2+} may be diffusing to the surface and reacting with O_2 or H_2O; this could be verified by X-ray fluorescence analysis of the outer sections of the crystal. If the analysis showed no excess concentration then the drop in conductance could be ascribed to complexing with anions throughout the entire crystal. Alternatively the centre section may have a specific conductance similar to that of the original crystal before exposure to $O_2 + H_2O$. This would indicate the process was confined to a surface region and arose from a reduction of surface conductance.

4.02 Treatment of conductivity data.

There is no exact, direct analytical procedure which can be employed to determine the conductivity parameters from the available data. As mentioned in 1.07 a determination of the mobility ratio $\phi = \mu_2/\mu_1$ usually involves approximations, an exact method is only possible when $\phi > 1$ then from 1.07.25 and 26, σ/σ_0 exhibits a minimum given by $\sigma/\sigma_0 = 2\sqrt{\phi}/(1 + \phi)$. Unfortunately in KCl $\phi < 1$ and the method does not apply. The only attempt at determining ϕ for KCl has been described above and involves the somewhat dubious procedure of drawing tangents to the intrinsic region. Rolfe (1.08) with the additional information provided by anion doping had to neglect association at high temperatures in the extrinsic region in order to find ϕ for KBr.

For these reasons it was decided that a better approach might be to compute theoretical log (σT) versus 1/T curves and obtain the parameters by fitting these curves to the experimental results. In order to achieve this an autocode program was written for the Atlas computer (the actual program is given in Appendix 1). The fitting was accomplished using Atlas Routine 970 (Rossenbrook, 1960) provided by the London University Institute of Computer Science. This routine, based on the method of steepest

descents, will find the position of the minimum of a function of several variables. To fit the data the function F was to be minimised

4.02.1

$$F = 100 \left[\frac{1}{L-1} \sum_{L} [\log (\sigma T) \text{ calculated} - \log (\sigma T) \text{ experimental}]^2 \right]^{\frac{1}{2}}$$

where L is the number of data points. The way by which log (σT) was calculated, starting with the conductivity parameters is as follows. K_1 and K_2 were computed from the expressions

1.02.19 $$K_1 = e^{-(h-Ts)/kT}$$

1.06.9 $$K_2 = 12e^{5/kT}$$

The cubic equation,

1.06.7 $$x_2^3 + x_2^2(c + K_1K_2) - x_2K_1 - K_2K_1^2 = 0$$

was then solved for x_2 using the numerical values of K_1, K_2 and the mole fraction of divalent impurities c. In order to determine the nature of the roots of 7 the discriminant Δ was examined

4.02.2

$$\Delta = K_2^2K_1^4 - \frac{2}{3}(c + K_2K_1)K_2K_1^3 - \frac{4}{27}K_1^3 - \frac{4}{27}(c + K_2K_1)^3K_2K_1^2 - \frac{1}{27}(c + K_2K_1)^2K_1^2$$

The only positive term in Δ is $K_2^2K_1^4$; on collecting similar terms this is reduced to $\frac{8}{27} K_2^2K_1^4$. By comparison with the term, $-\frac{4}{27} K_1^3$, it is seen that a sufficient condition for Δ to be negative is

$$1 > 2K_2^2K_1$$

Typical values of K_1 at the highest temperature are about 10^{-10} and $K_2 \sim 5 \times 10^3$ for $\zeta = 0.5$ eV and with these values the condition is fulfilled. Since the discriminant is negative, the cubic will have three real roots and may be solved by the trigonometrical method. The solution is

4.02.3

$$x_2 = \left[\frac{4}{3}[K_1 + \frac{1}{3}(c + K_2K_1)^2]\right]^{\frac{1}{2}} \cos[\tfrac{1}{3}(2n\pi \pm \theta)] - \tfrac{1}{3}(c + K_2K_1)$$

$$\text{where } \theta = \cos^{-1}\left[\frac{[K_2K_1^2 - \frac{2}{27}(c + K_2K_1)^3 - \frac{K_1}{3}(c + K_2K_1)]3\sqrt{3}/2}{[K_1 + \frac{1}{3}(c + K_2K_1)^2]^{3/2}}\right]$$

By Descartes' rule of signs the cubic 1.06.7 will have 1 positive and 2 negative roots; clearly it is the positive root which is required. This root will occur for the maximum of the three values for the trigonometrical term in 3, since the remaining term is negative; it was obtained by setting $n = 0$ and finding the value of θ between 0 and $\pi/2$. Although this method is correct it

failed in the extrinsic region when x_2 is a small difference of two relatively large numbers represented by the two terms in the expression for x_2. This was overcome by obtaining x_2 at the highest temperature using the above equation; x_2 at the next temperature was found by Newton's method using x_2 from the highest temperature as a starting value. This procedure was repeated for all the following determinations, the previous value being used as a first approximation for Newton's method. To ensure this technique was working, a print out of x_1, x_2, K_1 and K_2 was obtained for a pure crystal and the crystal with the highest doping level. The cubic was found to be satisfied at all temperatures when the appropriate values were substituted in it. Having found x_2, the value of x_1 was obtained from

1.06.2 $$K_1 = x_1 x_2$$

The mobilities of the defects were computed from 1.07.9 thus

4.02.4 $$T\mu_1 = \frac{4ea^2\nu_1}{k} e^{-(\Delta h_1 - T\Delta s_1)/kT}$$

4.02.5 $$T\mu_2 = \frac{4ea^2\nu_2}{k} e^{-(\Delta h_2 - T\Delta s_2)/kT}$$

Since it is not clear what numerical values should be

inserted for ν_1 and ν_2 they were both set equal to $\nu = 4.25 \times 10^{12} sec^{-1}$. This value is the frequency for transverse vibrations in KCl as determined from I.R. absorption measurements (Barnes, 1932). One might anticipate that the actual frequencies would be less than ν but in the absence of more precise information no accurate values could be used for ν_1 and ν_2. The value used for ν has no effect on any of the parameters except Δs_1 and Δs_2 and a self-consistent correction for this can be made later. Log (σT) was then obtained from the expression for σT which is,

$$\sigma T = Ne(T\mu_1 x_1 + T\mu_2 x_2)$$

There are in all 8 conductivity parameters Δh_1, Δs_1, Δh_2, Δs_2, h, s, ζ and c. This is a large number for a fitting routine and the final answer is slightly dependent upon the initial guesses and the order in which the parameters are varied by Routine 970. The main program was written in such a way as to allow any desired order of the parameters to be chosen, and each parameter to be either held constant or varied. The initial approximate parameters were based on Allnatt's results (Table 4). Δs_1 and Δs_2 needed to be corrected since the value of a (equations 4 and 5) was taken by Allnatt

to be the cation-cation separation, $a\sqrt{2}$; whereas it should be the anion-cation separation, a (the distance travelled in the direction of the field, 1.07.6). In addition, $\nu = \nu_1 = \nu_2$ was taken as $4.51 \times 10^{12} sec^{-1}$ by Allnatt. With these two corrections in the pre-exponential of 4 the value of Δs_1 becomes

$$10^3 \Delta s_1 = 0.114 - 10^3 k \ln(\tfrac{1}{2} \times 4.25/4.51)$$

$$\Delta s_1 = 0.179 \times 10^{-3} \text{ eV/deg.}$$

A number of different values of Δh_2 and Δs_2 were tried as considerable errors could be introduced by Allnatt's method of finding these. This is shown above where $|\Delta h_1 - \Delta h_2|$ found by Gründig and by Allnatt are vastly different.

Values for the parameters were found by fitting the data for the pure crystals used in runs 6, 9 and 10. Run 9 was included in the hope that the long intrinsic region, showing definite curvature, would enable a better estimate of Δs_2 and Δh_2 to be arrived at. It was found necessary while doing this to prevent the fitting routine from making c negative, for when this occurred the program faulted as the inverse cosine in 3 went out of range. To rectify this a large number was put into F whenever c went negative; the fitting routine recorded this as a

bad fit and so made c positive again. The only other difficulty encountered was with run 9. Since there is very little extrinsic conductivity data for this run the data fit is very insensitive to $\mathcal{S}$. Thus $\mathcal{S}$ had to be held constant to prevent the fitting routine from changing it drastically in an attempt to alter F. The final fit was obtained from a program in which F was minimised for each crystal for all eight cyclic permutations of the fitting order of the parameters, one of which is h, s, $\mathcal{S}$, c, Δh_1, Δs_1, Δh_2, Δs_2. Having found a set of parameters yielding the lowest F values for the three pure crystals, the data for each of the doped crystals was fitted allowing only Δs_1, Δh_1 and $\mathcal{S}$ to vary. The value of c was fixed at the average of the two values determined by X-ray fluorescence and the other parameters were held at the average values from fitting the data for the pure crystals. All six permutations of order of the three parameters were tried for each run. Finally c was allowed to vary in addition to Δs_1, Δh_1 and $\mathcal{S}$ and fits were obtained for the four cyclic permutations of $\mathcal{S}$, c, Δh_1, Δs_1.

The accuracy with which the theoretical curve of log σT versus 1/T fits the data is demonstrated in Figs.16 and 17 for the pure crystal used in run 6 and Figs.18 and

and 19 for the data from run 8; the best fit is plotted in each case. The parameters and F values for the best fits of the pure crystals are listed in Table 19. The value of ξ for the best fit of run 6, was 0.430 eV. Where several fits are almost as good they are all included in Table 19.

TABLE 19

Conductivity parameters obtained from the best fits of the data for the pure crystals.

Run	F	h (eV)	s (10^{-3} eV/deg.)	Δh_1 (eV)	Δs_1 (10^{-3} eV/deg.)	Δh_2 (eV)	Δs_2 (10^{-3} eV/deg.)
6	1.42	2.252	0.463	0.711	0.156	1.045	0.543
9	2.12	2.250	0.461	0.708	0.156	1.071	0.551
9	2.16	2.250	0.461	0.709	0.155	1.062	0.544
9	2.17	2.250	0.460	0.709	0.155	1.060	0.542
10	1.54	2.276	0.462	0.708	0.156	1.016	0.535
10	1.58	2.273	0.466	0.708	0.155	1.021	0.535
Average of means for each run		2.259	0.463	0.709	0.155	1.043	0.541

Every fit which was obtained is not included as variations in the parameters for a given run were less than the overall variations in Table 19. Values of log ($\sigma_i T$) and

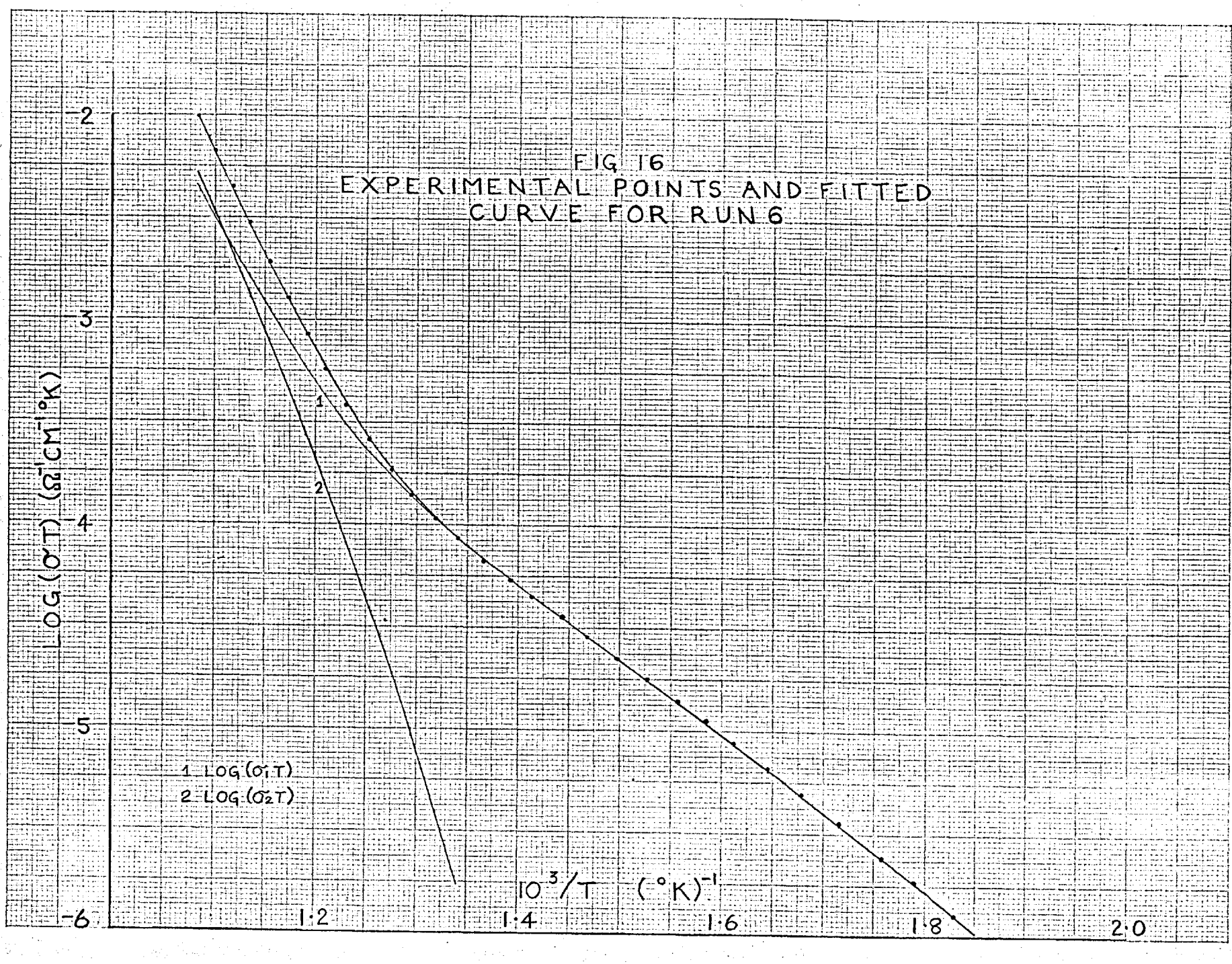
FIG 16
EXPERIMENTAL POINTS AND FITTED CURVE FOR RUN 6
LOG (σT) (Ω⁻¹CM⁻¹°K)
-2
-3
-4
-5
-6
1
2
1 LOG (σ₁T)
2 LOG (σ₂T)
10³/T (°K)⁻¹
1·2
1·4
1·6
1·8
2·0

FIG 17
DIFFERENCE PLOT FOR THE FIT
OF RUN 6 F = 1·42

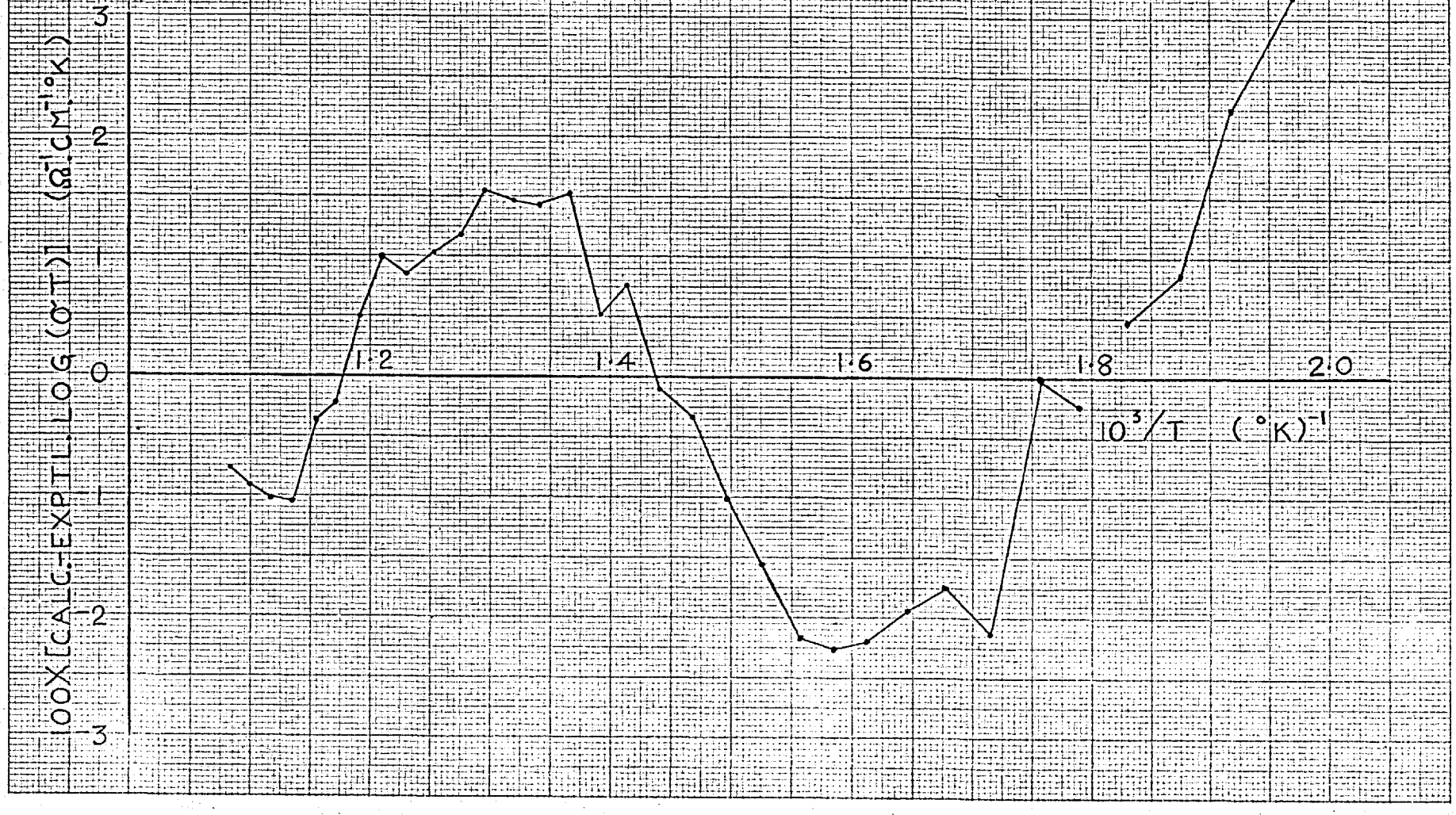

FIG 18
EXPERIMENTAL POINTS AND FITTED CURVE FOR RUN 8

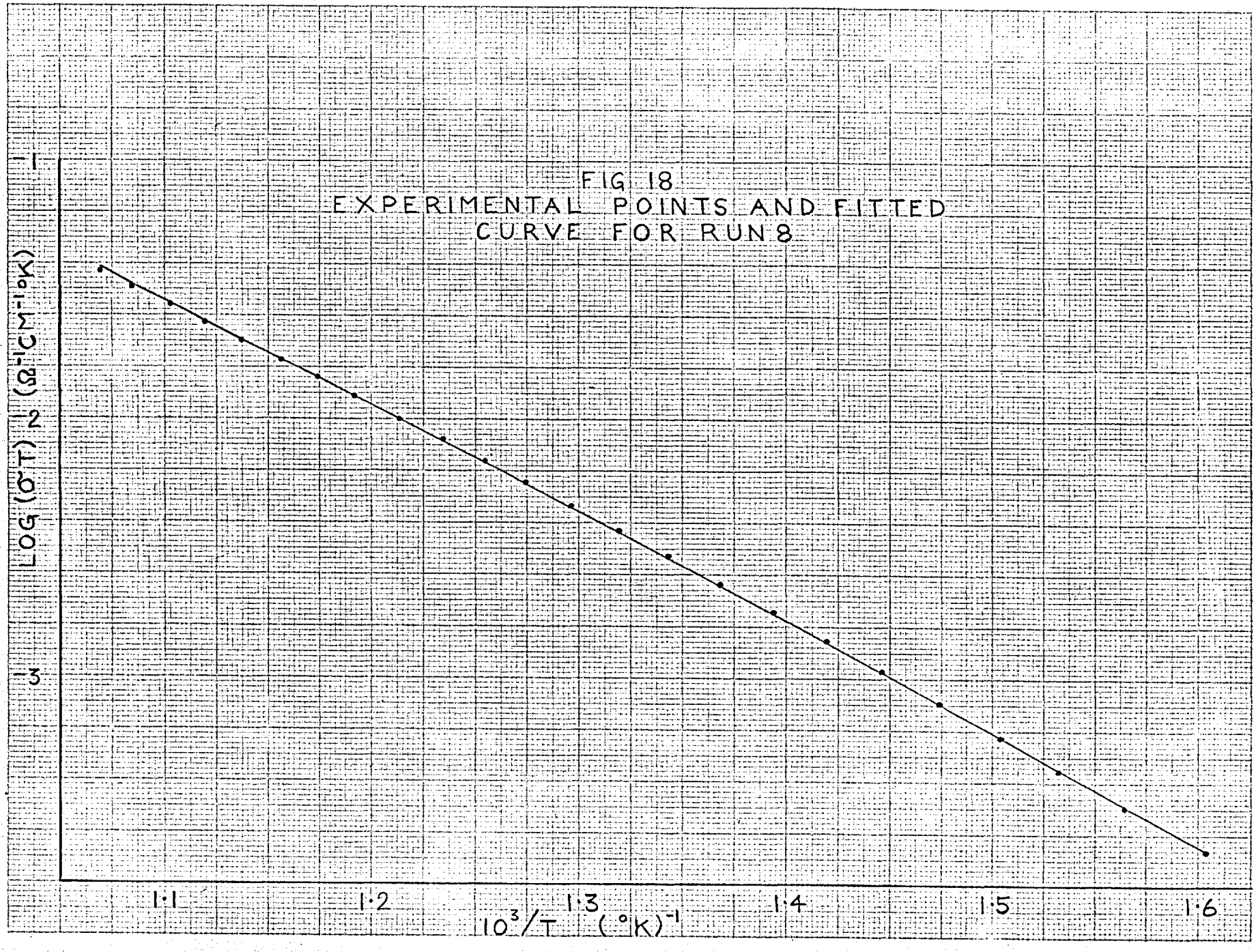

FIG 19
DIFFERENCE PLOT FOR A FIT
OF RUN 8 F=0·908

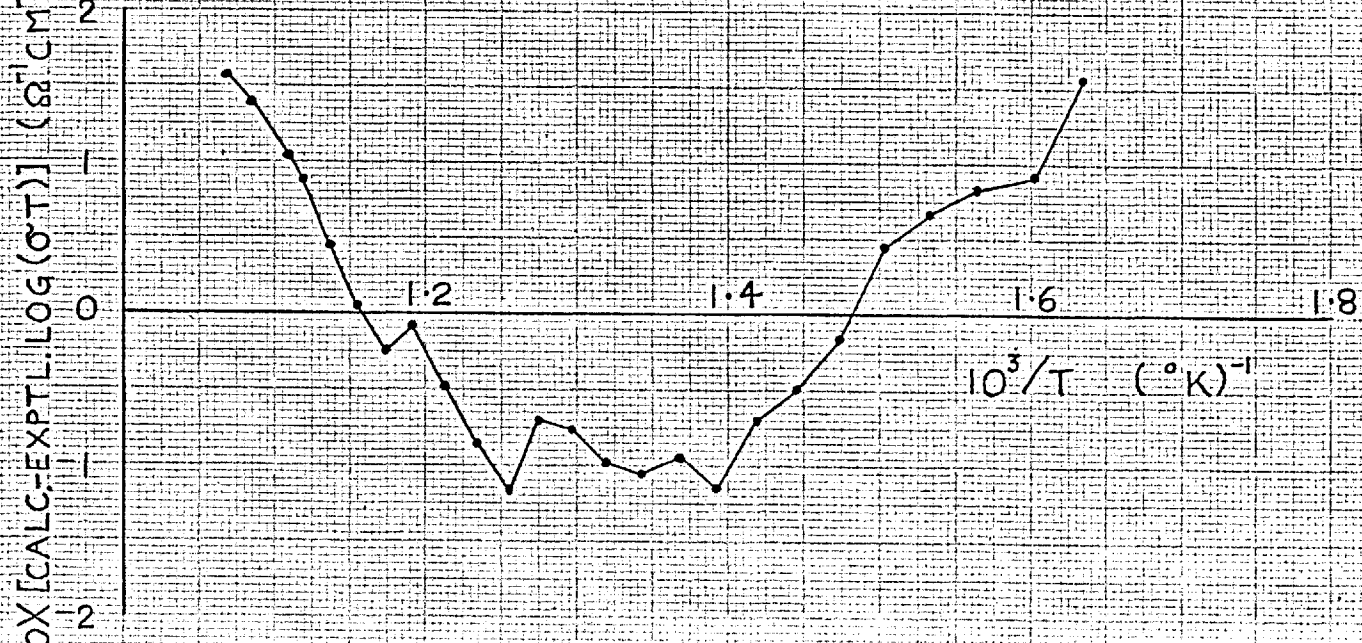

log ($\sigma_2 T$) computed from the best fit parameters for run 6 (Table 19) have also been plotted in Fig.16. Two observations may be made from these. The first is that it is not valid to draw a tangent to log (σT), just above the knee and assume it represents log ($\sigma_1 T$) (4.01). The second stems from the curvature of the log ($\sigma_1 T$) and log ($\sigma_2 T$) plots above the knee temperature. This demonstrates that the impurities are influencing conductance above the knee since when $x_1 >> c$, plots of log ($\sigma_1 T$) and log ($\sigma_2 T$) should be straight lines. This is confirmed by the experimental data (Fig.8) which shows that although the knee is at about $10^3/T = 1.3/^oK$ results taken after oxygen treatment indicate the conductivity is only intrinsic above $10^3/T = 1.2/^oK$.

Fig.20 shows t_1 the transference number for the cation vacancies, computed from the best fit parameters for runs 6, 9 and 10. For comparison the values obtained by Kerkhoff and the single value of Haven (1.08) are also included. Now from 1.08.1

$$t_1 = 1/(1 + \sigma_2/\sigma_1)$$

thus when $c << x_1$ i.e. at high temperatures for a pure crystal, this may be combined with the two terms from 1.07.14 giving

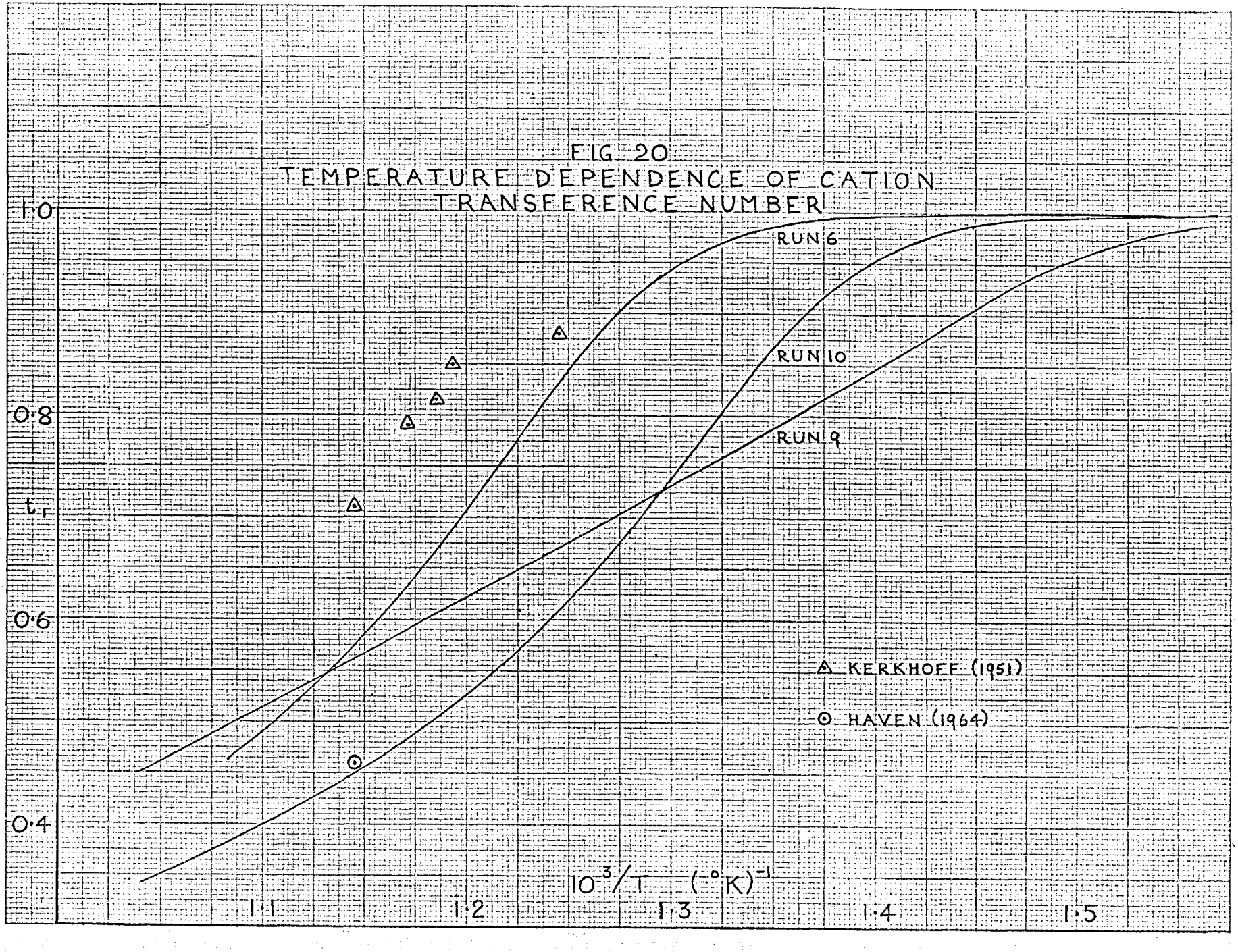
FIG 20
TEMPERATURE DEPENDENCE OF CATION TRANSFERENCE NUMBER
1·0
0·8
0·6
0·4
t_+
RUN 6
RUN 10
RUN 9
KERKHOFF (1951)
HAVEN (1964)
$10^3/T$ (°K)$^{-1}$
1·1
1·2
1·3
1·4
1·5

$$t_1 = 1/\{1 + \exp[T(\Delta s_2 - \Delta s_1) + \Delta h_1 - \Delta h_2]/kT\}$$

This condition should be well satisfied for runs 10 and 9 at the highest temperatures but small variations in Δs_1, Δs_2, Δh_2 and Δh_1 will have a considerable effect upon t_1 which is sensitive to the relatively small differences in these parameters. This largely accounts for the lack of agreement of the high temperature data in Fig.20; however, for run 6 the impurity level is sufficiently high to affect t_1 up to temperatures at least as high as $10^3/T = 1.2/^oK$. Of the three sets of data, that for run 10 is probably the most reliable. The measurements for this run extend to higher temperatures than those for run 6 giving more scope for the fitting routine to determine accurate values of Δh_2 and Δs_2, the effect of anion conduction being significantly more dominant in this region. In addition run 10 had an extremely good fit over the intrinsic region. Although the measurements for run 9 also extend to high temperatures, the fit for this was not as good as that for run 10, probably because there was very little data in the extrinsic region to help locate the parameters. The single value found by Haven agrees well with the data for run 10. This may be somewhat fortuitous but it seems very clear that

Kerkhoff's values are too high. These lie on a curve almost parallel with that for runs 10 and 6 in a region where impurities are still influencing t_1. This would indicate that the crystal used for his measurements was more impure than that used for run 6. This observation is confirmed by the conductivity measurements taken by Kerkhoff after performing his transference number measurements. These show the knee at $10^3/T = 1.2/^oK$, whereas for run 6 it was at $10^3/T = 1.3/^oK$.

From equation 1.02.17

$$s = -kz[\ln(\nu_A^V/\nu) + \ln(\nu_B^V/\nu)]$$

Thus assuming $\nu_A^V = \nu_B^V = \nu'$ it is possible to calculate the ratio of the frequency of the nearest neighbours to a vacancy along the line joining the vacancy and nearest neighbour centres ν' to their frequency in the absence of the vacancy ν . Using the average value of $s = 0.463 \times 10^{-3}$ eV/deg.(Table 19)

$$\nu/\nu' = 1.56$$

This may be compared with the values of 1.96 for KCl (Allnatt and Jacobs, 1962), 1.32 for NaCl (Etzel and Maurer, 1950) and 1.51 for KBr (Rolfe, 1964). If ν is taken as 4.25×10^{12}/sec, which is the frequency of transverse vibrations in KCl as found from absorption measurements

(Barnes, 1932), then $\nu' = 2.72 \times 10^{12}$/sec.

The presence of a vacancy will probably reduce the vibrational frequency of the next nearest neighbour ions, though not to the same extent as it affects the nearest neighbours. However, a lower limit for the effective frequency of the next nearest neighbours to the vacancy may be obtained by equating it to ν'. (This is a somewhat inconsistent approach since the derivation of the expression used to calculated ν' (1.02) only assumed nearest neighbours were affected but this will not affect the fact that ν' is a lower limit). For consistency upper limits may be calculated for Δs_1 and Δs_2, the only two parameters dependent upon the value taken for the next nearest neighbour vibrational frequency. The upper limits are

$$10^3 \Delta s_1 = 0.155 + 10^3 k \ln (4.25/2.72)$$

$$10^3 \Delta s_1 = 0.155 + 0.038$$

$$\Delta s_1 = 0.193 \times 10^{-3} \text{ eV/deg (upper limit value)}$$

similarly

$$\Delta s_2 = 0.579 \times 10^{-3} \text{ eV/deg (upper limit value).}$$

The concentrations of impurities in the pure crystals, as found from the fitting procedure are for run 6,

1.75×10^{-6}; for run 9, 6.7×10^{-8}; and for run 10, 4.2×10^{-7} mole fraction. These are in the correct order according to the relative positions of the extrinsic regions.

Table 20 lists the average values of the parameters for the doped crystals. The range refers to the F values for which an average was taken; thus a range of 5% means that the average is over all the fits with an F value within approximately 5% of that for the best fit for that particular run. Included within these averages are the parameters obtained when c was allowed to vary. The variations in ζ and Δh_1 when c was allowed to vary were well within those when c was fixed at the analysed values. It is clear from the scatter in Fig.11 that c was not known very precisely. To show this did not significantly affect the determination of ζ and Δh_1, Table 21 lists average values of the parameters obtained in an earlier fitting run. For these, the value of c was fixed at that determined by the first X-ray fluorescence analysis (Table 5) and the other parameters were fixed at $\Delta h_2 = 1.00$ eV, $\Delta s_2 = 0.472 \times 10^{-3}$ eV/deg, $h = 2.28$ eV, $s = 0.469 \times 10^{-3}$ eV/deg. The general agreement between these two sets of values demonstrates that ζ and Δh_1 are not very

TABLE 20

Conductivity parameters obtained by fitting the data for the Sr^{2+} doped crystals

Run	Range	F	No. averaged	Δh_1 (eV)	Δs_1 (10^{-3} eV/deg.)	ζ (eV)
8	1%	0.995-1.02	5	0.707	0.143	0.434
	5%	0.995-1.02	5	0.707	0.143	0.434
		0.995-1.42	10	0.710	0.149	0.434
11	1%	1.75 -1.77	4	0.717	0.171	0.408
	5%	1.75 -1.78	7	0.709	0.164	0.417
		1.75 -2.36	10	0.709	0.163	0.417
12	1%	1.39 -1.41	4	0.719	0.183	0.398
	5%	1.39 -1.51	7	0.706	0.171	0.411
		1.39 -2.71	10	0.708	0.169	0.410
13	1%	1.56 -1.58	4	0.702	0.171	0.432
	5%	1.56 -1.64	8	0.705	0.173	0.429
		1.56 -2.18	10	0.709	0.171	0.423
14	1%	1.92 -1.94	4	0.708	0.149	0.427
	5%	1.92 -2.02	7	0.707	0.147	0.429
		1.92 -2.24	10	0.709	0.149	0.430
Average of all the fits				0.709	0.160	0.423
Mean of the 1% range averages				0.710	0.163	0.420

TABLE 21

Conductivity parameters obtained by fitting the data for the Sr^{2+} doped crystals

Run	Range	F	No. averaged	Δh_1 (eV)	Δs_1 (10^{-3} eV/deg)	(eV)
8	1%	.908-.917	3	0.702	0.130	0.436
11	0%	1.74	3	0.714	0.170	0.414
12	0%	1.34	2	0.717	0.198	0.409
13	0%	1.50	4	0.711	0.186	0.426
14	0%	1.89	2	0.706	0.145	0.429
Averages				0.710	0.166	0.423

dependent upon a precise knowledge of c and the other fixed parameters. The reason for this is that the fitting procedure determines $\mathcal{S}$ from the temperature dependence of conductivity rather than the concentration dependence as in the analytical methods (1.07). Since the conductivity is apparently relatively insensitive to concentration dependence of association compared to temperature dependence, the errors in c become less important. However, Δs_1 is rather more dependent upon an accurate knowledge of c. Below the knee changes in Δs_1 merely displace the extrinsic region as a whole relative to the log σT axis; this is exactly what changes in c do in the absence of association. Thus one might expect to find more scatter in Δs_1 from run to run when c is not known accurately. In agreement with this the fits for which c, when varied lay closest to the straight line in Fig.11 (within 6% of values on the line) had the following values for Δs_1: run 8, 0.154; run 11, 0.155; run 12, 0.155; run 13, 0.155; run 14, 0.155(10^{-3} eV/deg.). These are virtually identical to Δs_1 obtained by fitting the pure crystals.

The results in Tables 20 and 21 show that $\mathcal{S}$ increases slightly as the concentration of impurities decreases. This may indicate that long range coulombic interactions are having some effect on the degree of

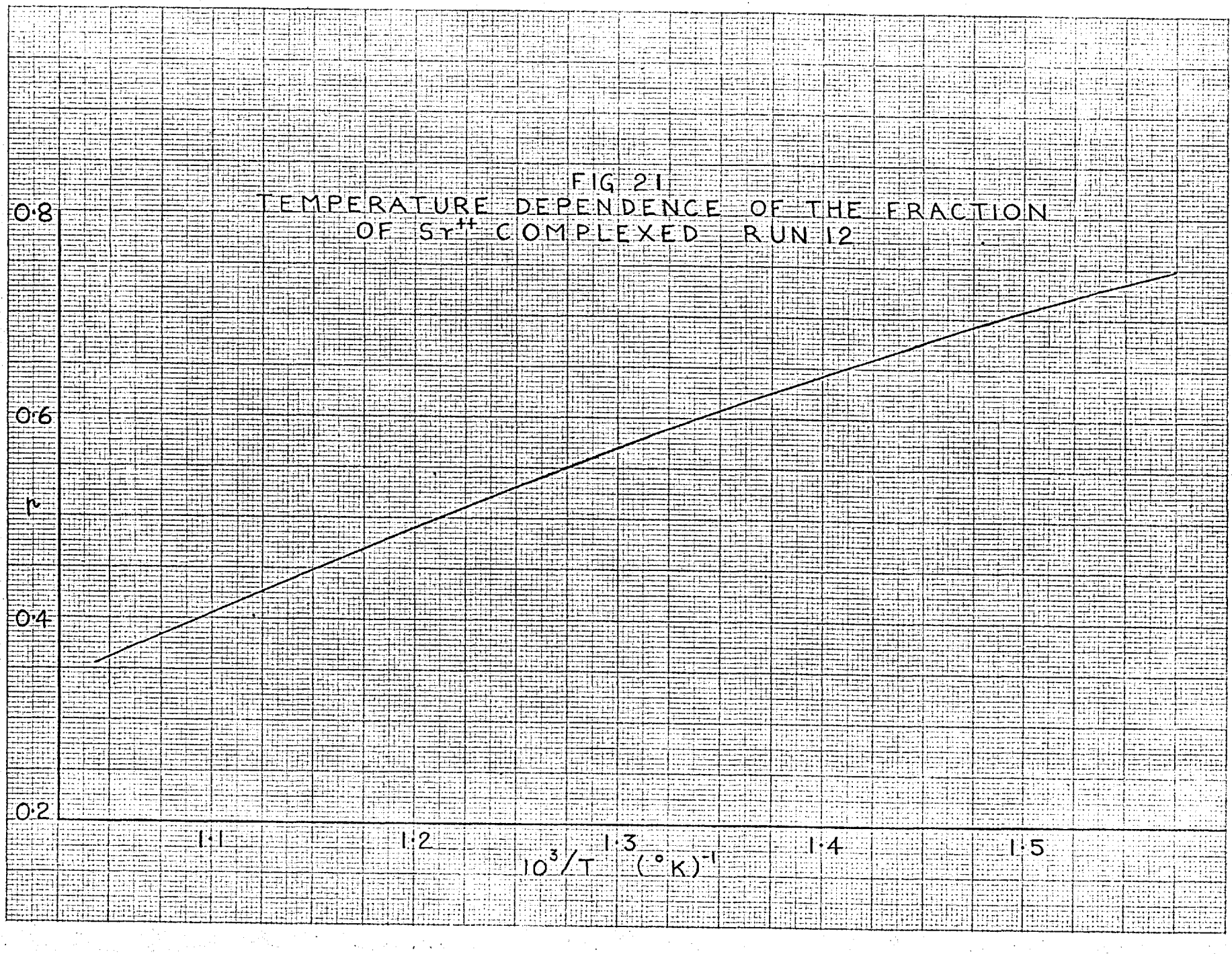
FIG 21
TEMPERATURE DEPENDENCE OF THE FRACTION OF Sr^{++} COMPLEXED RUN 12
0·8
0·6
r
0·4
0·2
1·1
1·2
1·3
1·4
1·5
$10^3/T$ $(°K)^{-1}$

association (Lidiard, 1957) but the evidence is not very substantial. The average value of $\mathcal{E}$ = 0.42 eV lies between the theoretical values of the association energies E_1 and E_2 (Table 2). These calculations indicate that excited states of the complex should be considered (1.06.8 and 1.06.10) but this would have introduced additional parameters which, judging by the excellent fit of the temperature dependence, is apparently not necessary. To show the effect of association Fig.21 is a plot of the fraction of impurities complexed $p = x_k/c$ against 1/T. The computed curve is for one of the fits of run 12 with $c = 4.17 \times 10^{-4}$ mole fraction, $\mathcal{E}$ = 0.426 eV and the remaining relevant parameters equal to the average values from Table 19.

4.03 Development of the A.C. space charge capacitance theory for partially blocking electrodes.

In an attempt to reconcile some of the disagreements between the capacitance results and the predictions of Macdonald's space charge capacitance theory outlined in 1.09 (the lack of agreement will be demonstrated in 4.04), the theory was extended to include partial discharging of ions at the electrodes. The case of partial blocking has been considered before by Chang and Jaffé (1952) but

their expression does not satisfy Poisson's equation and has been criticised by Macdonald (1953). Friauf (1954) has also considered discharging of ions but although his treatment satisfies Poisson's equation, he does not give an explicit formula for the space charge capacitance. Instead his results are presented as a series of lengthy complex expressions from which he computes values for a few special cases applicable to AgBr.

The expression obtained here is specifically for doped KCl. Only negative charge carriers (cation vacancies) are assumed to be mobile and the generation and recombination of these carriers is neglected as in Friauf's treatment. The effect of generation and recombination was examined by carrying out the calculation below, retaining the two extra terms in 1.09.14, but in the absence of a knowledge of k_1 and k_2 approximations cannot be made to determine whether a simple expression is obtainable.

The equation of detailed balance for the cation vacancies, neglecting generation and recombination is from 1.09.14

4.03.1 $$\frac{\partial n}{\partial t} = D\left(\frac{\partial^2 n}{\partial x^2}\right) + \mu \frac{\partial}{\partial x}(nE)$$

where $n(x,t)$ is the number of vacancies per unit volume and μ and D are respectively their mobility and diffusion

coefficient. Poisson's equation relates the electric field E(x,t) to the charge distribution and is

$$4.03.2 \qquad \frac{\partial E}{\partial x} = \beta(c_o - n)$$

where c_o is the number of dissociated Sr^{2+} ions per unit volume and $\beta = 4\pi e/\epsilon$ (e is the electronic charge and ϵ the dielectric constant). One boundary condition for the solution of 1 and 2 (1.09.17) is

$$4.03.3 \qquad V_1 e^{i\omega t} = \int_o^L E(x,t)dx$$

where $V_1 e^{i\omega t}$ represents the sinusoidal applied voltage and the length of the crystal is L. The final boundary condition introduces the partially blocked electrode. Equations 1.09.18 and 1.09.19 no longer apply, instead the current at the electrodes is assumed to be proportional to the excess concentration of cation vacancies Δn over that existing for zero applied voltage. Consider the crystal under the conditions in Fig.22a. In this diagram the direction of the field relative to the x direction is consistent with the derivation of 1. The flux F of negative charges through the crystal in the positive x direction is

$$4.03.4 \qquad F = -D\frac{\partial n}{\partial x} - \mu n E$$

FIG 22

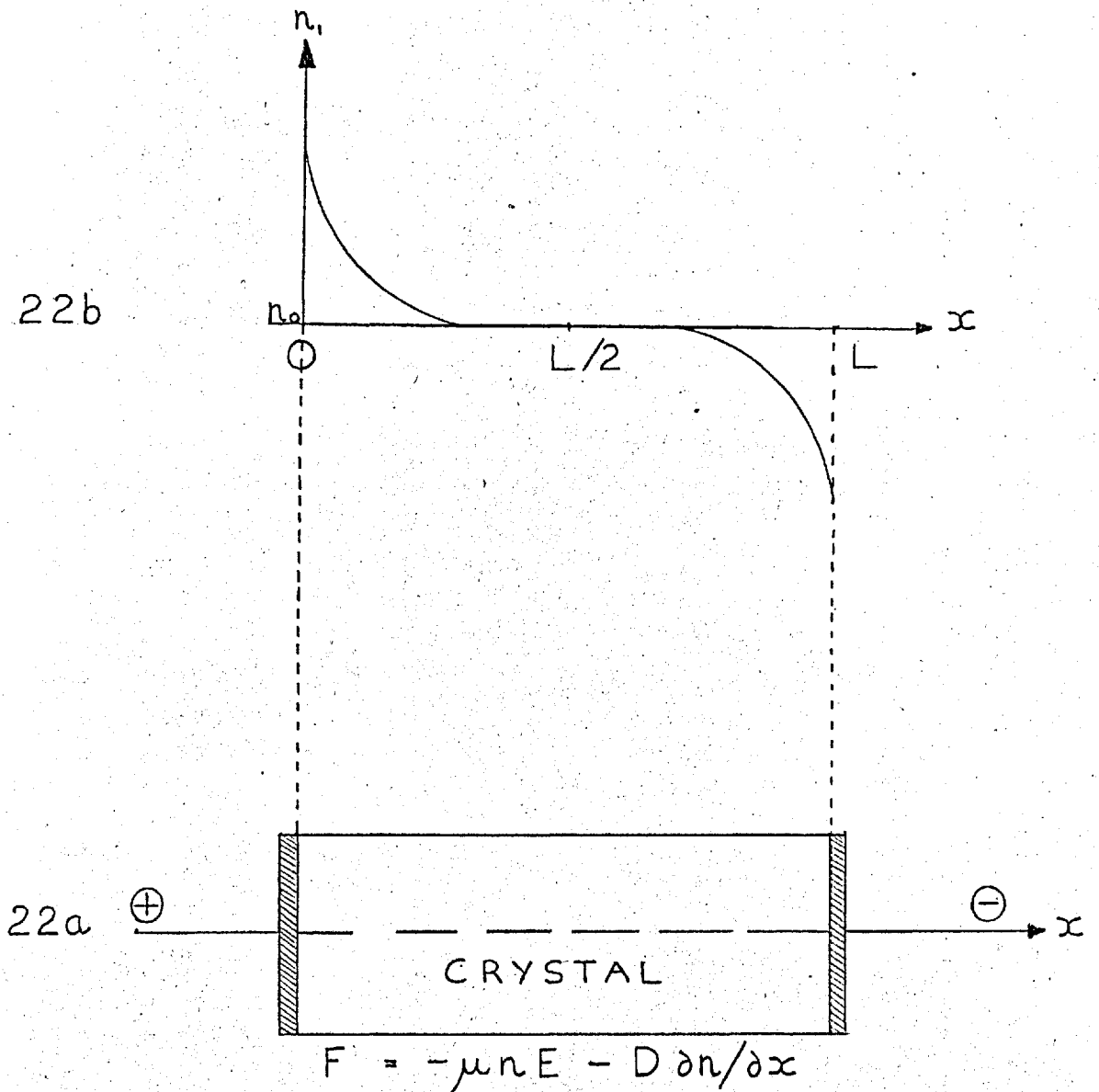

and thus the current in the crystal j due to the vacancies is

4.03.5 $$j = eD\frac{\partial n}{\partial x} + \mu n E e$$

The discharge current at x = L and 0 is given by

4.03.6

$$j(L,t) = -\rho e \Delta n(L,t) D/L$$

$$j(0,t) = \rho e \Delta n(0,t) D/L$$

where ρ is a dimensionless parameter which may be interpreted (Friauf, 1954) by considering a symmetrical free energy barrier of height ΔW to exist at the electrodes. Then the current flowing across the crystal surface at x = 0 will be

4.03.7 $$j(0,t) = \Delta n(0,t) e a \nu_0 e^{-\Delta W/kT}$$

and the blocking parameter is therefore

4.03.8 $$\rho = a \nu_0 (L/D) e^{-\Delta W/kT}$$

where a is the interionic distance and ν_0 the vibrational frequency of an ion in the lattice. Clearly for a completely blocked electrode $\rho = 0$ and for a completely free electrode $\rho = \infty$. The boundary condition may be found by equating the cation vacancy current in the crystal adjacent to the electrodes to the discharge current across

the electrodes thus

4.03.9

$$\mu nEe + D\frac{\partial n}{\partial x}e = -\rho e\,\Delta n(D/L) \qquad \text{at } x = L$$

$$\mu nEe + D\frac{\partial n}{\partial x}e = \rho e\,\Delta n(D/L) \qquad \text{at } x = 0$$

Since the equations 1 and 2 are non linear the current through the crystal will contain all harmonics of the applied potential. However, for small voltages such that $eV_1 \ll kT$ the proportion of higher harmonics to that of the fundamental will be small. It is, therefore, a valid approximation for small voltages, to neglect the higher harmonics (this procedure is adopted throughout the literature) and assume that n and E are of the form

4.03.10 $$n(x,t) = n_o(x) + n_1(x)e^{i\omega t}$$

4.03.11 $$E(x,t) = E_o(x) + E_1(x)e^{i\omega t}$$

Following Macdonald (1953) it is now assumed that $n_o(x) = c_o$ and is thus homogeneous throughout the crystal. As a consequence of this assumption $E_o(x) = 0$. Thus 10 and 11 become

4.03.12 $$n = c_o + n_1 e^{i\omega t}$$

4.03.13 $$E = E_1 e^{i\omega t}$$

On substituting these expressions in 1 and retaining only the linearised part of the equation

4.03.14 $$\frac{d^2n_1}{dx^2} = (i\omega n_1 - \mu c_o \frac{dE_1}{dx})/D$$

By substituting 12 and 13 into 2

4.03.15 $$\frac{dE_1}{dx} = -\beta n_1$$

Consequently 14 simplifies to

4.03.16 $$\frac{d^2n_1}{dx^2} = (i\omega + \mu c_o \beta)n_1/D$$

Substituting 12 and 13 into 3 and 9, and using 12 for Δn

4.03.17 $$V_1 = \int_o^L E_1 dx$$

4.03.18

$$\mu c_o E_1 + D\frac{dn_1}{dx} = -\frac{D\rho}{L} n_1 \qquad \text{at } x = L$$

$$\mu c_o E_1 + D\frac{dn_1}{dx} = \frac{D\rho}{L} n_1 \qquad \text{at } x = 0$$

The equations 15 to 18 may now be solved to find $n_1(x)$. Equation 16 is of the general form

$$\frac{d^2n_1}{dx^2} = m^2 n_1$$

The general solution of this equation is

$$n_1 = A \sinh mx + B \cosh mx$$

However, n_1 must be antisymmetric about the centre of the crystal (Fig.22b) as the time dependence is merely given by multiplying by a sinusoidally varying factor. Thus only the sinh function may be retained and this must have its origin at the centre of the crystal. The solution will therefore be of the form

4.03.19 $$n_1 = A \sinh m(x - L/2)$$

4.03.20 where $$m = \left(\frac{\mu c_o \beta + i\omega}{D}\right)^{\frac{1}{2}}$$

The value of A may be determined as follows. From 15 and 19

$$E_1 = -\beta \int A \sinh m(x - L/2)dx + K$$

4.03.21 $$E_1 = -\frac{\beta A}{m} \cosh m(x - L/2) + K$$

The integration constant K may be eliminated by substitution in 18

4.03.22 $$\mu c_o\left[-\frac{\beta A}{m} \cosh m(x-L/2) + K\right] = -D\left(\frac{\rho n_1}{L} + \frac{dn_1}{dx}\right) \text{ at } x=L$$

Substituting 19 into 22 and putting x = L

4.03.23

$$K = \frac{A}{\mu c_o}\left[\frac{\mu c_o \beta}{m} \cosh(mL/2) - \frac{D\rho}{L} \sinh\left(\frac{mL}{2}\right) - Dm \cosh(mL/2)\right]$$

$$K = \frac{A}{\mu c_o} \cosh(mL/2) \left[\frac{\mu c_o \beta}{m} - D\left[\frac{\rho}{L} \tanh(mL/2) + m\right]\right]$$

A may now be found by substituting 21 into 17

4.03.24

$$V_1 = A \int_0^L -\frac{\beta}{m}\cosh m(x-L/2) + \frac{1}{\mu c_o}\cosh(mL/2)\left[\frac{\mu c_o \beta}{m} - D\left[\frac{\rho}{L}\tanh(mL/2) + m\right]\right] dx$$

Carrying out the integration

4.03.25

$$A = -V_1\left[\frac{2\beta}{m^2}\sinh(mL/2) - \frac{Lm}{\mu c_o}\cosh(mL/2)\left[\frac{\mu c_o \beta}{m^2} - D\right] + \frac{D\rho}{\mu c_o}\sinh(mL/2)\right]^{-1}$$

This may be simplified by substituting for m^2 using 20

4.03.26

$$A = -V_1\left[\sinh(mL/2)\left[\frac{2\beta}{m^2} + \frac{i\omega L}{m\mu c_o}\coth(mL/2) + \frac{D\rho}{\mu c_o}\right]\right]^{-1}$$

The current density j(x,t) within the crystal will be given by the sum of the displacement current (1.01) and the current due to the motion of vacancies thus

4.03.27

$$j(x,t) = \frac{\epsilon}{4\pi}\frac{\partial E}{\partial t} + e[\mu n E + D\frac{\partial n}{\partial x}]$$

The total current density J, flowing into the crystal may be obtained by taking a space average over the whole crystal thus

4.03.28 $$J = \int_0^L j(x,t)\,dx \Big/ \int_0^L dx$$

Using 3, 12 and 13 to carry out the integration

4.03.29

$$J_1 = Y_1 V_1 = \frac{i\omega\epsilon}{4\pi}\frac{V_1}{L} + \frac{e}{L}\left[\mu c_o V_1 + D\left\{n_1(L) - n_1(o)\right\}\right]$$

For convenience this may be written as

4.03.30 $$Y_1 = \frac{i\omega\epsilon}{4\pi L} + \frac{e\mu c_o}{L} + Z$$

where $$Z = \frac{eD}{LV_1}\left\{n_1(L) - n_1(o)\right\}$$

Y_1 is to be regarded as the complex admittance of unit area of the crystal, viewed as one lumped circuit element and may be equated to the equivalent parallel combination of conductance and capacitance, $G + i\omega C'$. Thus the conductance G comprises a term corresponding to the crystal conductance in the absence of polarisation, namely, $\mu c_o e/L$ and the real part, $(1/R)_p$, of Z. The capacitance C' is composed of the capacitance in the absence of microscopic charges $\epsilon/4\pi L$ and the imaginary part of Z divided by ω. The latter component is the space charge capacitance C_p and is found experimentally by subtracting the high frequency capacitance $\epsilon/4\pi L$ from the total capacitance. The expressions for C_p and $(1/R)_p$ are thus

4.03.31 $$\omega C_p = \mathrm{Im}(Z)$$

4.03.32 $$(1/R)_p = \mathrm{Re}(Z)$$

From equation 19

4.03.33 $$Z = \frac{eD}{V_1 L}\, 2A \sinh(mL/2)$$

Substituting 26 for A

4.03.34

$$Z = -\frac{2eD}{L}\left[\frac{2\beta}{m^2} + \frac{i\omega L}{m\mu c_o}\coth(mL/2) + \frac{D\rho}{\mu c_o}\right]^{-1}$$

In order to separate the real and imaginary parts of Z it was found convenient to let

4.03.35 $$m = A + iB$$

4.03.36 $$\coth(mL/2) = F + iH$$

(This A is not to be confused with the A in 33 which will not appear in any of the following expressions). In terms of these abbreviations

4.03.37

$$Z = -\frac{2eDm^2}{L}\left[\frac{i\omega L}{\mu c_o}(A + iB)(F + iH) + 2\beta + \frac{m^2 D\rho}{\mu c_o}\right]^{-1}$$

Substituting 20 for m^2 in the brackets and collecting terms

4.03.38

$$Z = -\frac{2eDm^2}{L}\left[-\frac{\omega L}{\mu c_o}(BF + AH) + \beta(2+\rho) + \frac{i\omega L}{\mu c_o}(AF-BH + \rho/L)\right]^{-1}$$

This expression was rationalised; the result with 20 substituted for the remaining m^2 term is

4.03.39

$$Z = -\frac{2e}{L}\,\frac{\left[-\omega L\beta(BF + AH) + \beta^2\mu c_o(2+\rho) + \frac{\omega^2 L}{\mu c_o}(AF-BH+\rho/L)\right] + i\omega\left[-\frac{\omega L}{\mu c_o}(BF+AH) + \beta(2+\rho) - L\beta(AF-BH+\rho/l)\right]}{\frac{\omega^2L^2}{(\mu c_o)^2}(A^2+B^2)(F^2+H^2) + \beta^2(2+\rho)^2 - \frac{2\beta\omega L}{\mu c_o}(2+\rho)(BF+AH) + \frac{\rho\omega^2 L}{(\mu c_o)^2}(\frac{\rho}{L} + 2AF - 2BH)}$$

The values of A and B were determined by expressing 20 in its trigonometrical form and using De Moivre's theorem to find the square root. The result which may readily be checked is

4.03.40

$$A + iB = \left(\frac{\mu c_o \beta}{2D}\right)^{\frac{1}{2}}\left[\left[\left(1 + \frac{\omega^2}{(\mu c_o\beta)^2}\right)^{\frac{1}{2}} + 1\right]^{\frac{1}{2}} + i\left[\left(1 + \frac{\omega^2}{(\mu c_o\beta)^2}\right)^{\frac{1}{2}} - 1\right]^{\frac{1}{2}}\right]$$

F and H were found by rationalising coth mL/2 with A + iB substituted for m thus

$$F + iH = (e^{L(A+iB)} + 1)/(e^{L(A+iB)} - 1)$$

$$F + iH = \frac{\cos(LB)e^{LA} + 1 + i\sin(LB)e^{LA}}{\cos(LB)e^{LA} - 1 + i\sin(LB)e^{LA}}$$

Multiplying the top and bottom by the complex conjugate of the denominator

$$F + iH = \frac{e^{2LA} - 1 - 2i\sin(LB)e^{LA}}{1 + e^{LA}[e^{LA} - 2\cos LB]}$$

Multiplying top and bottom by e^{-LA} and collecting terms

4.03.41 $$F + iH = (\sinh LA - i\sin LB)/(\cosh LA - \cos LB)$$

In order to simplify the expression for C_p obtainable from 39, numerical values were computed for A, B, F and H for the conditions under which the experimental data were obtained. To aid the substitution of numbers, the Nernst-Einstein relation $\mu/D = e/kT$ (1.07.23) was used to eliminate D, and μ was expressed in terms of the conductivity $\mu = \sigma/c_o e$. The value used for ϵ (to be precise, the permittivity) was 5.21×10^{-12} F/cm, for e, 1.602×10^{-19} coulombs and for k, 1.380×10^{-23} J/°K. From 40 with $\beta = 4\pi e/\epsilon$ and $\omega = 2\pi f$ where f is the frequency of the applied voltage in c/sec.

4.03.42

$$A + iB = \left(\frac{2\pi e^2 c_o}{kT\epsilon}\right)^{\frac{1}{2}} \left[\left[\left(1 + \left(\frac{f\epsilon}{2\sigma}\right)^2\right)^{\frac{1}{2}} + 1\right]^{\frac{1}{2}} + i\left[\left(1 + \left(\frac{f\epsilon}{2\sigma}\right)^2\right)^{\frac{1}{2}} - 1\right]^{\frac{1}{2}}\right]$$

For $\sigma = 10^{-5}$ (ohm cm)$^{-1}$ and f = 1000 cps

4.03.43

$$(f\epsilon/2\sigma)^2 \sim 6 \times 10^{-8} \ll 1$$

This approximation holds well for $f < 10^4$ cps and $\sigma > 10^{-6}$ (ohm cm)$^{-1}$, the maximum value for these limits being $\sim 6 \times 10^{-4}$. Thus it is valid to write

4.03.44

$$A \sim \sqrt{2}\left(\frac{2\pi e^2 c_o}{kT\epsilon}\right)^{\frac{1}{2}}$$

For $c_o = 3 \times 10^{18}/cm^3$ corresponding to a mole fraction of $\sim 2 \times 10^{-4}$ and at T = 650°C,

4.03.45 $$A = 3.84 \times 10^6$$

From equation 42

4.03.46

$$B = (2\pi e^2 c_o/kT\epsilon)^{\frac{1}{2}}\left[\left\{1 + (f\epsilon/2\sigma)^2\right\}^{\frac{1}{2}} - 1\right]^{\frac{1}{2}}$$

Since $(f\epsilon/2\sigma)^2 \ll 1$ the binomial expansion may be used and the expression simplifies to

4.03.47 $$B = (2\pi e^2 c_o/kT\epsilon)^{\frac{1}{2}}\, f\epsilon/2\sqrt{2}\sigma$$

For f = 500 cps, T = 650°C, $\sigma = 10^{-4}$ (ohm cm)$^{-1}$ and $c_o = 3 \times 10^{18}/cm^3$.

4.03.48 $B = 7.86$

With these two approximations in 41

4.03.49 $F \sim \sinh LA/\cosh LA \sim 1$

4.03.50 $H \sim \sin LB/\cosh LA \sim 0$

since whatever the value LB, sin LB and cos LB must lie between 0 and 1 and will be negligible compared with sinh LA $\sim$ cosh LA $\sim e^{LA}$. The hyperbolic terms will be very large; for L $\sim$ 0.4 cms they will be of the order e^{10^5}. Thus the approximations 49 and 50 are very sound and will be valid for all the experimental data, in fact they will hold for all frequencies for which a space charge capacitance can be measured.

Using 49 and 50 together with 31 and 39 and neglecting B^2 in comparison with A^2 (45 and 48)

4.03.51

$$C_p = \frac{2e}{L}\left[\frac{1\beta(A + \rho/L) - \beta(2+\rho) + \omega LB/\mu c_o}{\beta^2(2+\rho)^2 - \frac{2\beta B\omega L(2+\rho)}{\mu c_o} + \frac{\omega^2}{(\mu c_o)^2}[L^2A^2 + \rho L(2A+\rho/L)]}\right]$$

4.03.52

$$C_p = \frac{2e\beta(\mu c_o)^2}{\omega^2 L^2 A}\left[\frac{1 - (2/LA) + (\omega B/\mu c_o \beta A)}{1 + \left(\frac{\beta\mu c_o}{\omega LA}\right)^2(2+\rho)^2 - \frac{2\beta B\mu c_o}{\omega LA^2}(2+\rho)+(2A+\rho/L)\rho/A^2L}\right]$$

The magnitudes of the terms in the numerator may now be compared. From 45, for L = 0.4 cm,

4.03.53 $$2/LA \sim 10^{-6}$$

Using 45 and 48 and the corresponding values used to obtain these

4.03.54 $$\omega B/\mu c_o \beta A = \epsilon f B/2\sigma A = 2.65 \times 10^{-11}$$

Both these terms are negligible compared with 1 and were dropped. Comparing terms in the denominator, those not involving ρ are 1, $4(\beta\mu c_o/\omega LA)^2$ and $-4\beta B\mu c_o/\omega LA^2$. Using the typical values above

4.03.55 $$-4\beta B\mu c_o/\omega LA^2 = -8\sigma B/\epsilon f LA^2 = -5.47 \times 10^{-7}$$

4.03.56 $$(2\beta\mu c_o/\omega LA)^2 = 32(\sigma/\epsilon f LA)^2 = 3.21 \times 10^{-1}$$

55 may be neglected in comparison with unity but 56 must be retained. The terms with ρ as a factor are the same as 53, 56 and half of 55, of these three only $\rho(2\beta\mu c_o/\omega LA)^2$ need be retained. The terms with ρ^2 as a factor are $1/A^2L^2$ and $(\beta\mu c_o/\omega LA)^2$, and from above the first term is negligible compared with the second. With these approximations and using the expressions 44 and 47 for A and B,

4.03.57
$$C_p = \left(\frac{\pi kT}{\epsilon c_o}\right)^{\frac{1}{2}} \frac{4\sigma^2}{\omega^2 L^2 e}\left[1 + \frac{\pi kT}{\epsilon c_o}\,\frac{4\sigma^2}{\omega^2 L^2 e^2}\,(2+\rho)^2\right]^{-1}$$

This is the final expression for the space charge capacitance per unit area, which will be used in the next section in an attempt to interpret the experimental data. It is worthy of note that all the approximations used to derive 57 from 39 improve as the frequency tends to zero, so a zero-frequency limiting polarisation capacitance can be obtained from 57. This is

$$4.03.58 \qquad C_o = e(\epsilon c_o/\pi kT)^{\frac{1}{2}}/(2+\rho)^2$$

When $\rho = 0$ (i.e. for complete blocking) this reduces to Macdonald's (1953) zero-frequency capacitance for blocked electrodes and complete dissocation. The term outside the square brackets in 57 corresponds to that used by Jacobs and Maycock (1963, b) to interpret their data but it would not be valid to neglect the rest of the expression which becomes increasingly importance if ρ is large (e.g. if $\rho \sim 10$).

By substituting 39 into 32 an expression for the polarisation conductance per unit area may be obtained

$$4.03.59 \qquad (1/R)_p = -\frac{2e(\mu c_o)^2}{\omega^2 L^3 A^2}\left[\frac{-\omega L\beta B + \beta^2 \mu c_o(2+\rho) + (A+\rho/L)\omega^2 L/\mu c_o}{1 + \frac{\pi kT}{\epsilon c_o}\cdot\frac{4\sigma^2}{\omega^2 L^2 e^2}(2+\rho)^2}\right]$$

This may be approximated for KCl in the experimental frequency range giving

4.03.60

$$(1/R)_p = -\frac{2e\beta^2(\mu c_o)^3(2+\rho)}{\omega^2 L^3 A^2} / [1 + \frac{\pi kT}{\epsilon c_o} \cdot \frac{4\sigma^2}{\omega^2 L^2 e^2} (2+\rho)^2]$$

On substituting for A (44) and β

4.03.61

$$(1/R)_p = -\frac{8\sigma^3 \pi kT(2+\rho)}{\omega^2 L^3 e^2 c_o \epsilon} / [1 + \frac{\pi kT}{\epsilon c_o} \cdot \frac{4\sigma^2}{\omega^2 L^2 e^2} (2+\rho)^2]$$

Using 57 this conductance may be expressed in terms of the space change capacitance thus,

4.03.62

$$(1/R)_p = -(2+\rho)(2\sigma/Le)(\pi kT/\epsilon c_o)^{\frac{1}{2}} C_p$$

4.04 Treatment of capacitance data.

The most direct test of equation 4.03.57 is via the frequency dependence for a doped crystal. Thus a plot of $1/\omega^2 C$ against $1/\omega^2$ should yield a straight line of slope $(2+\rho)^2/e(\epsilon c_o/\pi kT)^{\frac{1}{2}}$ $(= 1/C_o)$ and intercept $(\epsilon c_o/\pi kT)^{\frac{1}{2}} L^2 e/4\sigma^2$. Moreover, according to the very approximate equation used by Jacobs and Maycock (1963,b) this line should have the same intercept but zero gradient. Fig.23 shows the data for run 13 taken before the high

FIG 23

PRE-ANNEAL CAPACITANCE FOR RUN 13 (L = 0·343 CM)

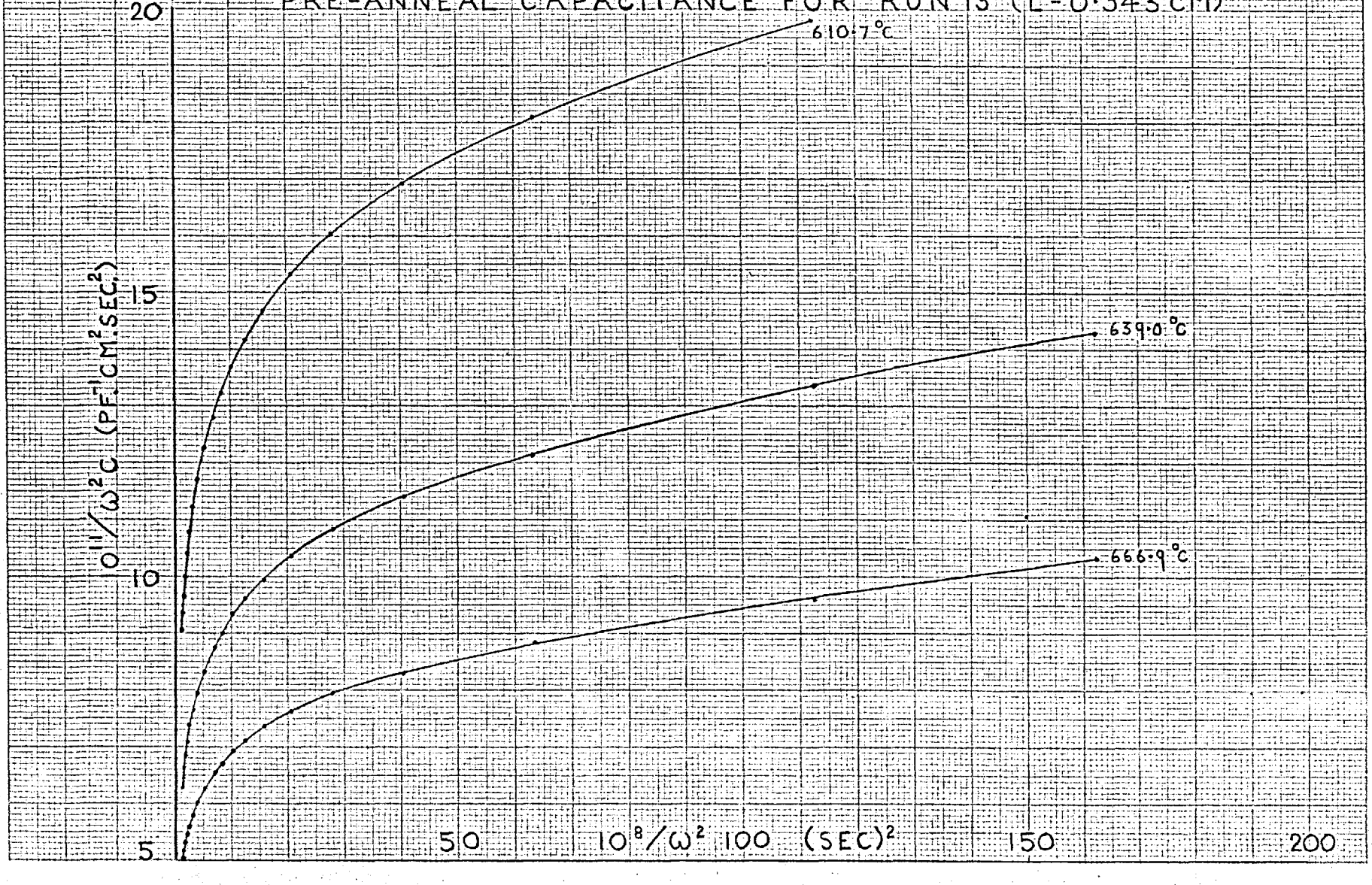

FIG 24
EXPERIMENTAL AND THEORETICAL CAPACITANCE
FOR RUN 13 AT 666·9°C

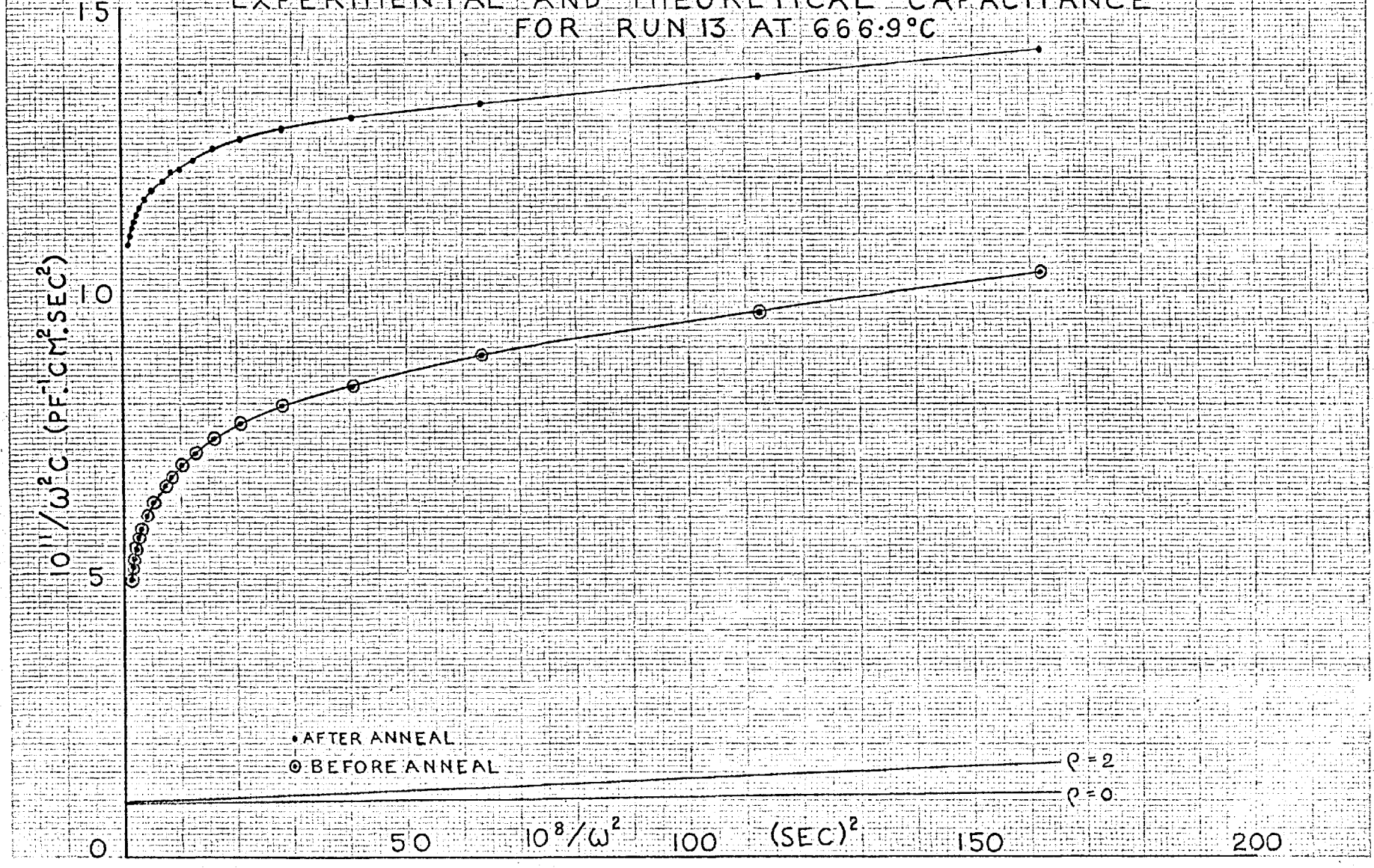

temperature anneal and with increasing temperature. In Fig.24 the data for the 666.9°C isotherm is replotted together with that measured after a high temperature (~680°C) anneal. The theoretical lines for two ρ values have also been included in this figure. The theoretical data were computed using $\epsilon = 5.73 \times 10^{-12}$ F/cm, this being a theoretical high temperature value (600°C) (Havinga, 1961). On the basis of these results the theory seems to provide but a very crude approximation to the actual behaviour although it does predict a capacitance of the correct order of magnitude (contrast Friauf, 1954).

Now from 4.03.8, the Nernst-Einstein equation 1.07.23, and the expression for the cation vacancy mobility 1.07.9,

$$\rho = \frac{L}{4a} e^{(\Delta g_1 - \Delta W)/kT}$$

Since a, the lattice parameter is 3.13×10^{-8}, L/4a is of the order of 10^7. Thus ΔW must be considerably greater than Δg_1, otherwise the value of ρ will be very large and there will be no blocking. As a consequence ρ should increase with increasing temperature and since the gradient of the isothermal plots $\propto (2 + \rho)^2 T^{\frac{1}{2}}$, their slope should also be greater at higher temperatures. From Fig.23 this is the reverse of the observed behaviour of a tangential slope at a particular frequency; the same is

true of the data taken after a high temperature anneal. Unfortunately this prevents any realistic estimate of ρ from these plots. However, if ρ is extremely small, 10^{-2} to 10^{-3}, then over the experimental frequency range C will be insensitive to variations in ρ and additional effects may be causing this contradictory behaviour.

The same type of frequency dependence was exhibited by the data from run 15, for which carbon electrodes were used (Fig.25). The one noticeable difference between these results and those obtained using platinum electrodes is in the magnitude of the capacitance. The crystals used for runs 15 and 13 had roughly similar conductance and impurity concentration (Fig.11) but Figs.24 and 25 show the results for run 15 are much closer in magnitude to the predicted value.

Fig.26 shows the frequency dependence of C exhibited in the same manner as that used by Jacobs and Maycock (1963, b), together with the theoretical plots for a series of ρ values. The fact that the experimental plots are almost linear shows that this method of displaying the data is apparently not a very stringent test of the form of the frequency dependence. Finally, Fig.27 shows log C plotted against log f for run 13 at two temperatures. The experimental plots are almost linear and the slopes for the data taken after annealing are -1.90. Over the

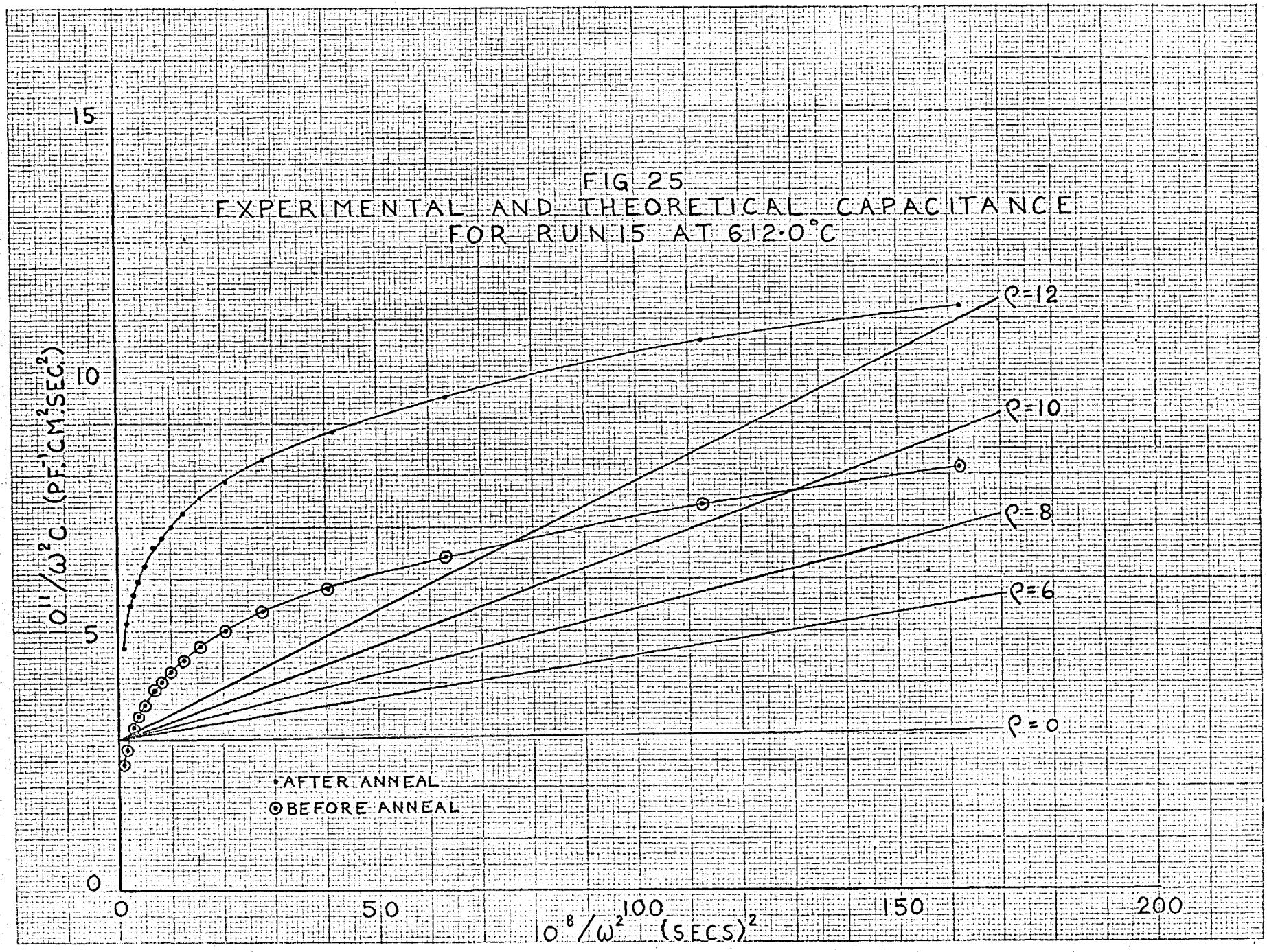
FIG 25
EXPERIMENTAL AND THEORETICAL CAPACITANCE
FOR RUN 15 AT 612·0°C
$10^{11}/\omega^2 C$ (P.F.$^{-1}$C.M.^{2}SEC.^{2})
$10^8/\omega^2$ (SECS)^2
ρ=12
ρ=10
ρ=8
ρ=6
ρ=0
•AFTER ANNEAL
⊙BEFORE ANNEAL
0
5
10
15
0
50
100
150
200

FIG 26
EXPERIMENTAL AND THEORETICAL CAPACITANCE
FOR RUN 13 AT 666·9°C

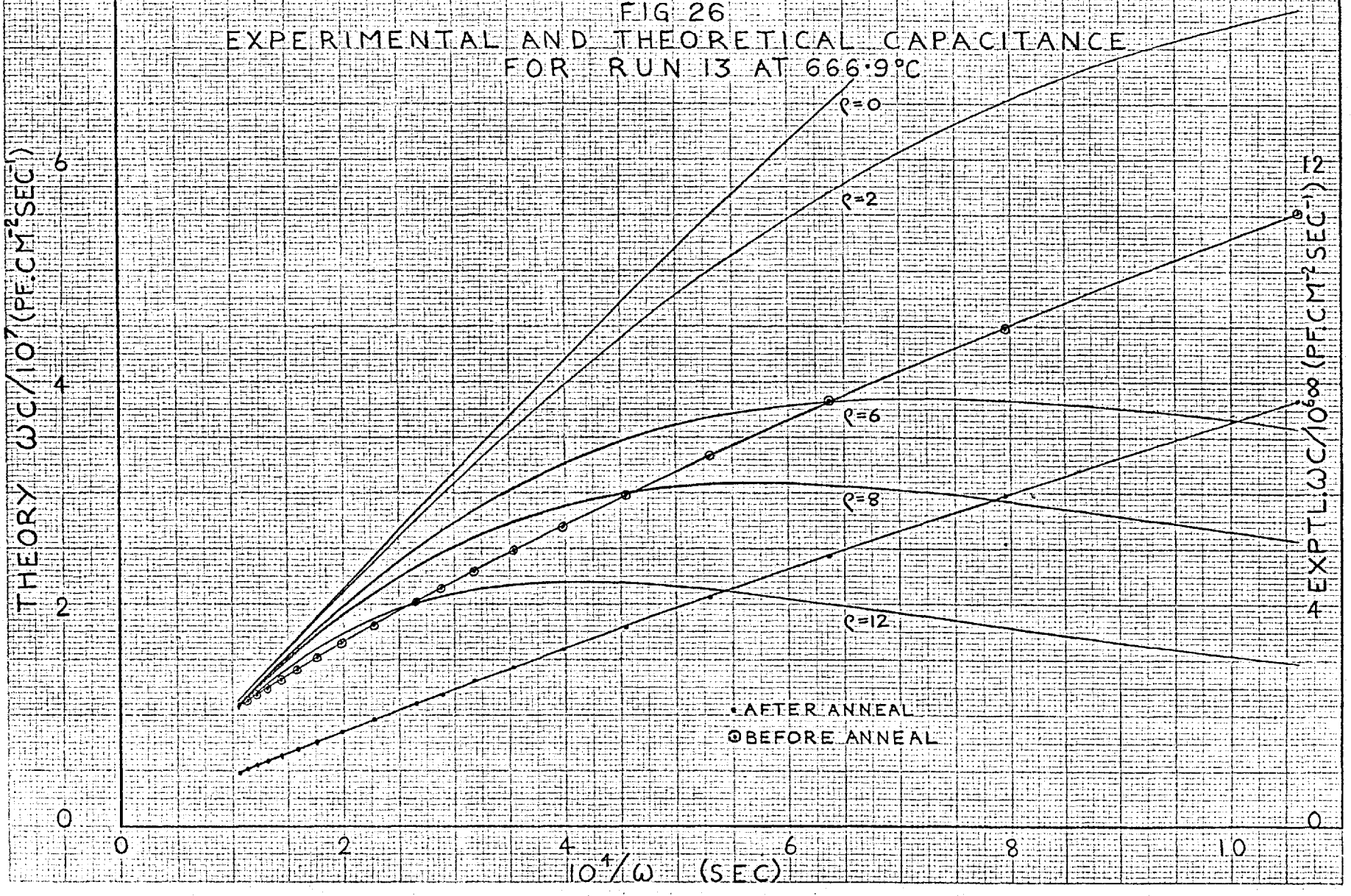

FIG 27
EXPERIMENTAL AND THEORETICAL CAPACITANCE FOR RUN 13

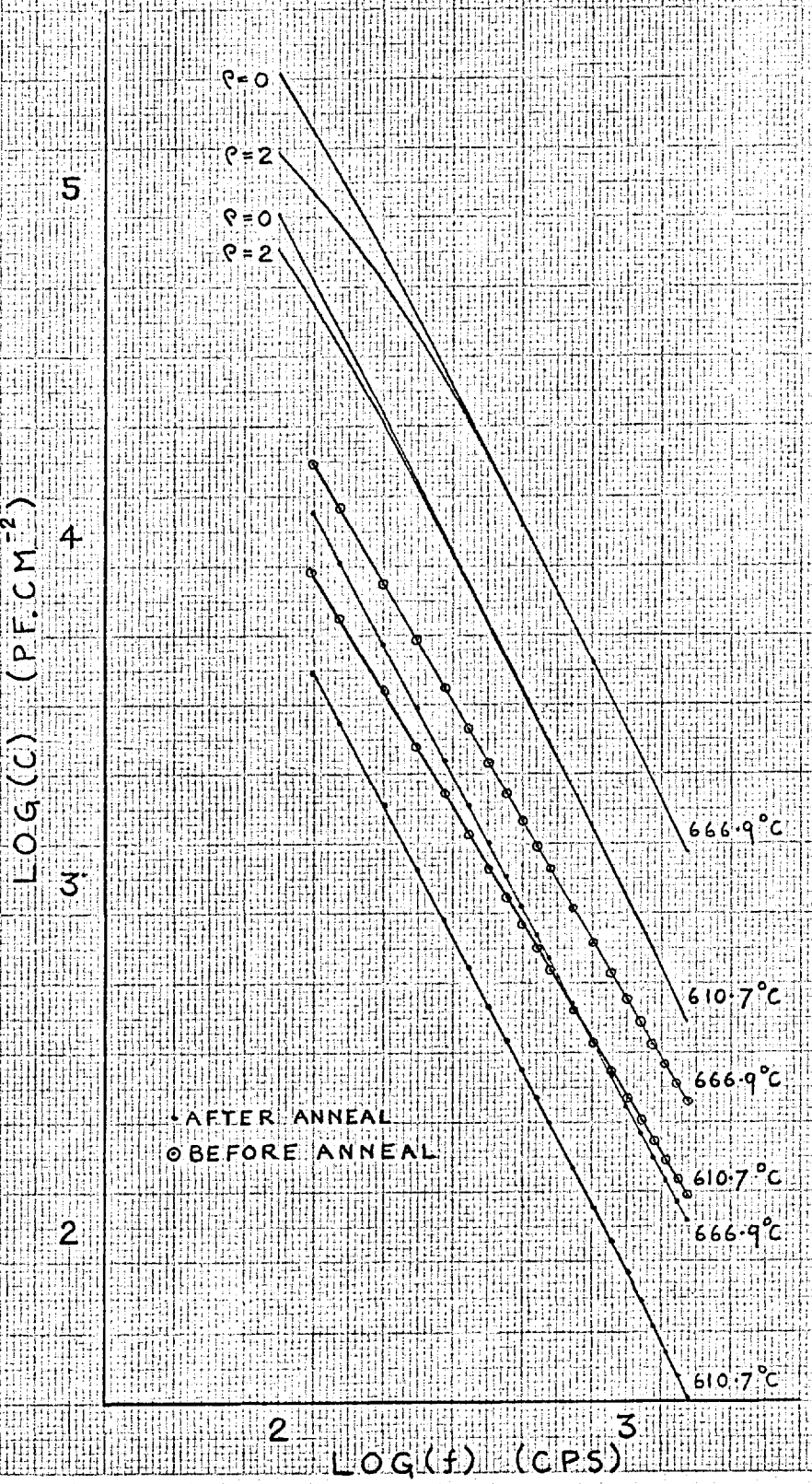

same frequency region the slopes of the theoretical plots for completely blocked electrodes are -1.99. Clearly a value of $\rho > 0$ does not improve the agreement with the observed frequency dependence.

On the basis of these results the theory only accounts for the frequency dependence in an extremely approximate manner. The introduction of partial blocking does not seem to have improved the agreement. One possible explanation of the observed behaviour within the framework of the present theory is in terms of a distribution of ρ values over the crystal electrode interface. (Strictly this makes the problem a three-dimensional one with fields and concentration gradients at right angles to the direction of the applied field.) If a portion of the crystal surface was in perfect contact with the crystal ($\rho \sim 0$) this could account for the experimental results being generally lower in magnitude than is predicted. If the remainder of the crystal surface was in varying degrees of contact with the electrode, the total capacitance would have to be written as a sum of capacitances given by 4.03.57 but with the appropriate area and ρ value. Such an expression would not necessarily have the same frequency dependence as 4.03.57. The reduction in capacitance on annealing could then be explained largely in terms of the

development of a better crystal electrode contact. A similar reduction of capacitance with time has been observed by Friauf (1953) for AgBr. Although no attempt was made to verify this suggestion quantitatively, it is not inconceivable that the experimental plot in Fig.26 could be constructed from theoretical curves similar to those shown but suitably adjusted to reduced areas. The scatter of points in Fig.13 also demonstrates the lack of a tendency for the magnitude of the capacitance to achieve a definite limiting value as a result of annealing.

The only feature which shows good agreement with the theory is the temperature dependence of the capacitance (Table 18) which obeys the predictions of the simple expression used by Jacobs and Maycock (1963, b). However, they plotted log C versus 1/T rather than log ($CT^{3/2}$) and did not attempt to obtain activation energies as their plots showed a high degree of curvature, more than may be accounted for by leaving out the $T^{3/2}$ factor. The straight line plots obtained in this work suggest an effective ρ value near to zero in agreement with the conclusions from the frequency dependence.

Fig.28 shows the frequency-dependent resistance for run 15 at 612°C prior to annealing. According to 4.03.61 this plot should be linear. The theoretical lines

FIG 28
EXPERIMENTAL AND THEORETICAL POLARISATION CONDUCTANCE FOR RUN 15 AT 612°C

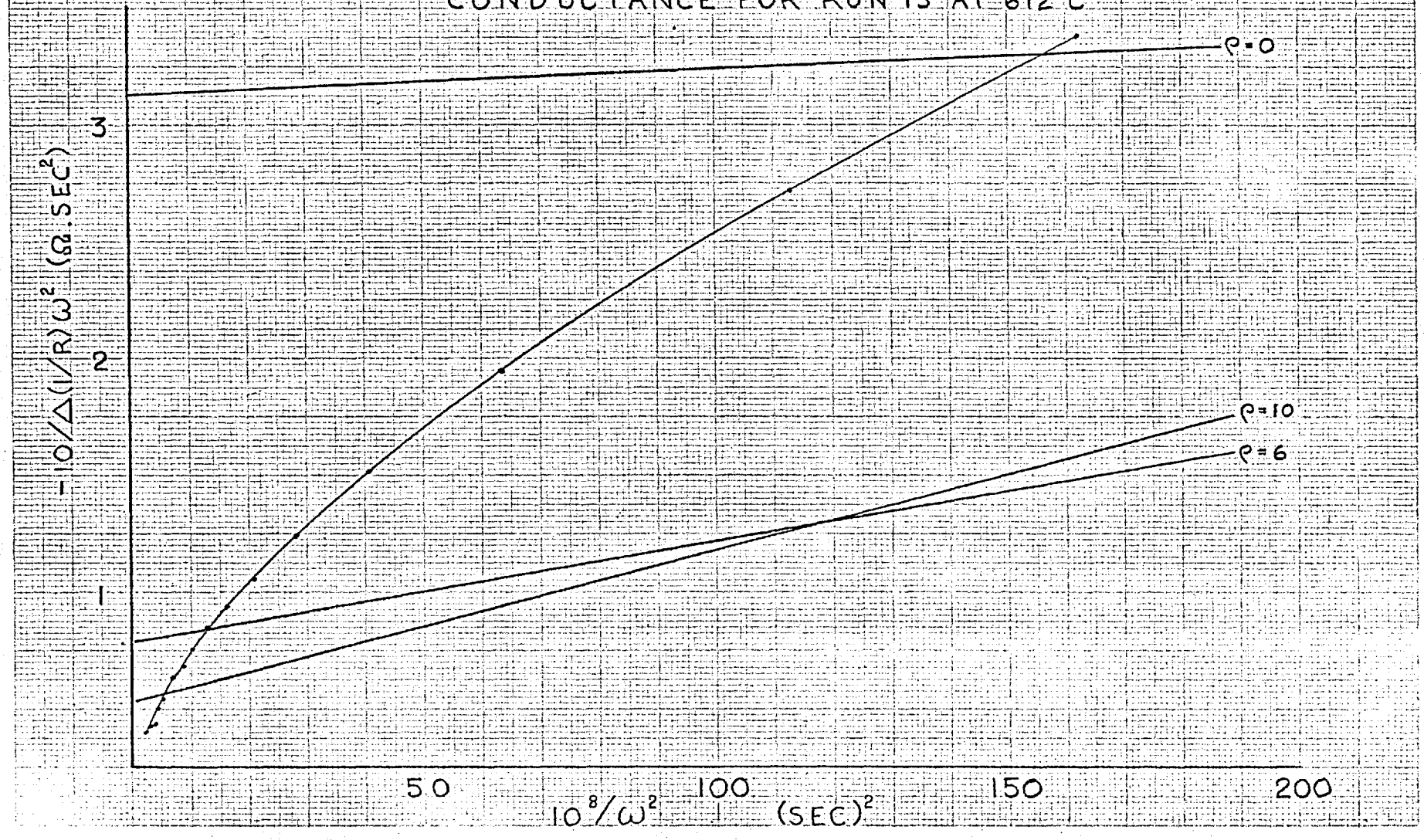

for three values of ρ, calculated according to 4.03.61, with the appropriate crystal area, show that the magnitude of the polarisation conductance is approximately correct but the frequency dependence shown by the data is not as predicted. However, the experimental plot is nearer to a straight line than the similar presentation of capacitance. No great significance may be attached to these results since the variation in resistance was extremely small. However, the logarithmic plot (Fig.15) shows the empirical relation $\Delta(1/R) \propto 1/\omega$ is approximately obeyed which agrees with the result found by Allnatt and Jacobs (1961) using platinum electrodes but a very highly doped crystal with 7×10^{-3} mole ratio Sr^{2+}. The reduction in $\Delta(1/R)$ on annealing (3.04) may be interpreted as an improvement of electrical contact between the crystal and electrode, consistent with the similar interpretation of the reduction in C_p. The fact that both $\Delta(1/R)$ and C_p were both greater when graphite electrodes were used seems to indicate that graphite makes a poorer contact than platinum.

Thus the theory accounts for the temperature dependence of capacitance and approximately predicts the correct frequency dependence and magnitude; it also predicts the correct order of magnitude of $\Delta(1/R)$. These results

make it not unreasonable to assume the origin of the polarisation lies in the formation of a space charge at the electrodes. Some of the lack of agreement may be due to the approximations involved in linearisation of the initial differential equations. Thus the neglect of harmonic terms is only valid if $eV_1/kT \ll 1$. To satisfy this the measuring voltage should have been well below 0.08 volts. Although this condition could not be satisfied, within the limits of experimental error, no variation in capacitance or resistance was observed between voltages of 0.04 and 45. The rather simple form assumed for the rate of discharge at the electrodes (4.03.6) does not represent rectification. The neglect of this possibility was also necessary as a result of the linearisation which requires $n_1(x)$ to be antisymmetric about the centre of the crystal.

A straightforward way of resolving the problem of whether the lack of agreement with the predicted capacitance stems from partial discharge, would be to use blocking electrodes. This may be done by inserting layers of dielectric material between the electrodes and the crystal but would create considerable practical difficulties. The dielectric layers would have to be extremely thin and preferably of a high permittivity so that their total

capacitance may be negligible compared with that of the crystal. In addition they would have to be inert with respect to the crystal and electrode and have a high electrical resistance at temperatures up to $\sim 680^{\circ}C$. Such an experiment was attempted using mica as the dielectric but a sufficiently thin layer was not used and its impedance was much too high.

APPENDIX 1

The computer program used for fitting conductivity data to the theoretical expression is given below. It was written in Extended Mercury Autocode for the London University Atlas computer. A title and part of some input data for run 6 are included to help clarify some of the remarks to be made on the program. The program utilises a minimisation routine (Routine 970), which may be obtained from the London University Institute of Computer Science.

Chapter 1 of the program is a private post mortem which prints out the contents of some of the registers, starting with the present values of the parameters. This is only entered if the program faults. At the start of Chapter 0 the input data is read in and Routine 970 entered. F is calculated starting at label 1). At label 2) the parameters and F Value for each minimum found by Routine 970 are printed out and the accuracy of fit is tested (see below). That part of the program below label 20) puts increasingly larger numbers into F when c is made negative by Routine 970. This has the effect of making the Routine correct c back to a positive value.

A brief explanation of the form of input and output data follows.

Input

a) The constants N, ν_1, ν_2, e, a, $10^3/k$ are read in this order into the registers W_0, W_1,...,W_5

b) A jump label S' is read which initially must be 6.

c) The number of data points is read into L followed by the ratio of length: area for the crystal, which goes into H. The experimental data is then read in the repeated form of a temperature in degrees centigrade, the first one goes into register C_0, followed by the corresponding resistance of the crystal which goes into G_0. Thus the data occupies the registers C_0 to C_{L-1} and G_0 to G_{L-1}.

d) A jump condition is read into T' which initially is set to 1.

e) The number of parameters to be varied is read into N.

f) An integer in the range 0 to 7 is read into I' followed by the value of the parameter h, which goes into YI'. This reading order is repeated for all the possible integers and all the initial 'guesses' of the parameters. The order of the parameters must be h, 10^3s, $\mathfrak{Z}$, c, Δh_1, $10^3\ \Delta s_1$, Δh_2, $10^3 \Delta s_2$, but the integers can be in any order; they specify the order in which the parameters are to be varied by Routine 970. Thus the first parameter to be varied will be the one

with the integer 0 directly preceding it, i.e. it will be in register Y_0. If e.g. N has been read as 3 then only the parameters in registers Y_0, Y_1, Y_2 will be varied in this order.

g) The steplength used by Routine 970 for varying the parameters is read into F.

h) The required accuracy of the final fit is read into A. The condition used to stop the fitting program is

$$|F_2 - F_1| / F_2 < A$$

where F_1 is the final fit F value and F_2 is the preceding fit F value.

This completes the input of the first group of data. Having executed this, more data may be read in starting with the jump label S' (the constants are only read in the first time).

1) If S' is read as 6 and T' as 1 a complete set of new data must be read exactly as above, starting at b).

2) If S' is read as 6 and T' as -1 then only new experimental data is read in, the remaining data being the same as before.

3) If S' is read as 6 and T' as 0, experimental data, accuracy and steplength must be read in again.

4) If S' is read as 7 then the number of parameters to be varied, the parameters, the steplength and accuracy must be read.

5) If S' is read as 8 a new steplength and accuracy must be read in.

6) If S' is read as 50 the program ends.

Output.

The parameters appear in the order in which they were varied followed by the value of F appropriate to them. Several lots of parameters and F values are printed out, each corresponding to a minimum found by Routine 970. Finally, when two consecutive F values satisfy the accuracy condition specified in register A, the exact F value for the last set of parameters is printed out again (it might not correspond precisely to the F value immediately preceding it, this stems from the way Routine 970 is written). This is followed by the experimental data and data calculated from the last set of parameters. The data appears in headed columns (see the caption in Chapter 0). The columns labelled experimental and inverse temp are log σT and $10^3/T$ respectively, computed directly from the experimental data. The difference between log σT calculated from the parameters and the experimental value is in the column labelled

calc.-exptl. In addition calculated values of log $\sigma_1 T$, log $\sigma_2 T$, t_1 and $p(=x_k/c)$ are also printed out.

PROGRAM

```
JOB
LSCIIPFI, BEAUMONT MINIMISATION RUN I/2 7/7
COMPUTING 50000 INSTRUCTIONS
OUTPUT
0 LINE PRINTER 4000 LINES
STORE 32 BLOCKS
COMPILER EMA

MAIN → 1200
AUXILIARY (0,1000)
DEPTH0
DUMPS0

ROUTINE 970
  ⌘ ⌘
TITLE
MINIMISATION OF PARAMETERS
(FOR IONIC CONDUCTIVITY)
CHAPTER I
A→100
B→100
C→100
D→100
U→100
X→100
V→100
Z→100
E→100
F→4
G→100
H→100
W→10
Y→10
£→10
I)NEWLINE
CAPTION
PRIVATE POST MORTEM
0=0(I)7
NEWLINE
PRINT(Y0)0,10
REPEAT
NEWLINE
0=0(I)4
NEWLINE
PRINT (W0)0,10
REPEAT
NEWLINE
NEWLINE
PRINT(H0)0,10
PRINT(V0)0,10
PRINT(Z0)0,10
NEWLINE
PRINT(X0)0,10
PRINT(B0)0,10
PRINT(U0)0,10
```

```
ACROSS5/0
CLOSE

CHAPTERO
VARIABLES 1

F2=0
U'↓0
V'↓120
K=0(1)5
READ(WK)
REPEAT

5)F2=0
READ(S')
S')=S')
JUMP(S')

6)READ(L)
L=L-1
READ(H)
K=0(1)L
READ(CK)
DK=CK+273.18
EK=1000/DK
READ(GK)
GK=XLOG(DKH/GK)
AK=0.434295GK
REPEAT

READ(T')
JUMP9,0>T'
JUMP8,T'=0
7)READ(N)
READ(1')
READ(Y1')
READ(J')
READ(YJ')
READ(K')
READ(YK')
READ(L')
READ(YL')

READ(M')
READ(YM')
READ(N')
READ(YN')
READ(O')
READ(YO')
READ(P')
READ(YP')


8)READ(F)
READ(A)
9)M=0
T)=1)
S)=2)
Q'=0
JUMPDOWN(R970)


NEWLINE 4
CAPTION
LOG SIGMA1 T LOG SIGMA 2 T*
INVERSE TEMP LOG SIGMA T
EXPERIMENTAL CALC-EXPTL
   P          T1


K=0(1)L
NEWLINE
PRINT(VK)0,4
PRINT(ZK)0,4
PRINT(EK)0,4
PRINT(BK)0,4
PRINT(AK)0,4
PRINT(UK)0,4
PRINT(HK)0,4
PRINT(XK)0,4
REPEAT
JUMP 5
50)END
```

*There are no carriage return line feeds in the actual program caption.

```
1)F=0
A'=XSORT(3)
K=0(1)L
W=XEXP(YJ'W5-Y1'w5EK)
W'=XEXP(YK'EKW5)
W'=12W'
JUMP10,K>0
X'=YL'+WW'
Y=XSQRT(0.3333333X'X'+W
Y'=YYY
X'=0.3333333X'
X=WWW'-2X'X'X'-WX'
X=1.5A'X/Y'
B'=XMOD(X)
JUMP20,B'>1
X=XARCCOS(X)
X=XCOS(0.3333333X)
X=2XY/A'
X=X-X'
10)C=XX
D=XC+CYL'+CWW'-WX-WWW'
D'=3C+2XWW'-W+2XYL'
E=X-D/D'
D=XMOD(E-X)
D=D/E
X=E
JUMP11,0.0000001>D
JUMP10
11)X'=W/X


HK=X-X'
HK=1+HK/YL'
Y'=XEXP(YN'W5-YM'EKW5)
Y'=4000W3W4W4W1Y'W5

Y=XEX>(YP'W5-EKY0'W5)
Y=4000W3W4W4W2YW5

Y'=WOW3Y'X'
VK=XLOG(Y')
VK=0.434295VK+18.7953105
Y=WOW3YX
ZK=XLOG(Y)
ZK=0.434295ZK+18.7953105
G=Y'+Y
XK=Y'/G
Z=XLOG(G)
BK=0.434295Z+18.7953105
UK=BK-AK
F=F+UKUK
REPEAT

F=F/L
RETURN
2)NEWLINE
NEWLINE
K=0(1)N
PRINT(YK)0,4
REPEAT
B=XSQRT(F)
B=100B
NEWLINE
PRINT(B)0,4
Q'=0

JUMP3,F2=0
M=M+1
JUMP4,M>9
F1=F
B=XMOD(F2-F1)
B=B/F2
JUMP4,A>B
F2=F1
RETURN
3)F2=F
RETURN
4)R=0
RETURN
100)ACROSS1/1
20)Q'=Q'+1
JUMP 100,Q'>10
NEWLINE
620,3
PRINT(Q')1,0
PRINT(R)1,0
K=0(1)7
PRINT(YK)Q,3
REPEAT
F=100Q'
RETURN
CLOSE
```

```
1.6166,22  4.25,12  4.25,12  1.6021,-19  3.139,-8  11.6049

6  33  0.5355

649.9  4.951,4
636.0  7.161,4
621.7  1.057,5
607.9  1.555,5
593.5  2.381,5
580.2  3.501,5
566.4  5.291,5
553.5  7.712,5
539.5  1.126,6
524.8  1.645,6
510.9  2.276,6
499.0  2.938,6
485.1  3.798,6
472.5  4.701,6
458.7  5.878,6
445.0  7.115,6
434.3  8.470,6
421.0  1.026,7
408.4  1.256,7
394.9  1.557,7
382.2  1.927,7
369.0  2.428,7
357.8  3.010,7
347.1  3.740,7
334.6  4.895,7
322.6  6.410,7
309.8  8.550,7
296.0  1.260,8
285.9  1.625,8
273.5  2.295,8
260.4  3.400,8
248.5  5.050,8
234.7  8.100,8

1   3
3   2.285
4   0.477
5   0.425
0   1.42,-6
6   0.708
7   0.224
1   1.02
2   0.594
```

```
0.05   0.05

7   3
3   2.285
4   0.477
5   1.42,-6
6   0.708
7   0.224
2   1.02
1   0.594

0.05   0.05
```

REFERENCES

Allnatt, A.R., 1959, Thesis, Univ. of London.

Allnatt, A.R., 1964, J.Phys.Chem., 68, 1763.

Allnatt, A.R., and Cohen, M.H., 1964, J.Chem.Phys., 40, 1860, 1871.

Allnatt, A.R. and Jacobs, P.W.M., 1961, J.Phys.Chem.Solids, 19, 281.

Allnatt, A.R. and Jacobs, P.W.M., 1962, Trans.Farad.Soc., 58, 116.

Arnilear, H.J. and Chemla, M., 1956, Compt.Rend., 242, 2132.

Aschner, J.F., 1954, Thesis, Univ. of Illinois.

Barnes, R.B., 1923, Z.Physik, 75, 723.

Barr, L.W., Hoodless, I.M., Morrison, J.A. and Rudham, R., 1960, Trans.Farad.Soc., 56, 697.

Barr, L.W., Morrison, J.A. and Schroeder, P.A., 1965, Preprint.

Bassani, F. and Fumi, F.G., 1954, Nuovo Cimento, 11, 274.

Beltrami, M., Cappelletti, R. and Fieschi, R., 1964, Physics Letters, 10, 279.

Biermann, W., 1960, Z.Physik.Chem.(Frankfort), 25, 90, 253.

Boswarva, I.M., 1965, Private communication.

Boswarva, I.M., and Franklin, A.D., 1965, Phil.Mag., 11, 335.

Brennecke, C.G., 1940, J.Appl.Phys., 2, 202.

Bucci, C. and Fieschi, R., 1964, Phys.Rev.Letters, 12, 16.

Bucci, C.A. and Riva, S.C., 1965, J.Phys.Chem.Solids, 26, 363.

Camagni, P. and Manara, A., 1965, J.Phys.Chem.Solids, 26 449.

Chang, H. and Jaffé, G., 1952, J.Chem.Phys., 20, 1071.

Compaan, K. and Haven, Y., 1956, Trans.Farad.Soc., 52, 786.

Cook, J.S. and Dryden, J.S., 1960, Australian J.Phys., 13, 260.

Dreyfus, R.W., 1961, Phys.Rev., 121, 1675.

Dreyfus, R.W. and Nowick, A.S., 1962, J.Appl.Phys.Supp., 33, 473.

Dryden, J.S., 1963, Proceedings of the International Conference on crystal lattice defects, J.Phys.Soc., Japan, 18, Supp.3, 129.

Dryden, J.S. and Meakins, R.J., 1957, Disc.Farad.Soc., 23, 39.

Eshelby, J.D., Newey, G.W.A., Pratt, P.L. and Lidiard, A.B., 1958, Phil.Mag., 3, 76.

Etzel, H.W. and Maurer, R.J., 1950, J.Chem.Phys., 18, 1003.

Etzel, H.W. and Patterson, D.A., 1958, Phys.Rev., 112, 1112.

Ewles, J. and Jain, S.C., 1957, Proc.Roy.Soc.A., 243, 353.

Fowler, R.H. and Guggenheim, E.A., 1952, Statistical Thermodynamics, Cambridge, P.545.

Frenkel, J., 1926, Z.Physik, 35, 652.

Friauf, R.J., 1954, J.Chem.Phys., 22, 1329.

Fröhlich, H., 1958, Theory of Dielectrics, Oxford.

Gründig, H., 1960, Z.Physik, 158, 577.

Gründig, H., 1965, Z.Physik, 182, 477.

Gründig, H. and Rühenbeck, C., 1965, Z.Physik, 183, 274.

Gründig, H. and Wassermann, E., 1963, Z.Physik, 176, 293.

Guccione, R., Tosi, M.P. and Asdente, M., 1959, J.Phys. Chem.Solids, 10, 162.

Haven, Y., 1964, Proceedings of the British Ceramic Society, No.1, 93.

Havinga, E.E., 1961, J.Phys.Chem.Solids, 18, 253.

Jacobs, P.W.M. and Maycock, J.N. 1963a, J.Phys.Chem.Solids, 24, 1693.

Jacobs, P.W.M. and Maycock, J.N., 1963,b, J.Chem.Phys., 39, 757.

Jaffé, G., 1933, Ann.Physik, 16, 217, 249.

Joffé, A.F., 1923, Ann.Physik, 72, 461.

Kanzaki, H., Kido, K. and Ninomiya, T., 1962, J.Appl.Phys., 33, 482.

Känzig, W. and Cohen, M.H., 1959, Phys.Rev.Letters, 3, 509.

Kelting, H. and Witt, H., 1949, Z.Physik, 126, 697.

Keneshea, F.J. and Fredericks, W.J., 1963, J.Chem.Phys., 38,1952.

Keneshea, F.J. and Fredericks, W.J., 1965, J.Phys.Chem. Solids, 26, 501.

Kerkhoff, F.Z., 1951, Z.Physik, 130, 449.

Kessler, A. and Mariani, E., 1965, Phys.Stat.Solidi, 8, K 149.

Kobayashi, K. and Tomiki, T., 1960, J.Phys.Soc.Japan, 15, 1982.

Kummer, J.T. and Youngs, J.D., 1963, J.Phys.Chem., 67, 107.

Laurent, J.-F. and Bernard, J., 1957, J.Phys.Chem.Solids, 3, 7.

Lehfeldt, W., 1933, Z.Physik, 85, 717.

Lidiard, A.B., 1954, a, Phys.Rev., 94, 29.

Lidiard, A.B., 1954,b, Report of the Conference on Defects in Crystalline Solids held at Bristol, p.283.

Lidiard, A.B., 1957, Handbuch der Physik, 20, 246.

Lüty, F., Anger,J. and Fritz, B., 1963, Z.Physik, 174, 240.

Macdonald, J.R., 1953, Phys.Rev., 92, 4.

Maurer, R.J., 1963, Technical Report No.7, Contract Nonr 1834 (19) NR 017-412, University of Illinois.

Maycock, J.N., 1962, Thesis, Univ. of London.

Ninomiya, T., 1960, J.Phys.Soc.Japan, 15, 1601.

Otterson, D.A., 1960, J.Chem.Phys., 33, 227.

Parker, N.S., 1954, Thesis, Univ. of Durham.

Patterson, D.A., 1962, Phys.Rev., 127, 1564.

Penley, J.C. and Witte, R.S., 1964, J.Chem.Phys., 40, 1550.

Phipps, T.E. and Partridge, E.G., 1929, J.Amer.Chem.Soc., 51, 1331.

Pierce, C.B., 1961, Phys.Rev., 123, 744.

Redfern, B.A.W. and Pratt, P.L., 1964, Proceedings of the British Ceramic Society, No.1, 173.

Roberts, M.H., 1951, Elec.Eng., 23, 51.

Rolfe, J., 1964, Canadian J.Phys., 42, 2195.

Rolfe, J., Lipsett, F.R. and King, W.J., 1961, Phys.Rev., 123, 447.

Rossenbrook, H.H., 1960, Computer J., 3, 175.

Sastry, P.V. and Srinivasen, T.M., 1963, Phys.Rev., 132, 2445.

Schottky, W., 1935, Z.Phys.Chem.Abt.B, 29, 335.

Stasiw, O. and Teltow, J., 1947, Ann.Physik, 1, 261.

Sutter, P.H. and Nowick, A.S., 1963, J.Appl.Phys., 34, 734.

Tharmalingam, K., 1963, J.Phys.Chem.Solids, 24, 1380.

Tharmalingam, K., 1964, J.Phys.Chem.Solids, 25, 255.

Tharmalingam, K. and Lidiard, A.B., 1961, Phil.Mag., 6, 1157.

Tosi, M.P. and Airoldi, G., 1958, Nuovo Cimento, 8, 584.

Tosi, M.P. and Fumi, F.G., 1958, Nuovo Cimento, 7, 95.

Tubandt, C., Reinhold, H. and Liebold, G., 1931, Z.anorg. allg.Chem., 197, 225.

Wagner, C. and Hantelmann, P., 1950, J.Chem.Phys., 18, 72.

Watkins, G.D., 1959, Phys.Rev., 113, 79.

Watkins, G.D., and Walker, R.M., 1956, Bull.Amer.Phys.Soc. Ser.2, 1,324.

Wert, C., 1950, Phys.Rev., 79, 601.